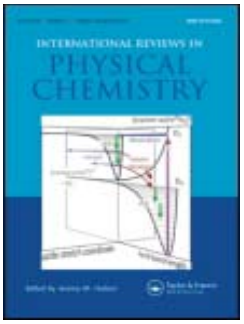

International Reviews in Physical Chemistry

ISSN: 0144-235X (Print) 1366-591X (Online) Journal homepage: http://www.tandfonline.com/loi/trpc20

Formation of resonantly stabilised free radicals via the reactions of atomic carbon, dicarbon, and tricarbon with unsaturated hydrocarbons: theory and crossed molecular beams experiments

Alexander M. Mebel & Ralf I. Kaiser

To cite this article: Alexander M. Mebel & Ralf I. Kaiser (2015) Formation of resonantly stabilised free radicals via the reactions of atomic carbon, dicarbon, and tricarbon with unsaturated hydrocarbons: theory and crossed molecular beams experiments, International Reviews in Physical Chemistry, 34:4, 461-514, DOI: 10.1080/0144235X.2015.1075280

To link to this article: http://dx.doi.org/10.1080/0144235X.2015.1075280

Published online: 13 Oct 2015.

International Reviews in Physical Chemistry, 2015
Vol. 34, No. 4, 461–514, http://dx.doi.org/10.1080/0144235X.2015.1075280

Formation of resonantly stabilised free radicals via the reactions of atomic carbon, dicarbon, and tricarbon with unsaturated hydrocarbons: theory and crossed molecular beams experiments

Alexander M. Mebel[a]* and Ralf I. Kaiser[b]*

[a]*Department of Chemistry and Biochemistry, Florida International University, Miami, FL 33199, USA;* [b]*Department of Chemistry, University of Hawaii at Manoa, Honolulu, HI 96822, USA*

(*Received 19 March 2015; final version received 15 July 2015*)

Resonance stabilised free radicals (RSFRs) play an important role in the growth of polycyclic aromatic hydrocarbons and ultimately in the production of soot and carbonaceous particles in combustion flames, in the interstellar medium, and in planetary atmospheres. This article reviews extensive experimental crossed molecular beams and theoretical *ab initio*/Rice–Ramsperger–Kassel–Marcus studies in the last two decades of the reactions of atomic carbon, $C(^3P)$, dicarbon, $C_2(X^1\Sigma_g^+/a^3\Pi_u)$, and tricarbon, $C_3(X^1\Sigma_g^+)$, with unsaturated hydrocarbons, from acetylene to benzene, showing that the reactions form various types of RSFR via C_n(n = 1–3)-for-H, C_n-for-CH_3, and C_n-for-C_xH_y exchange mechanisms. The RSFRs produced in these reactions include C_xH (x = 1–8), propargyl (C_3H_3) and its substituted analogues, 2,4-pentadiynyl-1 (i-C_5H_3) and 1,4-pentadiynyl-3 (n-C_5H_3) together with their methyl substituted counterparts, butatrienyl (i-C_4H_3) and its substituted analogues, and hexenediynyl, i-C_6H_3, as well as cyclic five-, six-, and seven-member ring radicals including aromatic phenyl, benzyl, and tolyls. The reactions of atomic carbon and dicarbon proceed by barrierless additions to double, triple, or 'aromatic' bonds of the unsaturated hydrocarbons, form highly exothermic products, and are fast even at very low temperatures, whereas the reactions of singlet tricarbon require high barriers to be overcome, often leading to endothermic products, and can occur only at high temperatures. The paper summarises typical reaction mechanisms for small carbon species (C, C_2, and C_3) with unsaturated hydrocarbons and describes implications of the considered reactions in combustion chemistry and astrochemistry.

Keywords: resonance stabilised free radicals; crossed molecular beams; *ab initio* calculations; reaction mechanism

Contents

*Corresponding authors. Email: ralfk@hawaii.edu; mebela@fiu.edu

1. Introduction

Hydrogen-deficient carbon bearing radicals stabilised by electron delocalisation or resonance stabilised free radicals (RSFRs) are believed to play an important role in the growth of polycyclic aromatic hydrocarbons (PAH) and ultimately production soot and carbonaceous particles in combustion flames [1–3], as well as in the interstellar medium (ISM) and planetary atmospheres [4–13]. The homogeneous formation of PAHs can be subdivided into two stages: (1) formation of the first aromatic ring (benzene, C_6H_6, or the phenyl radical, C_6H_5) or production of two fused aromatic rings from non-aromatic hydrocarbons and (2) the growth of PAHs starting from the first aromatic ring [3,14]. A unifying theme, which has emerged for both stages is the importance of RSFRs involved in crucial chemical reactions of formation and growth of aromatics [15–20]. For instance, the recombination of resonance stabilised propargyl radicals, C_3H_3, has been firmly established as a potential pathway for the synthesis of the first aromatic ring [21–25], whereas other possible routes include the reactions like n-$C_4H_3 + C_2H_2$, n-$C_4H_5 + C_2H_2$,3 and i-$C_5H_3 + CH_3$ [21,26] which also involve RSFRs. On the growth stage, propargyl radical addition to phenyl, benzyl and methylphenyl radicals, $C_6H_5/C_7H_7 + C_3H_3$, can lead to the formation of the simplest PAH, indene and naphthalene [27,28], and this motif can be continued with larger PAH species. But how RSFRs themselves can be produced? In combustion, they are formed through the pyrolysis of hydrocarbon molecules via C–H bond rupture, direct hydrogen atom abstraction, and β C–C bond scission and reach high concentrations in flames due to their higher stability and lower reactivity with respect to e.g. molecular oxygen as compared to conventional free radical species. Under low temperature conditions of ISM

and planetary atmospheres the pyrolytic pathway is not available, but hydrocarbon molecules can decompose photolytically. Another important reactions class for RSFR synthesis is represented by the reactions of carbon atoms and small carbon clusters with unsaturated hydrocarbons. Dicarbon, C_2, and tricarbon, C_3, are the simplest among bare carbon clusters and both species have been detected in high temperature combustion flames under fuel-rich conditions of incipient soot formation at concentrations near 10^{15} cm^{-3} [29]. The reactions of atomic carbon, dicarbon, and tricarbon with unsaturated hydrocarbons were suggested to convert those to larger hydrogen deficient hydrocarbon radicals, in particular RSFRs. These reactions are also important in chemical vapour deposition processes of nano diamonds [30], and are closely related to the growth of carbon clusters in carbon-rich stars as well as to the synthesis of diamonds in interstellar space [31–34].

In this article, we overview experimental and theoretical studies of the reactions of C, C_2, and C_3 with unsaturated hydrocarbons from C_2H_2 to C_6H_6, leading to the formation of various classes of RSFRs, which were performed in the last two decades in our groups and by other researchers. Our focus is on crossed molecular beam (CMB) experiments under single-collision conditions, which, together with theoretical investigations of the potential energy surfaces (PESs), allow us to establish intimate details of the reaction mechanism and to uncover the reaction dynamics. The results of CMB studies are compared with kinetics experiments in the gas phase and with the studies of the reactions in matrix isolation where available. The paper is organised as follows: after a brief description of the CMB experimental techniques and theoretical methods used for the calculations of PESs and reaction kinetics under single-collision conditions, we classify different types of RSFRs by their molecular formulae and chemical bonding and then consider particular reactions of C, C_2, and C_3 leading to the different RSFR types and characterise their mechanistic and dynamic features. This discussion is followed by a summary of the typical reaction mechanisms for C, C_2, and C_3 with unsaturated hydrocarbons and concluding remarks describing implications of the considered reactions in combustion chemistry and astrochemistry.

2. Experimental and theoretical methodology

The CMB technique gives a unique way to observe reactions between two molecules or radicals in the single collision regime, i.e. without wall effects or third body collisions [13]. This is accomplished by generating molecular beams of reactants in separate chambers and colliding them into each other in the main reaction chamber as shown in Figure 1. The generation of supersonic reactant beams of sufficiently high concentration to guarantee a detectable quantity of the final reaction product(s) is critical. In our experiments reviewed in subsequent sections, the 266 nm output of a Nd:YAG laser is focused onto a rotating carbon rod [35] and the ablated species (atomic carbon $C(^3P_j)$, dicarbon $C_2(X^1\Sigma_g^+/a^3\Pi_u)$, tricarbon $C_3(X^1\Sigma_g^+)$ are seeded in neat carrier noble gas (helium, neon, or argon) released by a Proch–Trickl pulsed valve [36]. In such laser-based ablation sources [7,9], the chemical composition of the supersonic beam and the peak velocity differ in distinct segments of the pulsed beam and electronically and/or vibrationally excited species may prevail in the predominantly faster and hence less cooled parts of the beam. Therefore, to select a reactant beam of a well-defined chemical composition and velocity distribution, fast rotating chopper wheels are often utilised [35,37]. A selected segment of the beam crosses a pulsed beam of a second reactant (a hydrocarbon molecule) released by a second pulsed valve perpendicularly under a well-

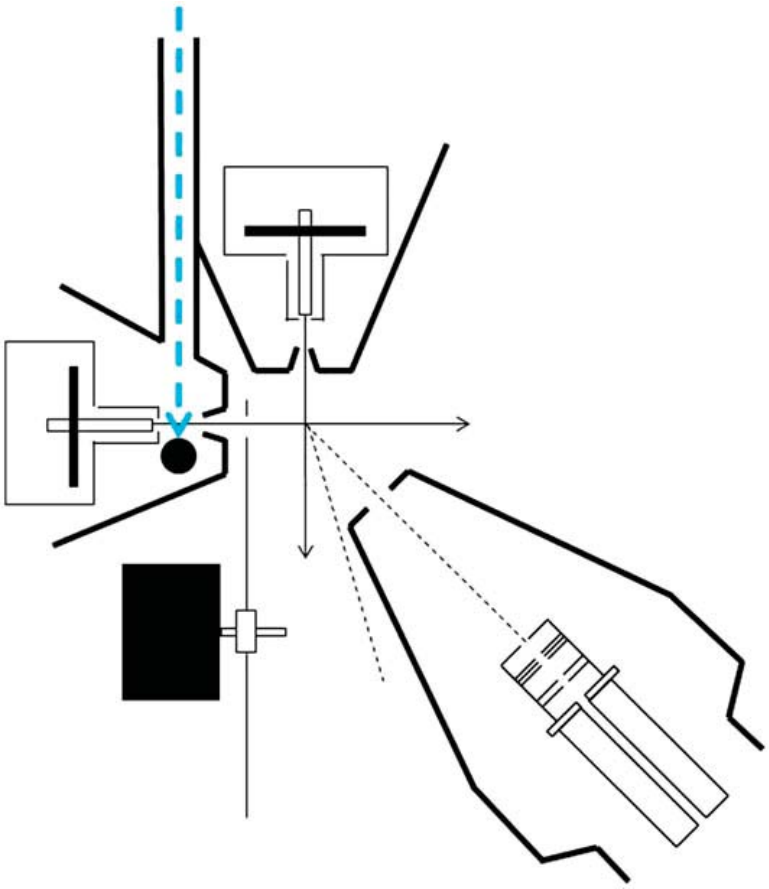

Figure 1. (Colour online) Schematic top view of a CMB apparatus. Shown are the primary source chamber with the ablation source and laser (dashed blue) channel (left), the secondary source chamber (top), the chopper wheel, and the triply differentially pumped detector.

defined collision energy in the interaction region. A chopper wheel is used to select a well-defined velocity of the pulsed radical beam, which in turn provides a specific kinetic energy of the primary beam reactant when undergoing reactive scattering with the secondary reactant. The reaction products are monitored by a rotatable, triply differentially pumped mass spectroscopic detector within the plane of the primary and secondary beams. The neutral products are universally electron impact ionised at 80 eV before being mass selected at a specific mass-to-charge ratio (*m/z*) and detected under ultra high vacuum conditions of typically a few 10^{-12} Torr. The reactive scattering signal at a specific *m/z* ratio is recorded at multiple angles exploiting the time-of-flight (TOF) technique. The ion counts of an ion of the selected *m/z* are recorded vs. the time. The collision between the radical and the hydrocarbon defines the 'time zero' in each experiment. At each angle, the TOFs are integrated furnishing us with the laboratory angular distribution, i.e. a distribution reporting the integrated ion counts at a defined *m/z* ratio vs. the laboratory angle. The laboratory data including laboratory angular distribution and TOF spectra are transformed into the centre-of-mass reference frame via a forward deconvolution technique. This yields two crucial functions, which – together with the laboratory data – assist us to extract the reaction dynamics and underlying reaction mechanisms: the centre-of-mass angular distribution ($T(\theta)$) and the product translational energy distribution ($P(E_T)$) [38]. For completeness, it should be

noted that vacuum ultraviolet (VUV) light instead of electrons can be also exploited to photoionize the neutral molecules [39–43]. However, the determination of braching ratios requires the knowledge of the photoionisation cross sections, which are often difficult to obtain. Further, pulsed beams can be replaced by continuous molecular beams coupled with soft electron impact ionisation of the reaction products [44–49]. This approach utilises electrons with low, tunable energy of typically 8–30 eV to reduce or even eliminate the problem of dissociative ionisation from interfering species. However, soft ionisation has one disadvantage: at electron energies of 8–30 eV, the ionisation cross sections of the newly formed molecules are *at least* a factor of 20 lower than the electron impact ionisation cross sections with 80 eV electrons. Therefore, continuous supersonic beams are crucial.

Obtaining accurate PESs for each crossed beam reaction is an integral part of elucidating the reaction mechanisms and products formed. In this review, we consider PESs for numerous chemical reactions covering theoretical work spanning over two decades and utilising a range of theoretical methods. Usually, structures of the reactants, products, intermediates, and transition states on their respective surfaces were optimised at the hybrid density functional B3LYP level [50–52] with the 6-311G** basis set and vibrational frequencies were calculated using the same B3LYP/6-311G** method. Connections between intermediates and transition states were normally verified by intrinsic reaction coordinate calculations. Higher level methods, such as various modifications of the G2 and G3 model chemistries [53–56], the coupled cluster CCSD(T) method [57] with Dunning's correlation-consistent cc-pVTZ basis set [58], or CCSD(T) extrapolated to the complete basis set (CBS) limit [59] were used to refine relative energies of various structures. Normally, such theoretical methods are capable to provide relative energies of various species including transition states accurate within 5–10 kJ mol^{-1}.

In CMB experiments, the reactions of C, C_2, and C_3 with unsaturated hydrocarbons were studied under single-collision conditions and hence we used the microcanonical version of Rice–Ramsperger–Kassel–Marcus (RRKM) theory for calculations of collision energy-dependent rate constants and relative yields of potential products. In this case, rate constant $k(E)$ at an internal energy E for a unimolecular reaction $A^* \rightarrow A^{\#} \rightarrow P$ can be expressed as [60]:

$$k(E) = \frac{\sigma}{h} \cdot \frac{W^{\#}(E - E^{\#})}{\rho(E)}$$

where σ is the reaction path degeneracy, h is the Plank constant, $W^{\#}(E - E^{\#})$ denotes the total number of states for the transition state (activated complex) $A^{\#}$ with a barrier $E^{\#}$, $\rho(E)$ represents the density of states of the energised reactant molecule A*, and P is the product or products. The available internal energy E is calculated as the reaction collision energy E_{col} (which is assumed to be predominantly converted into vibrational energy of collision complexes) plus the energy of chemical activation, i.e. the negative of the relative energy of an intermediate or a transition state with respect to the separated reactants.

If no distinct transition state exists on the PES (as for the case of a simple bond cleavage process), we considered different positions for the transition state along the reaction path and calculate rate constants corresponding to each of them. The minimum rate so obtained is the closest to the truth, assuming that quantum effects related to tunnelling and nonseparability are negligible. This procedure is called variational transition state theory (VTST) [61]. In the microcanonical VTST, the minimum in the micro-

canonical rate constant is found along the reaction path according to the following equation:

$$\frac{\mathrm{d}k(E)}{\mathrm{d}q^{\#}} = 0,$$

where $q^{\#}$ is the reaction coordinate, so that a different transition state is found for each different energy. The individual microcanonical rate constants are minimised at the point along the reaction path where the sum of states $W^{\#}(E - E_0)$ has a minimum. Thus, the reaction bottleneck is located where the minimal sum of states is found, i.e. the transition state's sum of states must be calculated along the reaction path. Each of these calculations requires values of the classical potential energy, zero-point energy, and vibrational frequencies as functions of the reaction coordinate.

Under collision-free molecular beam conditions, kinetic equations for unimolecular reactions can be expressed as follows:

$$\frac{\mathrm{d}[C]_i}{\mathrm{d}t} = \sum k_n[C]_j - \sum k_m[C]_i$$

where $[C]_i$ and $[C]_j$ are concentrations of various intermediates or products, k_n and k_m are microcanonical rate constants computed as described above. Steady-state approximation was used to solve the system of the kinetic equations. This approach allowed us to evaluate product branching ratios for chemical reactions under collision-free conditions starting from various initial collision complexes based on unimolecular rate constants for different isomerisation and dissociation steps [62], with the assumption that the reaction system behaves statistically and that the intramolecular vibrational redistribution (IVR) process is faster than any unimolecular reaction step – the basic assumption of RRKM theory.

How the CMB experimental data combined with the theoretical PESs allow us to unravel the reaction mechanism and dynamics? First, for those products born without internal excitation, the maximum translational energy of the $P(E_T)$ indicates the total available energy in the reaction, which is composed of the collision energy plus the reaction energy. Generally, the reaction energy can be used to identify the product formed in the reaction, either through comparison to reaction energies available in the literature or from the values computed theoretically. The situation becomes more complicated in some cases when multiple reaction channels and hence different isomers can be formed [63]. The position of the peak in translational energy distributions is indicative of the presence or absence of a tight exit transition state (an exit barrier) in the dissociation step leading to the final product formation. For instance, zero-peaking of the $P(E_T)$ normally means that such a step occurs without an exit barrier, via a loose variational transition state. Alternatively, the existence of a maximum away from zero translational energy indicates the existence of tight exit transition states and exit barriers above the separated products on the order of magnitude close to the $P(E_T)$ peak position. $P(E_T)$ also allows us to estimate the fraction of the total reaction energy converted to the translational degrees of freedom, which may be characteristic for indirect or direct reaction dynamics. The centre-of-mass angular distributions, $T(\theta)$ provide additional insights into the reaction dynamics. For example, angular distributions showing intensity over the full angular range are indicative of indirect, complex-forming reaction mechanisms, whereas a preferential backward or forward scattering observed in $T(\theta)$ may be due to direct dynamics. Further, if the $T(\theta)$ associated with the heavy product depicts a higher flux in the direction of a radical beam, then the lifetimes of the colli-

sion complexes are likely to be comparable and/or shorter than their rotational period, which is called osculating complex behaviour [64]. Thus, the rotational period of the complex can be used as a molecular clock to estimate its lifetime. The shape of the centre-of-mass angular distribution is also governed by the disposal of the total angular momentum, J. The reactants undergo rotational cooling in a supersonic expansion resulting in the initial total angular momentum, J, being equivalent to the orbital angular momentum L, and due to conservation of momentum, also equivalent to the final orbital angular momentum L_0, to give: $J \approx L \approx L_0$. The final recoil velocity vector v_0, is perpendicular to L_0 and therefore in the plane perpendicular to J. The centre-of-mass scattering angle θ, is defined as the angle between the initial relative velocity v and v_0, and depends on the values of J, M and M_0, where M and M_0 are the projections of J on the initial and final relative velocity, respectively. In a collision complex that dissociates with high M_0 values, the final relative velocity will be almost parallel to J and perpendicular to v and the products will be preferentially scattered at $\theta = 90°$. Thus, the angular distributions can characterise the structure of the decomposing complex and in particular the direction along which a light hydrogen atom is emitted when the final product is formed; this information can be compared with the theoretically computed structures of the decomposing complexes and dissociation transition states. When CMB experiments are carried out with (partially) isotopically labelled reactants (e.g. hydrocarbons deuterated in distinct positions), relative yields of ions with different *m/z* ratios (*H* loss vs. *D* loss) may characterise the position of atomic hydrogen elimination and, in comparison with the calculated PESs, provide further information on the reaction mechanism and dynamics. Finally, a comparison of the reaction products deduced from the experimental CMB data with theoretical product branching ratios computed using RRKM theory allow us to deduce whether the reaction follows statistical or non-statistical behaviour, which may also correlate with its indirect or direct character.

3. Discussion

Table 1 presents the list of RSFRs produced in various reactions of $C(^3P)$, $C_2(X^1\Sigma_g^+/a^3\Pi_u)$, and $C_3(X^1\Sigma_g^+)$ with unsaturated hydrocarbons ranging from acetylene (C_2H_2) to benzene (C_6H_6), while Figure 2 illustrates different types of structure of these radicals. In terms of their stoichiometry, four different classes of RSFR are formed: (i) C_xH (x = 3–8), (ii) C_xH_3 (x = 3–6), (iii) C_xH_5 (x = 4–9), and (iv) C_xH_7 (x = 6–7). Since the C_xH_y radicals can have numerous structural isomers, in the discussion to follow RSFRs are classified according to their structure and chemical bonding type rather than stoichiometry.

3.1. C_xH (x = 3, 5, 7)

C_xH radicals with an odd number of carbon atoms have two low energy isomers, linear with a $^2\Pi$ ground electronic state, and cyclic with a three-member carbon ring and a $^2B_2$ ground electronic state [65–69]. Electronic configuration of the linear structure can be best described in terms of two resonance structures, cumulenic and acetylenic, where the unpaired electron is placed on carbon atoms in the opposite ends of the molecule:

Table 1. Summary of the products of the $C/C_2/C_3$ reactions with unsaturated hydrocarbons.

(a) Products classified according to reaction counterparts.

	C	C_2	C_3
C_2H_2	C_3H	C_4H	C_5H
C_2H_4	C_3H_3	C_4H_3	C_5H_3
C_3H_4 (CH_3CCH)	C_4H_3	C_5H_3	C_6H_3
C_3H_4 (H_2CCCH_2)	C_4H_3	C_5H_3	C_6H_3
C_3H_6	C_4H_5	C_5H_5	
C_4H_2	C_5H	C_6H	C_7H
C_4H_4	C_5H_3	C_6H_3	
C_4H_6 ($C_2H_3C_2H_3$)	C_5H_5	C_6H_5	
C_4H_6 (CH_3CCCH_3)	C_5H_5	C_6H_5	
C_4H_6 ($H_2CCCH(CH_3)$)	C_5H_5	C_6H_5	
C_4H_6 ($HCCC_2H_5$)	C_5H_5	C_6H_5	
C_5H_8($C_2H_3C(CH_3)CH_2$)	C_6H_7	C_7H_7	
C_6H_6	C_7H_5	C_8H_5	C_9H_5

(b) Products classified by stoichiometry.

C_xH (x = 3–7)	C_xH_3 (x = 3–6)	C_xH_5 (x = 4–9)	C_xH_7 (x = 6–7)
C_3H	C_3H_3		
C_4H	C_4H_3	C_4H_5	
C_5H	C_5H_3	C_5H_5	
C_6H	C_6H_3	C_6H_5	C_6H_7
C_7H		C_7H_5	C_7H_7
		C_8H_5	
		C_9H_5	

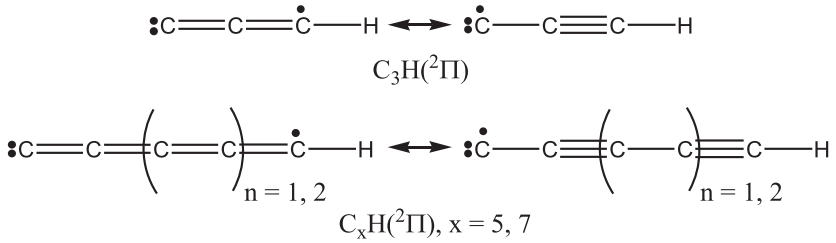

$C_3H(^2\Pi)$

$C_xH(^2\Pi)$, x = 5, 7

On the other hand, the cyclic structures represent σ radicals with the unpaired electron delocalized on the C_3 ring:

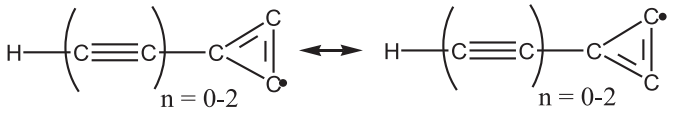

The cyclic structure is 11–12 kJ mol^{-1} more favourable than the linear one for C_3H but 11–21 kJ mol^{-1} less favourable for C_5H and C_7H.

The radicals can be produced in the reactions of $C(^3P)$ and $C_3(X^1\Sigma_g^+)$ with acetylene, diacetylene, and triacetylene,

$C + C_2H_2 \rightarrow C_3H_2 \rightarrow C_3H + H$

$C + C_4H_2 \rightarrow C_5H_2 \rightarrow C_5H + H$

$C + C_6H_2 \rightarrow C_7H_2 \rightarrow C_7H + H$

$C_3 + C_2H_2 \rightarrow C_5H_2 \rightarrow C_5H + H$

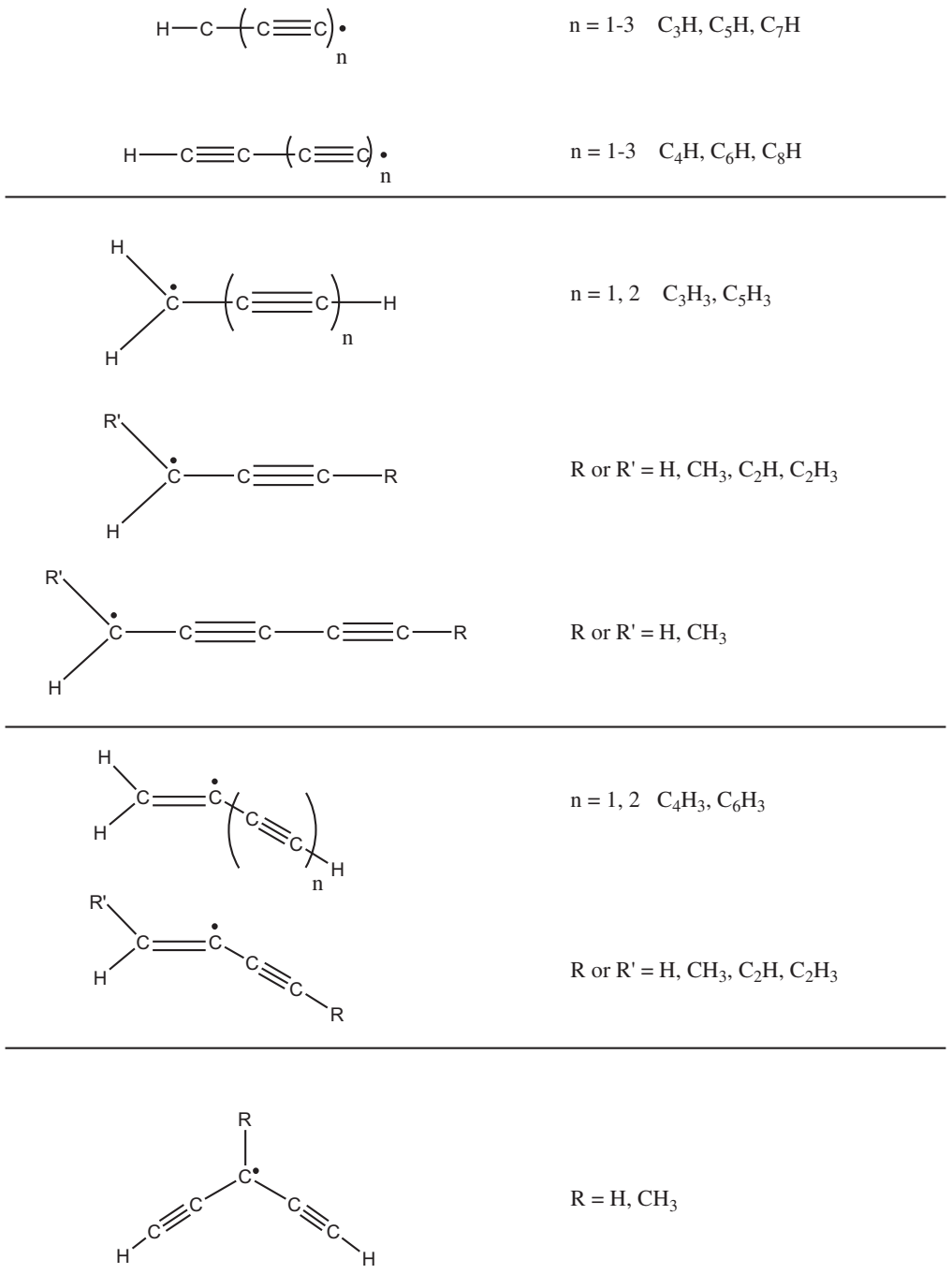

Figure 2. Types of RSFRs produced in the reactions of $C/C_2/C_3$ with unsaturated hydrocarbons.

$$C_3 + C_4H_2 \rightarrow C_7H_2 \rightarrow C_7H + H$$

The reaction of $C(^3P)$ with acetylene has been studied in great detail in CMB experiments in Kaiser's [70–77], Casavecchia's and Costes' groups [44–49, 78] in a broad range of collision energies, from 0.44 to 50 kJ mol^{-1}. The reaction was found to form both cyclic (c-C_3H) and linear (l-C_3H) isomers. In the first CMB experiments of carbon atoms with acetylene Kaiser *et al.* inferred, on the basis of the centre-of-mass angular distributions, the formation of c-C_3H and l-C_3H [69, 70]. At lower collision energies, the cyclic isomer was suggested to be produced through a short-lived triplet

cyclopropenylidene intermediate in a direct fashion, whereas the linear C_3H structure was synthesised via a long-lived 'symmetric' propargylene intermediate. With an increase of the collision energy, the centre-of-mass angular distributions became less forward scattering culminating in an isotropic distribution at the highest collision energy of 45.0 kJ mol^{-1}, which was attributed to the production of *l*-C_3H. Casavecchia and co-workers [44–47] also found the most stable *c*-C_3H isomer to be the dominant product at low collision energies, whereas at higher collision energies, the cross section for the *l*-C_3H formation increased and, at the highest E_c of 50.2 kJ mol^{-1} in their experiments, the cyclic and linear C_3H were produced approximately in equal amount. The special feature of the $C + C_2H_2$ reaction is that, besides $C_3H + H$, the $C_3(X^1\Sigma_g^+) + H_2$ products can be also formed. Molecular hydrogen elimination from C_3H_2 occurs on the singlet PES after intersystem crossing (ISC) from the triplet PES accessed when $C(^3P)$ initially reacts with acetylene. The efficiency of the singlet-triplet ISC decreases with the collision energy; the molecular hydrogen elimination pathway is favourable at low collision energies but becomes less important as E_c increases, with the branching ratios for the $C_3 + H_2$ measured in Kaiser's group experiments decreasing from $73 \pm 7\%$ at $E_c = 8$ kJ mol^{-1} via $42 \pm 5\%$ at 20 kJ mol^{-1} to $29 \pm 3\%$ at 31 kJ mol^{-1} [71]. This trend was corroborated by Casavecchia and co-workers who measured the relative yield of $C_3 + H_2$ to be about $50 \pm 10\%$ at 3.6 kJ mol^{-1} [46, 47], in line with the kinetic measurements by Bergeat and Loison carried out at room temperature [79]. The $C_3 + H_2$ branching ratio decreased with increasing collision energy to $36 \pm 7\%$ at 18.6 kJ mol^{-1}, $29 \pm 7\%$ at 29.3 kJ mol^{-1}, and to $13 \pm 4\%$ at 49.1 kJ mol^{-1} [46, 47]. The branching ratios obtained by Kaiser's and Casavecchia's groups agree well at the collisions energies of 19–20 kJ mol^{-1} and above but show significant disagreement at low E_c. Costes *et al.* [49] measured the branching ratios at very low collision energies from 0.44 to 4.8 kJ mol^{-1} relevant to low-temperature environments and found a strong domination of the non-adiabatic $C_3 + H_2$ channel (87–82%) and relatively small yields of *c*-C_3H (< 18%) and *l*-C_3H (<1%). The high yield of the $C_3 + H_2$ channel supports the results of the Kaiser's group [71] since extrapolation of their curve based on data at $E_c > 8$ kJ mol^{-1} gives the $C_3 + H_2$ branching ratio around 90% at lower collision energies.

The $C + C_2H_2$ reaction has been also a subject of numerous theoretical studies. Ochsenfeld *et al.* [80] calculated the molecular structure and energetics of stationary points on the triplet C_3H_2 PES and our group has studied singlet C_3H_2 isomers and transition states. Guadagnini *et al.* [81] used variational RRKM theory to compute the thermal rate constant for the $C(^3P) + C_2H_2$ reaction at 300 K. Buonomo and Clary [82] reported reduced-dimensionality quantum wave packet calculations in two degrees of freedom based on a two-dimensional PES constructed from CCSD(T)/cc-pVDZ calculations and deduced *l*-C_3H to be the dominant product at collision energies in the range of 5–70 kJ mol^{-1}. Later three- and two-degree-of-freedom quantum calculations by Takayanagi [83, 84] based on a B3LYP PES resulted in an opposite conclusion that *c*-C_3H is highly favoured. Park *et al.* [85] constructed full-dimensional triplet and singlet PESs related to the $C(^3P) + C_2H_2$ and used them in quasiclassical trajectory calculations of the reaction dynamics. On the triplet PES, *l*-C_3H was predicted to dominate at $E_c = 5$–40 kJ mol^{-1}, whereas on the singlet surface, both C_3H isomers as well as C_3 were computed to be formed in similar amounts. The only theoretical work thus far which took into account both triplet and singlet surfaces and the ISC between them was reported by us [86]. We combined CCSD(T)/CBS calculations of intermediates and transition states on the singlet and triplet C_3H_2 PESs with RRKM computations of

energy-dependent rate constants for isomerisation and dissociation steps within the same multiplicity and radiationless transition and non-adiabatic transition state theories for singlet-triplet ISC rates in order to predict product branching ratios. The results showed qualitative agreement with the observed experimental trends, as c-C_3H + H and $C_3 + H_2$ were predicted to be the most probable products at low collision energies, whereas l-C_3H + H to become the major product at higher E_c above 25 kJ mol^{-1}. Meanwhile, the relative yield of the non-adiabatic $C_3 + H_2$ products was significantly underestimated, especially at low collision energies, as compared to Kaiser's [71] and Costes' [49] results, indicating that the probability of ISC was undervalued in our calculations. This points at the necessity of further dynamics calculations on accurate triplet/singlet *ab initio* PESs including more accurate treatment of the non-adiabatic effects.

Another important question for the C(^{3}P) + C_2H_2 reaction concerns the energetics of the products channels. While the spin-forbidden $C_3 + H_2$ channel is highly exothermic, by −106 ± 16 kJ mol^{-1} according to various experimental measurements and theoretical calculations, the c-C_3H/l-C_3H + H channels are either slightly exothermic or thermoneutral. Ochsenfeld *et al.*'s [79] and our [85] calculations respectively gave the reaction exothermicities as 8.6 and 14.1 kJ mol^{-1} for c-C_3H vs. 1.5 and 3.1 kJ mol^{-1} for l-C_3H. Considering that the calculated relative energies may be accurate within ~5 kJ mol^{-1} in our calculations, it was still uncertain whether the l-C_3H + H channel is exothermic, or slightly endothermic, or thermoneutral. Costes *et al.* [49] went further and recomputed the reaction energetics more accurately, using CCSD(T)/cc-pV5Z optimised geometries and a more sophisticated extrapolation to the CBS limit from Hartree–Fock and correlation energies, which takes into account the slower convergence of the correlation energy. The reaction energies for the c-C_3H + H and l-C_3H + H channels were found to be −11.7 and +0.7 kJ mol^{-1}, which closely agreed with the experimental values of −12 and 0 kJ mol^{-1}, deduced from accurate fits of translational energy distributions at low E_c. Thus, the l-C_3H + H channel is concluded to be thermoneutral and, although it is still possible at very low temperatures characteristic for the ISM, its yield was found to be almost negligible under those conditions [49] Summarising, the C(^{3}P) + C_2H_2 reaction does produce resonance stabilised c-C_3H and l-C_3H radicals but they, especially the linear isomer, become the major products only at higher collision energies.

Experimental and theoretical studies [87–89] demonstrated that the next member in the series of C_xH species with odd x, the 2,4-pentadiynylidyne HCCCCC (l-C_5H, $X^2\Pi$) radical, can be produced under single-collision conditions in the reaction of C(^{3}P) with diacetylene. These studies showed that the reaction dynamics is indirect, as it proceeds via addition of the electrophilic carbon atom to the electron density of the diacetylene molecule yielding ultimately the carbene-like HCCCCCH structure in the triplet $X^3\Sigma_g^-$ state, which then emits a hydrogen atom resulting in the linear C_5H product exothermic by 40 kJ mol^{-1}. The yield of the cyclic c-C_5H isomers which is 10–15 kJ mol^{-1} less stable than l-C_5H appeared to be negligible according to RRKM calculations, and no evidence of the cyclic isomer was found in experiment. Thus, it was concluded that the C(^{3}P) + C_4H_2 exclusively forms l-C_5H. This allowed the authors to predict that reaction of carbon atoms with polyynes of the generic formula H(C≡C)$_n$H leads to the formation of hydrogen-terminated carbon radicals of the generic form HC_{2n+1}. Following this prediction it is expected, for example, that the reaction of C(^{3}P) with triacetylene C_6H_2 should produce the linear l-C_7H ($X^2\Pi$) radical, 1,3,5-heptatriynylidyne. The

prediction was later corroborated by theoretical *ab initio*/RRKM calculations, which gave *l*-C_7H as the sole product of the $C(^3P) + C_6H_2$ reaction [90].

The alternative routes to the C_xH (x = 5, 7) radicals involve the reaction of tricarbon C_3 with acetylene and diacetylene. The reaction of the ground-state $C_3(X^1\Sigma_g^+)$ with C_2H_2 was studied both experimentally [91] and theoretically [92]. The calculations indicated that different modes of addition of C_3 to acetylene require high barriers of 32–58 kJ mol^{-1} to be overcome. Moreover, the *l*-C_5H + H products were computed to be endothermic by 102 kJ mol^{-1}. The reaction products most favourable thermodynamically are *l*-$C_5(X^1\Sigma_g^+)$ + H_2, which are still endothermic but only by 17 kJ mol^{-1}. Reactive scattering of tricarbon with acetylene in CMB could be observed only at high collision energies, above the threshold value of 80–90 kJ mol^{-1}. The molecular hydrogen elimination pathway leading to C_5 was found to be closed and it was concluded that *l*-C_5H is the dominant reaction product. This conclusion is in agreement with the results of *ab initio*/RRKM calculations of product branching ratios in the collision energy range of 105–146 kJ mol^{-1} indicating that *c*-C_5H + H and *l*-C_5 + H_2 are only minor products with branching ratios below 2.5and 0.7%, respectively. A similar reaction of $C_3(X^1\Sigma_g^+)$ with diacetylene was proposed to form *l*-C_7H ($X^2\Pi$) via an analogous mechanism [93], but this was not verified experimentally thus far. In any case, due their entrance barriers and endothermicity of the products, the ground state reactions of tricarbon with (poly)acetylenes can contribute to the production of C_xH radicals only in high-temperature environments, such as in the outflows of carbon stars or in combustion flames.

Recently, Huang *et al.* [39] investigated the reaction of the electronically excited tricarbon $C_3(a^3\Pi_u)$ with acetylene in CMB with the use of photoionisation spectroscopy for characterisation of the reactants and products. Since the triplet state of C_3 is 204 kJ mol^{-1} higher in energy than the ground singlet states, the authors were able observe a reactive signal at a much lower collision energy of 46 kJ mol^{-1}. The only product detected was *l*-C_5H ($X^2\Pi$) and it appeared to be exothermic by 96 ± 16 kJ mol^{-1} (80 kJ mol^{-1} according to theory [93]). Theoretical calculations showed that $C_3(a^3\Pi_u)$ adds to acetylene without an entrance barrier producing a triplet C_5H_2 complex, which eventually emits a hydrogen atom. Due to the absence of the barrier and overall exothermic character, the $C_3(a^3\Pi_u) + C_2H_2$ reaction may represent an important route to *l*-C_5H even at low temperatures in the environments where the electronically excited tricarbon is available, for instance, in a C_2H_2 rich environment like discharge or combustion of acetylene where triplet tricarbon can be synthesised, e.g. via the radiative association $C(^3P) + C_2(^1\Sigma_g^+) \rightarrow C_3(a^3\Pi_u) + h\nu$.

3.2. C_xH (x = 4, 6, 8)

C_xH radicals with an even number of carbon atoms have only one low-lying linear isomer, which possesses two relatively low-energy electronic states, $^2\Sigma^+$ and $^2\Pi$. Whereas for the smallest radical in the series, ethynyl C_2H, the $^2\Sigma^+$ state lies 43 kJ mol^{-1} lower in energy than $^2\Pi$ [94], for C_4H, C_6H, and C_8H, the ground state is $^2\Pi$, and the $^2\Sigma^+$ states reside 3 [95], 7–25, and 23 [96] kJ mol^{-1} higher in energy, respectively. Also, the lowest cyclic isomers, four-member ring C_4H, six-member ring C_6H, and six-member ring C_8H, were computed to lie 95 [67], 41 [95], and about 135 [67] kJ mol^{-1} higher in energy than the linear forms. Hence, we focus here on the formation of the linear isomers. The electronic configuration of the $^2\Pi$ and $^2\Sigma^+$ states can be described in terms of the following resonance structures:

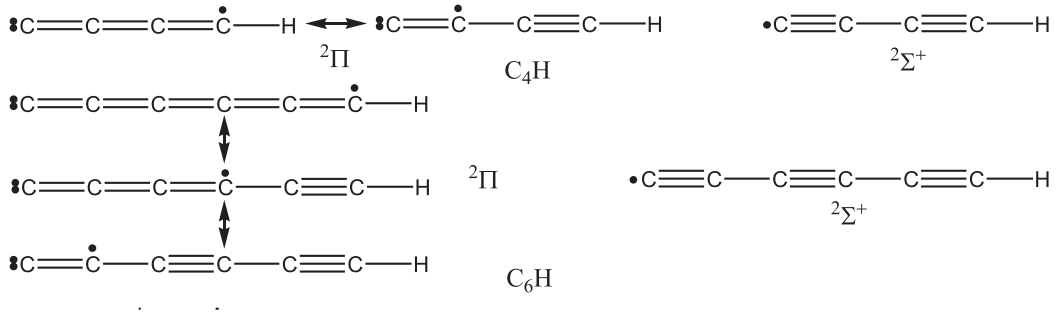

The stability of the $^2\Pi$ state relative to $^2\Sigma^+$ increases with the number of resonance structures the $^2\Pi$ state can be represented with.

The *l*-C_4H radical, 1,3-butadiynyl, can be produced in the reactions of dicarbon, $C_2(^1\Sigma_g^+/^3\Pi_u)$, with acetylene, which has been carefully studied by several groups both experimentally and theoretically [46, 92, 97–106]. Although kinetic studies have shown that the reactions of both singlet and triplet dicarbon with C_2H_2 are fast, close to the collision kinetics limit even at very low temperatures down to 24 K [103, 104], the reaction products were first identified in our CMB experiment [100]. The measurements at the collision energy of 24 kJ mol^{-1} combined with theoretical calculations showed that only one channel is open for both reactions – the channel leading to the formation of the 1,3-butadiynyl radical plus atomic hydrogen. The *l*-C_4H + H products were computed to be exothermic by 33 and 40 kJ mol^{-1} for the singlet and triplet reactions, respectively; the experimental reaction exothermicity was determined to be 39.9 ± 5.0 kJ mol^{-1} [101]. On the singlet surface, the reaction has no entrance barrier, is indirect, and proceeds by the addition of $C_2(X^1\Sigma_g^+)$ to the C≡C triple bond of C_2H_2 to a C_4H_2 complex, which eventually isomerizes to the $D_{\infty h}$-symmetric diacetylene molecule and then loses a hydrogen atom to form 1,3-butadiynyl without an exit barrier. The fragmentation of the symmetric C_4H_2 precursor results in a forward-backward symmetric product angular distribution. On the triplet surface, the reaction begins with addition of $C_2(^3\Pi_u)$ to a terminal carbon atom in acetylene and then proceeds by an H loss from the short lived adduct leading to *l*-C_4H over an exit barrier of ~26 kJ mol^{-1}; the short lifetime of the triplet complex is reflected in the forward-scattered angular distribution of the products. The difference in the lifetimes of the singlet and triplet C_4H_2 intermediates was attributed to their well depths with respect to the reactants, 577 and 180 kJ mol^{-1}, respectively. The reactions of $C_2(^1\Sigma_g^+/^3\Pi_u)$ with C_2H_2 were later re-investigated in CMBs at six different collision energies between 10.6 and 47.5 kJ mol^{-1} and these studies were extended by similar experiments involving three acetylene isotopomers, C_2D_2, C_2HD, and $^{13}C_2H_2$ to elucidate the role of ISC and of the symmetry of the reaction intermediate(s) on the centre-of-mass functions [101]. The singlet reaction was confirmed to proceed through an indirect mechanism involving a diacetylene intermediate, which fragmented to *l*-C_4H + H via a loose exit transition state. The $D_{\infty h}$ symmetry of the decomposing diacetylene intermediate led to collision-energy invariant, isotropic (flat) centre-of-mass angular distributions of this microchannel. Isotopic substitution experiments suggested that at least at the collision energy of 29 kJ mol^{-1}, the diacetylene isotopomers are long-lived with respect to their rotational periods. In the meantime, the centre-of-mass angular distributions varied from a forward scattered distribution at the lowest collision energy to a backward scattered distribution with at the highest collision energy. The observed asymmetry of angular distributions was

attributed to the involvement of the triplet surface where the C_4H_2 intermediates are short-lived, in particular to the impact-parameter dictated reaction dynamics of barrierless entrance channels on the triplet surface and also to a possible increase of the fraction of the $^3\Pi_u$ state in the dicarbon beam. No evidence was found that at the investigated collision energies ISC is effective and provides any contribution to the reaction dynamics. Casavecchia and co-workers reported CMBs experiments on $C_2(^1\Sigma_g^+/^3\Pi_u)$ + C_2H_2 at two collision energies of 13.6 and 37.4 kJ mol^{-1} using a continuous dicarbon beam and soft electron impact ionisation for the product detection [46, 105]. While their results agreed with ours in terms of the reaction products, 1,3-butadiynyl + H, they found different angular distributions, isotropic at the low E_{col} and forward-scattered at the high $E_{col.}$ Casavecchia *et al.* argued that, according their LIF characterisation of the C_2 beam, the relative concentrations of the $^1\Sigma_g^+$ and $^3\Pi_u$ states in the beam were approximately the same at the two collision energies. Based on this, they proposed an alternative explanation of the observed behaviour: formation of a long-lived complex which starts osculating when the energy available to the complex itself shortens its lifetime at the high collision energy (i.e. the lifetime of the collision complex decreases with increasing E_{col} to reach a value comparable to the rotational period), thus resulting in the forward-scattered angular distribution. If the concentration of triplet dicarbon in the beam is comparable to that of singlet dicarbon, both should similarly contribute to the recorded signal and the observed forward scattering could be primarily due to the triplet reaction, for which the lifetime of the complex is expected to be significantly shorter than that at the lower E_{col} because the wells of the triplet intermediates are much more shallow than that of the very stable singlet diacetylene. The observed differences in the details of the reaction mechanism can be resolved in the future by further experiments and quantum dynamical calculations. Nevertheless, despite these differences, 1,3-butadiynyl is firmly confirmed as the exclusive product of the C_2 + C_2H_2 reactions.

The *l*-C_6H radical, 1,3,5-hexatriynyl, was found to be formed in the reactions of singlet and triplet dicarbon with diacetylene [107]. In particular, our CMBs experiments at two collision energies of 12.1 and 32.8 kJ mol^{-1} indicated that *l*-C_6H + H are the only products of both $C_2(^1\Sigma_g^+/^3\Pi_u)$ + C_4H_2 reactions. Based on the observed forward-backward symmetric angular distributions, the reaction dynamics were concluded to be indirect, to involve singlet and triplet C_6H_2 intermediates, and to be dictated by an initial addition of C_2 to the C≡C triple bond of diacetylene. On the singlet surface, the linear triacetylene molecule, $C_6H_2(X^1\Sigma_g^+)$, resulting from isomerisation of the initial adduct, decomposed to 1,3,5-hexatriynyl without an exit barrier. On the triplet surface, the dynamics suggested at least a tight exit transition state, located 24.4 kJ mol^{-1} above the separated products according to theory and involved in the fragmentation of a triplet C_6H_2 intermediate to yield *l*-$C_6H(X^2\Pi)$ + H. The experimental results and the derived reaction mechanisms were fully corroborated by *ab initio* of the singlet and triplet C_6H_2 PESs. The computed exothermicities for the singlet and triplet reactions were 44 and 55 kJ mol^{-1}, respectively, in agreement with the experimentally observed margins of 51 ± 20 kJ mol^{-1}. The indirect dynamics and forward-backward symmetric angular distributions observed for $C_2(^1\Sigma_g^+/^3\Pi_u)$ + C_4H_2 are in contrast to the asymmetry of the angular distributions for C_2 + C_2H_2 attributed to the triplet reaction. The difference may be explained by a deeper well associated with the decomposing triplet C_6H_2 intermediate, 209 kJ mol^{-1}, resulting in a longer lifetime for this species.

The reaction of $C_2(^1\Sigma_g^+/^3\Pi_u)$ with triacetylene, C_6H_2, producing *l*-$C_8H(X^2\Pi)$ + H was recently investigated for the first time by Lee's group [40]. The authors recorded

the translational energy and angular distributions and the photoionisation spectrum of the C_8H product in a CMB apparatus using synchrotron VUV ionisation. The produced C_8H was identified as octatetranyl based on the maximal translational-energy release corresponding to the reaction exothermicity of 25.5 ± 8.4 kJ mol^{-1} consistent with the computed theoretical values of 18.4 and 34.3 kJ mol^{-1} for the singlet and triplet reactions, respectively, and the ionisation threshold 8.9 ± 0.2 eV, also in agreement with the calculated value for the adiabatic ionisation potential of 8.87 eV for *l*-$C_8H(X^2\Pi)$. Kinematic constraints accounted for the nearly isotropic angular distribution. The quantum-chemical calculations showed that both exothermic reactions $C_2(^1\Sigma_g^+/^3\Pi_u) + C_6H_2 \rightarrow$ *l*-$C_8H(X^2\Pi)$ can proceed without entrance and exit barriers if the dicarbon unit first adds to a triple C≡C bond in triacetylene, inserts into this bond, and then a C_8H_2 tetracetylene singlet or triplet complex emits a hydrogen atom. However, the observed non-zero peaking of the translational energy distribution at ~15 kJ mol^{-1} is rather indicative of a contribution of the triplet reaction channel in which the initial addition of $C_2(^3\Pi_u)$ to the terminal carbon atom of triacetylene is immediately followed by H loss from the attacked carbon atom occurring via an exit barrier of 17 kJ mol^{-1}.

3.3. C_xH_3 (x = 3, 5)

Resonance stabilised propargyl, C_3H_3, and 2,4-pentadiynyl-1, *i*-C_5H_3, radicals are described by the general formula $H_2C–(C\equiv C)_n–H$ (*n* = 1–2, Figure 1) and can be represented by the following resonance structures in their ground $^2B_1$ electronic state:

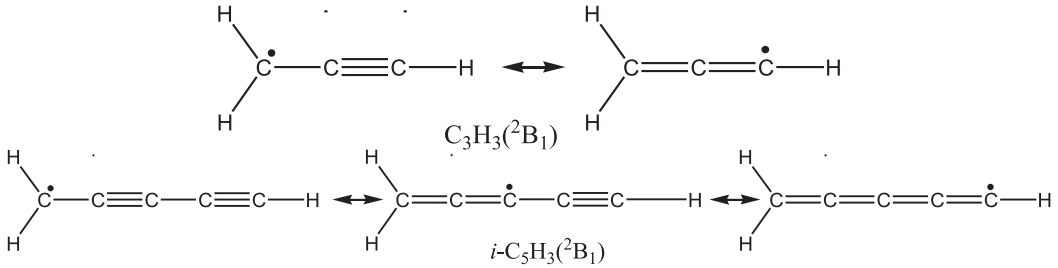

For the C_3H_3 radical, the propargyl isomer is by far more stable than any other structure; the next isomer in the order of stability, *c*-C_3H_3, lies 131 kJ mol^{-1} above propargyl [108]. Alternatively, for C_5H_3 another low-lying isomer exists, 1,4-pentadiynyl-3, $HCCCHCCH(^2B_1)$ or *n*-C_5H_3, which resides only 4–6 kJ mol^{-1} higher in energy than *i*-C_5H_3 [26, 109] and can be described in terms of the following resonance structures:

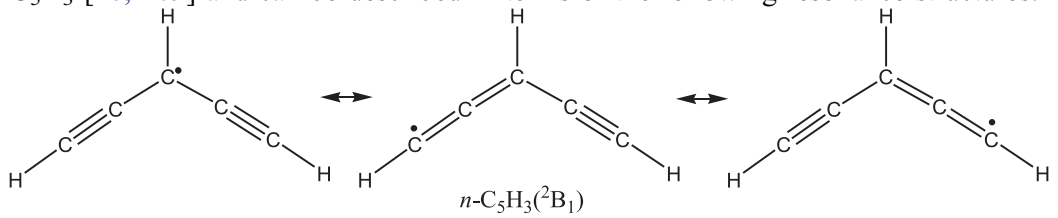

3.3.1. *Propargyl radical, C_3H_3*

The simplest reaction to produce propargyl is $C(^3P) + C_2H_4$. The reaction was found to be very fast, with rate constants in the range of 10^{-10} cm^3 mol^{-1} s^{-1}, both at room temperature [78] and at low temperatures down to 15 K [110]. Bergeat and Loison [78] have also estimated the absolute product branching ratio of H atoms to be 0.92 ± 0.04,

implying that the dominant heavy-atom reaction product should be C_3H_3. However, the first compelling characterisation of the products of the $C(^3P) + C_2H_4$ reaction came from CMB experiments, which were carried out at two collision energies of 17.1 and 38.3 kJ mol^{-1} [111]. A fit of the recorded product angular distributions and TOF spectra gave a maximum energy release and angular distributions consistent with the formation of the propargyl radical in its ground electronic state. Based on the experimental data, two microchannels were identified; in the first one the initially formed triplet cyclopropylidene complex rotates in a plane roughly perpendicular to the total angular momentum vector around its *C*-axis, undergoes ring opening to triplet allene, and decomposes via H emission through a tight transition state to the propargyl radical. Here, the initial and final orbital angular momenta L and L' are weakly coupled resulting in an isotropic centre-of-mass angular distribution. A second microchannel arises from *A*-like rotations of the cyclopropylidene complex, followed by ring opening and H-atom elimination. In this case, a strong L–L' correlation leads to a forward-scattered centre-of-mass angular distribution. The details of the reaction mechanism were later confirmed by our *ab initio*/RRKM calculations [112], which showed that at the initial step carbon atom attacks the π-orbital ethylene producing triplet cyclopropylidene without entrance barrier and then the initial adduct isomerizes to the triplet allene via ring opening. The latter either splits an H atom producing the propargyl radical with the overall reaction exothermicity of 190 kJ mol^{-1} or undergoes a 1,2-H shift to vinylmethylene, which in turn gives propargyl. The propargyl radical was concluded to be a nearly exclusive reaction product. RRKM calculations at the collision energy of 38.3 kJ mol^{-1} showed that about 93% of propargyl comes from fragmentation of triplet allene and 7% from vinylmethylene. The only alternative products predicted by the calculations were $CH_2(^3B_1) + C_2H_2$ (only 2%, via the vinylmethylene).

The $C(^3P) + C_2H_4$ reaction was later revisited by several experimental groups. Costes and Casavecchia's groups [48] used complementary CMB techniques with pulsed supersonic beams coupled with laser-induced fluorescence detection of hydrogen atoms and measured integral and differential cross sections in a broad range of collision energies of 0.49–24.9 kJ mol^{-1}. They confirmed the barrierless character of the carbon atom addition to ethylene and the formation of propargyl as the major reaction pathway, dominant at low collision energies. In the meantime, the authors have also proposed a minor hydrogen atom elimination pathway, which was attributed to the formation of either 1-propynyl, H_3CCC, or *c*-C_3H_3 isomers. According the measured differential reaction cross sections, the minor channel contributed 2, 5, and 14% to the total C_3H_3 yield at E_{col} = 9.1, 17.2, and 30.8 kJ mol^{-1}, respectively. While the formation of propargyl was suggested to proceed via an osculating complex mechanism following addition of the carbon atom to the double bond of ethylene, the dynamics of formation of the less stable isomers is going through a long-lived complex, as supported by an isotropic angular distributions. The authors also argued against the description of the reaction dynamics in terms of two microchannels proposed by Kaiser *et al.* [110]; in their view, the observed translational energy distributions and angular distributions as well as integral and differential reaction cross sections can be interpreted in terms of an additional C_3H_3 product channel, i.e. a formation of a higher-energy isomer, rather than different microchannels leading to the same propargyl product. However, later studies have not confirmed the formation of other C_3H_3 isomers, at least at the collision energy as low as 14.6 kJ mol^{-1}. Lee and co-workers [41] investigated the $C(^3P) + C_2H_4$ reaction in a CMB apparatus using synchrotron radiation as an ionisation source; the C_3H_3 products were identified based on photoionisation

cross sections measured between 9.5 and 11.6 eV. The only C_3H_3 species identified based on the ionisation energy of 8.6 ± 0.2 eV together with the maximal kinetic-energy release of 205 kJ mol^{-1} was propargyl in agreement with Kaiser *et al.* [110]. The authors argued that their work had better temporal resolution and signal-to-noise ratios, as well as less interference from reactions of $C(^1D)$ atoms and C_2 with ethylene than the previous studies. Another, very low-collision energy study (0.7 to 5.5 kJ mol^{-1}) of the $C(^3P) + C_2H_4$ reaction using Doppler–Fizeau spectroscopy by Costes and co-workers [113] also showed no evidence for the formation of C_3H_3 isomers other than propargyl. The authors determined the reaction energy for the formation of the propargyl radical to be -190 kJ mol^{-1}, very close to the value predicted by the earlier theoretical calculations [111]. Summarising, it can be concluded that although higher-energy C_3H_3 isomers may not be ruled out completely as minor products of the $C(^3P) + C_2H_4$ reaction at high collision energies (very high temperatures), the propargyl radical is the dominant or nearly exclusive reaction product. Note that the reaction of electronically excited carbon atoms $C(^1D)$ with ethylene also form the propargyl radical via stripping dynamics [114].

In addition to the $C + C_2H_4$ reaction where the propargyl radical is formed via the C-for-H exchange mechanism, this radical can be also produced in reactions of C or C_2 with larger unsaturated hydrocarbons. For instance, Lee *et al.* [42, 43] detected the $C_3H_3 + CH_3$ channel in the reaction of $C(^3P)$ with propene, C_3H_6, studied in CMB at $E_{col} = 15.9$ kJ mol^{-1}, with the maximal translational energy release and photoionisation spectra of C_3H_3 being consistent with the production of the propargyl radical (exothermic by 228 kJ mol^{-1}). The CH_3-loss channel had a nearly forward and backward peaked angular distribution enhanced in the forward direction. The branching ratio for the propargyl + CH_3 channel in the $C(^3P) + C_3H_6$ reaction at $E_{col} = 16.7$ kJ mol^{-1} was evaluated to be 78% from *ab initio*/RRKM calculations and 75% from experiment; the theoretical results were not sensitive to the collision energy in the 0–16.7 kJ mol^{-1} range. Theoretically, we have also predicted the formation of propargyl in the reaction of singlet dicarbon with 1,3-butadiene via the $C_2(^1\Sigma_g^+) + H_2CCHCHCH_2 \rightarrow C_3H_3 + C_3H_3$ channel, the branching ratio for which was evaluated as 31–35% in the collision energy range of 0–34 kJ mol^{-1} [115]. The reactions of singlet C_2 with C_5H_8 isomers isoprene [116] and 1,3-pentadiene [117] were also predicted to form minor amounts of propargyl, together with its methyl-substituted counterparts, C_4H_5. However, due to a signal interference from dissociative ionisation of primary reaction products, it was not possible to positively identify C_3H_3 as a product of dicarbon reactions with 1,3-butadiene and C_5H_8 isomers in CMB experiments.

3.3.2. *C_5H_3 radicals*

The *i*- and *n*-C_5H_3 radicals are produced in the reaction of atomic carbon with vinylacetylene, C_4H_4 [108]. We investigated the reaction dynamics of $C(^3P_J) + C_4H_4$ by combining CMB experiments at collision energies of 18.8 and 26.4 kJ mol^{-1} with *ab initio*/RRKM calculations of PES and product branching ratios. We found the reaction to be governed by indirect scattering dynamics and to proceed without an entrance barrier through a long-lived collision complex, triplet C_5H_4, which eventually decomposes to yield the *i*- and *n*-C_5H_3 products via tight exit transition states, with theoretical branching ratio of the two isomers being 3:2. The reaction pathway depends on the direction of the initial carbon atom attack toward the π electron density of vinylacetylene, to the double or triple carbon-carbon bond. The triple bond addition almost

exclusively produces *i*-C_5H_3, whereas the double bond addition favours *n*-C_5H_3 vs. *i*-C_5H_3 with a 5:1 ratio of the yields. The calculations predict no other product channels to be feasible, except for trace amounts of HCCCH(^{3}B) + C_2H_2, in excellent with the experiment, where no products other than C_5H_3 were observable. The calculated branching ratios appeared to be insensitive to the collision energy in the range of 0–26.4 kJ mol^{-1}. The computed reaction exothermicities leading to *n*-C_5H_3 and *i*-C_5H_3 were 206 and 212 kJ mol^{-1}, respectively, which is somewhat higher than the value derived from the maximal translational energy release in experiment, 170 ± 36 kJ mol^{-1}. The difference was attributed to the low fraction of energy of only 25–27% channelling into the translational degrees of freedom of the C_5H_3 products. While it was not possible to distinguish between the C_5H_3 isomers because of their closeness in energy, some experimental indication of which isomer is preferred arose from the centre-of-mass angular distribution. According to the calculated transition state structures leading to *i*-C_5H_3, the preferential direction of H loss is perpendicular to the principal rotation axis of the molecule, which should result in a preference of sideways scattering. Alternatively, for *n*-C_5H_3 the angle between the departing hydrogen atom and the primary rotation axis has a value in the 30°–60° range leading a broader/isotropic centre-of-mass angular distribution. Hence, from the fact that the experimental centre-of-mass angular distribution was sideways scattered, we concluded *i*-C_5H_3 to be the predominant product and, since angular distribution could be also fit within the errors limit with an isotropic distribution, *n*-C_5H_3 isomer to be formed to with a lower relative yield. This observation correlates well with the computed product branching ratio.

The C_5H_3 radicals are also formed in the reactions of $C_2(^1\Sigma_g^+/^3\Pi_u)$ with C_3H_4 isomers allene and methylacetylene. The reactions of singlet dicarbon with methylacetylene, CH_3CCH (X^1A_1), was first investigated by *ab initio*/RRKM calculations [118] which showed that the $C_2(^1\Sigma_g^+)$ can add to methylacetylene without a barrier producing three-member or four-member ring singlet C_5H_4 intermediates, which quickly rearrange to the most stable $H_3CCCCCH$ isomer. $H_3CCCCCH$ then loses a hydrogen atom from the CH_3 producing *i*-C_5H_3. Alternatively, H atom migrations followed by H loss can lead to *n*-C_5H_3. RRKM computed product branching ratios gave *i*-C_5H_3 (64–66%) and *n*-C_5H_3 (34–30%) as the major reaction products, with other possible minor products, HCCCCCH + H_2, HCCCHCC + H_2, C_3H_3 + C_2H, and *c*-C_3H_2 + C_2H_2 contributing only 1–2% or less to the total products yield if the energy randomisation is complete. The relative product yields were found to be nearly independent on the collision energy in the E_{col} range of 0–50 kJ mol^{-1}. In the $C_2(^3\Pi_u)$ + CH_3CCH reaction on the triplet surface, barrierless addition of dicarbon to bridge the triple C≡C bond is followed by stepwise insertion of the C_2 unit in this bond via a rhombic and a three-member ring intermediate leading to triplet $H_3CCCCCH$, which then loses an H atom producing, via a tight exit transition state, *i*-C_5H_3 as the dominant reaction product. A small amount of *n*-C_5H_3 (up to 7%) can be formed via an alternative pathway involving H migrations. In CMB experiments, the chemical dynamics of the $C_2(^1\Sigma_g^+/^3\Pi_u)$ + CH_3CCH reactions was studied at four collision energies between 13.9 and 50.3 kJ mol^{-1} [102, 119]. The experimental reaction exothermicity to synthesise C_5H_3 isomer(s) plus atomic hydrogen was derived to be 181 ± 12 kJ mol^{-1} from the maximum energy release observed in the translational energy distribution. This value is in a reasonably close agreement with the computed reaction exothermicity to form *i*- and *n*-C_5H_3, 191–192 and 200–201 kJ mol^{-1}, on the singlet and triplet PESs, respectively. The translational energy distribution of the C_5H_3 isomer(s) peaked away from zero velocity; a relatively broad peak was observed between 15 and 40 kJ mol^{-1}.

This indicated that at least one reaction channel to form the C_5H_3 isomer(s) has a tight exit transition state hence proposed an involvement of the triplet PES because the triplet methyldiacetylene loses an H atom via a significant exit barrier, whereas singlet C_5H_4 isomers emit H without exit barriers. The angular distribution showed non-zero intensity over the entire 0°–180° range, which supports indirect scattering dynamics and the participation of at least one C_5H_4 complex in the entrance channel. In line with the RRKM-computed product branching ratios, the measured angular distribution showed that the formation of the *i*-C_5H_3 isomer is somewhat favoured, at least on the triplet surface, as compared to *n*-C_5H_3. In particular, sideways-peaking of the angular distribution between 85° and 120° was observed implying that that the light hydrogen atom was emitted favourably in a direction nearly perpendicular to the rotating plane of a decomposing C_5H_4 complex, like in the singlet and triplet $H_3CCCCCH$ intermediates, the precursors of *i*-C_5H_3. Alternatively, *n*-C_5H_3 can be produced from $H_2CCCHCCH$ intermediates, which emit an H atom either perpendicularly (singlet) or parallel (triplet) to the molecular plane. Further insight on the formation of the *i*- and *n*-C_5H_3 isomers was provided by the experimental study of the reaction of C_2 with isotope-labelled methylacetylene, CD_3CCH [120]. Only D atom elimination was observed and no H atom elimination, indicating that the leaving H(D) atom originates from the methyl group, which is consistent with the production of only *i*-C_5H_3 on the triplet surface and both *i*- and *n*-C_5H_3 on the singlet surface. The isotope-labelled study completely ruled the possibility of the formation of the higher energy D_3CCCCC isomer. The results of the $C_2(^1\Sigma_g^+/^3\Pi_u) + CD_3CCH$ CMB experiments confirmed the RRKM-computed product distribution in the reaction at least qualitatively.

The dynamics of singlet and triplet dicarbon reactions with another C_3H_4 isomer allene, $H_2CCCH_2(X^1A_1)$, was probed in a theoretical *ab initio*/RRKM study combined with CMB experiments at four collision energies in the 13.6–49.4 kJ mol^{-1} range [121]. The results showed that both the singlet and the triplet reactions exhibit no entrance barrier, are indirect, and proceed through C_5H_4 intermediates after addition of C_2 to the C=C double bond (singlet) and to the terminal or central carbon atoms (triplet) of allene. The initial adducts undergo direct (singlet) or stepwise (triplet) insertion of the C_2 unit into the C=C bond to form singlet or triplet pentatetraene $H_2CCCCCH_2$ intermediates, respectively, that emit an H atom to produce *i*-C_5H_3. This reaction mechanism is reflected in symmetric centre-of-mass angular distributions. However, at higher E_{col} the angular distributions show an increasing backward bias, which may be due to a decreasing lifetime of the decomposing intermediates becoming shorter than their rotation period. A second product channel was found on the triplet surface, in which a non-symmetric intermediate $HCCCH_2CCH$ is formed by 1,5-H migration in the initial complex where C_2 was attached to the terminal carbon atom of allene. The intermediate decomposes by H loss to *n*-C_5H_3 also contributing to the backward scattered centre-of-mass angular distributions observed at higher collision energies. According to RRKM computed relative yields, the reaction channels leading to *i*-C_5H_3 dominate. The formation of *n*-C_5H_3 from the $HCCCH_2CCH$ precursor contributes only 1–2% to the total product yield in the collision energy range of 0–50 kJ mol^{-1}, although its branching ratio does increase with E_{col}. Nevertheless, another evidence that a minor amount of *n*-C_5H_3 can be formed comes from the shape of the experimental translational energy distributions, which show a broad peak between 3 and 40 kJ mol^{-1} and thus suggest an existence of at least one fragmentation channel proceeding via a tight exit transition state. Since both singlet and triplet pentatetraenes lose hydrogen without exit barriers, the fragmentation of triplet $HCCCH_2CCH$ proceeding via an exit

barrier of 133 kJ mol^{-1} is a plausible candidate to account for the observed behaviour. The computed reaction exothermicities of both *i*- and *n*-C_5H_3, 194–195 and 202–203 kJ mol^{-1} on the singlet and triplet PESs, respectively, are in close agreement with the experimental value of −183 ± 15 kJ mol^{-1}.

The reaction of tricarbon, $C_3(^1\Sigma_g^+)$, with ethylene represents another route to produce C_5H_3 radicals. We have studied this reaction in crossed beams at E_{col} = 73 kJ mol^{-1} in conjunction with theoretical calculations of its PES [90]. We found that tricarbon reactant formally 'inserts' into the C=C double bond of ethylene leading to the singlet pentatetraene $H_2CCCCCH_2$ intermediate, which then loses one of its H atoms producing *i*-C_5H_3 as the exclusive product. The insertion is not feasible in a single step, instead C_3 either adds to C_2H_4 in a side-on manner to form a five-member ring C_5H_4 complex, which then ring-opens to pentatetraene, or the addition takes place end-on to form a three-member ring structure, which undergoes a two-step rearrangement to the five-member ring intermediate to merge the reaction pathways. The highest barriers computed for the two channels were 48 and 42 kJ mol^{-1}, respectively, in close agreement with the characteristic threshold energy of 40–50 kJ mol^{-1} measured in experiment. The reaction exothermicity to form *i*-C_5H_3, 56 kJ mol^{-1}, is within error bars of the experimental value of 47 ± 10 kJ mol^{-1} derived from the maximal translational energy release. However, the calculations indicated that the H loss from pentatetraene takes place without an exit barrier, in contradiction with peaking of the translational energy distribution away from zero, around 40 kJ mol^{-1}. This finding can be explained by the fact that the decomposing intermediate is very short-lived, at the borderline between direct and indirect dynamics, which is due to the large collision energy. The short lifetime of the intermediate is evidenced by the large fraction of the available energy, ~50%, channelling into the translational degrees of freedom. The very short lifetime apparently resulted in the observed off-zero peaking of the centre-of-mass translational energy distributions. Hence, the experimental and theoretical data on the $C_3(^1\Sigma_g^+) + C_2H_4$ reaction suggested the presence of a short-lived $H_2CCCCCH_2$ intermediate decomposing 'directly' to form *i*-C_5H_3.

Summarising the reactions forming C_5H_3 radicals overviewed in this section, we conclude that, although the *i*- and *n*-C_5H_3 isomers are nearly isoergic, due to peculiarities of the reaction mechanisms, *i*-C_5H_3 forms preferably in most cases. Significant amounts of *n*-C_5H_3 can be produced only in $C(^3P)$ + vinylacetylene and $C_2(^1\Sigma_g^+)$ + methylacetylene reactions. A small yield of *n*-C_5H_3 might expected in the $C_2(^3\Pi_u)$ + methylacetylene/allene reactions, at least according to theoretical calculations, albeit experimental evidence for this is rather tentative if any. Finally, the $C_2(^1\Sigma_g^+)$ + allene and $C_3(^1\Sigma_g^+)$ + ethylene reactions produce exclusively *i*-C_5H_3.

3.4. *Substituted propargyl radicals, R'HCCCR*

3.4.1. *Methylpropargyl and dimethylpropargyl radicals*

Hydrogen atom substitutions by a methyl group in the propargyl radical give rise to 1- and 3-methylpropargyl radicals. The methylpropargyl products were first identified in the reaction of $C(^3P)$ with propene, C_3H_6, investigated in CMBs at collision energies of 23.3 and 45.0 kJ mol^{-1}, based on the measured maximum energy release and angular distributions [122]. The authors proposed that the reaction proceeds on the lowest triplet surface via an initial addition of the carbon atom to the π-orbital to form a triplet methylcyclopropylidene adduct followed by ring opening to triplet 1,2-butadiene

(methylallene). Within 0.3–0.6 ps, triplet 1,2-butadiene emits a hydrogen atom to produce methylpropargyl radical isomers. The translational energy distribution indicated an existence of a tight exit transition state for the hydrogen atom loss. At lower collision energy, the angular distribution was found to be isotropic and symmetric suggesting that the decomposing C_4H_6 complex has a lifetime longer than its rotational period. Alternatively, a bias to forward scattering was found at higher collision energy, which pointed at a reduced lifetime of the C_4H_6 intermediate and suggested an osculating complex that decomposes before one full rotation elapses. Further, forward peaking at higher collision energy requires that the carbon atom and the leaving hydrogen atom must be located on opposite sites of the rotation axis of the decomposing complex. These hypotheses were corroborated by *ab initio*/RRKM calculations of the reaction PES [123]. The calculations showed that the addition of $C(^3P)$ to propene is barrierless and that both 1- and 3-methylpropargyl can be produced with exothermicities of 190 and 201 kJ mol^{-1}, respectively, via exit barriers in the range of 18–23 kJ mol^{-1}. In addition, the calculations predicted two other products, $H_2CCCHCH_2$ (resonance stabilised 1,3-butadienyl-2/1,2-butadienyl-3) + H and propargyl + CH_3 exothermic by 193 and 228 kJ mol^{-1}, respectively. The C + C_3H_6 reaction was later revisited by Lee's group [42, 114], who combined the CMB technique with the product detection using photoionisation spectroscopy employing a synchrotron light source. Among the observed C_4H_5 products, they identified not only 1- and 3-methylpropargyl, but also $H_2CCHCCH_2$, but could not distinguish between 1- and 3-methylpropargyl because both have very close ionisation energies, 7.89 and 7.87 eV, respectively. More accurate and detailed *ab initio*/RRKM calculations in their work [42] (built upon another theoretical study) [124] provided the reaction exothermicities to produce 1-methylpropargyl + H, 3-methylpropargyl + H, 1,3-butadienyl-2 + H, and propargyl + C_3H_3 as 187, 198, 188, and 228 kJ mol^{-1}, in close agreement with our earlier values. Theoretically, the branching ratios for these products were computed as 7:5:10:78, respectively, at the collision energy of 16.7 kJ mol^{-1}. The experimental yield ratio of $H_2CCCHCH_2$ to methylpropargyl isomers, about 1.4, obtained from the C_4H_5 photoionisation cross sections, was similar to the RRKM-predicted ratio of 1.2. Also, the calculated branching ratios closely correlated with the experimentally measured yield ratios of 17:8:75 for the C_4H_5, C_4H_4 and C_3H_3 species; here, C_4H_4 were proposed to be formed from vibrationally hot primary C_4H_5 products. Interestingly, the H-loss (C_4H_5) and 2H-loss (C_4H_4) channels were found to have nearly isotropic angular distributions, in contrast, to the CH_3-loss channel (C_3H_3), which exhibited a forward and backward peaked angular distribution with a forward bias [114]. Kinetics measurements for the $C(^3P)$ + C_3H_6 reaction at room temperature were reported by Loison and Bergeat [125] who reported the rate constant to be high, $2.6 \pm 0.4 \times 10^{-10}$ cm^3 mol^{-1} s^{-1}, which is consistent with the barrierless character of the atomic carbon addition. They have also determined the absolute branching ratio for the H atom production (C_4H_5 + H and C_4H_4 + 2H) to be 0.51 ± 0.08, a significantly higher value than that obtained by Lee's group, 0.33, considering that two hydrogen atoms were produced together with C_4H_4. The difference is likely due to the fact that Loison and Bergeat's experiments were carried out not under single-collision conditions but in a low-pressure fast-flow reactor, where secondary reactions and wall effects, although taken into account, have complicated the analysis of the results and may have affected the accuracy of determination of the H branching ratio.

Although the production of dimethylpropargyl radicals has not yet been observed experimentally in reactions of carbon atoms or dicarbon with unsaturated hydrocarbons,

a theoretical study indicated such a possibility. In particular, Li *et al.* [126] investigated the triplet PES for the reaction of $C(^3P)$ with trans-2-butene, C_4H_8. They found that the initial addition of the carbon atom to the C=C bond of 2-butene is barrierless and leads to a triplet three-membered cyclic isomer, which subsequently ring-opens process to a chain triplet $CH_3CHCCHCH_3$ isomer. The latter further decomposes to either 1,3-dimethylpropargyl by hydrogen atom loss or 1-methylpropargyl by CH_3 elimination, with the two paths predicted to be the most favourable reaction channels and to be exothermic by 208 and 237 kJ mol^{-1}, respectively. The kinetic study by Loison and Bergeat [124] gave the room temperature rate constant for the $C(^3P)$ + trans-2-butene reaction as $1.9 \pm 0.6 \times 10^{-10}$ cm^3 mol^{-1} s^{-1} and the absolute yield of hydrogen atoms as 0.33 ± 0.08; it is likely that atomic hydrogen is formed together with 1,3-dimethylpropargyl.

3.4.2. *Vinylpropargyl and divinylpropargyl radicals*

Vinyl substituted propargyl radicals can be formed in the reactions of carbon atoms with C_4H_6 isomers. For instance, the $C(^3P)$ + 1,3-butadiene ($H_2CCHCHCH_2$) reaction was probed by CMB experiments at three collision energies between 19.3 and 38.8 kJmol^{-1} in combination with *ab initio*/RRKM calculations of the PES and product branching ratios [127,128]. The results showed that, similar to smaller alkenes, the carbon atom adds barrierlessly to one of the π-orbitals of the 1,3-butadiene molecule producing vinylcyclopropylidene, which rotates in a plane almost perpendicular to the total angular momentum vector *J* around its *C*-axis. Next, the initial adduct ring opens to a long-lived vinyl-substituted triplet allene structure, $H_2CCCHCHCH_2$. Reations with partially deuterated reactants showed that the latter decomposes via three distinct pathways, including two different hydrogen atom loss channels producing 1- and 3-vinylpropargyl radicals, $HCCCHC_2H_3$ and $H_2CCCC_2H_3$, and elimination of the vinyl radical, C_2H_3, forming propargyl. According to the observed product translational distributions, the hydrogen elimination processes proceed via tight exit transition states, which were computed to reside about 20 kJmol^{-1} above the products. Also, the maximal translational energy release for the C_5H_5 products gives the reaction exothermicity as 215 ± 15 kJ mol^{-1}, which is consistent with the formation of 1- and 3-vinylpropargyl radicals, exothermic by 210 and 196 kJ mol^{-1} according to the computation. Although the $HCCCHC_2H_3$ and $H_2CCCC_2H_3$ products could not be distinguished experimentally, the former fits better the experimental reaction energy, and the calculated branching ratio of 1- vs. 3-vinylpropargyl radical was ~8:1. A minor channel of less than 10% – the formation of vinyl, C_2H_3, and propargyl, C_3H_3, was not seen in experiment but was predicted by theory. The angular distributions showed a forward-backward symmetric flux profile supporting indirect reaction dynamics via a long-lived C_5H_6 complex.

3-vinylpropargyl was assigned as a minor product of the $C(^3P)$ + 1,2-butadiene reaction [129]; we discuss this reaction later in Section 3.7 devoted to methylbutatrienyl radicals. Another possible source of vinylpropargyl radicals is the reactions of dicarbon $C_2(X^1\Sigma_g^+/a^3\Pi_u)$ with propene [130]. The CMB study of these reactions at E_{col} about 21 kJ mol^{-1}, which also included the partially deuterated D3 counterparts of propene (CD_3CHCH_2, CH_3CDCD_2) and was combined with *ab initio*/RRKM calculations, revealed that the reactions involve indirect scattering dynamics and are initiated by the addition of dicarbon to the C=C double bond of propene, both on the singlet and triplet surfaces. These initial adducts complexes rearrange via several isomerisation steps and eventually undergo hydrogen atom loss from the former methyl and vinyl groups

producing mostly 3- and 1-vinylpropargyl radicals. Both triplet and singlet methylbutatriene species were assigned to be important precursors to the products. From the maximal translational energy release, the reaction was determined to be exothermic by 200 ± 40 kJ mol^{-1}, which correlated closely with the computed exothermicities to form 1- and 3-vinylpropargyls, 235 and 221 kJ mol^{-1} on the singlet PES and 243–245 and 231 kJ mol^{-1} on the triplet surface, respectively. The observation of a relatively broad maximum of the centre-of-mass translational energy distribution starting from zero translational energy up to 20 kJ mol^{-1} indicated that at least one reaction channel involves a tight exit transition state and this channel was attributed to the triplet reaction where the exit barriers for hydrogen eliminations were computed to be in the 17–20 kJ mol^{-1} range; the H loss reaction steps were found to be barrierless on the singlet surface. The angular distribution was forward−backward symmetric indicating that decomposing C_5H_6 reaction intermediate(s) were long-lived, i.e. longer than their rotational period, and hence the reaction was concluded to follow indirect scattering dynamics via C_5H_6 complexes. The maximum at 90° in the angular distribution (sideways scattering) suggested that the atomic hydrogen is lost preferentially perpendicularly to the plane of the decomposing complex and almost parallel to the total angular momentum vector; this conclusion was corroborated by the calculated geometry of the decomposing complexes and H loss transition states (on the triplet PES). The studies of the reactions of C_2 with D3-propenes showed that hydrogen atoms can be eliminated both from the methyl and vinyl groups and the branching ratios of the two channels were derived as 75 ± 10% and 25 ± 10%, respectively. The computed product branching ratios at E_{col} = 21 kJ mol^{-1} were the following for the singlet reaction: 3-vinylpropargyl – 45% (formed by H loss from the methyl group), 1-vinylpropargyl – 12% (hydrogen losses from methyl/vinyl groups in the ration of ~1:2), cyclopentadienyl – 6% (H loss from the methyl group), and *i*-C_4H_3 + CH_3 – 29%, with few other minor products contributing under 1–3%. The branching ratios differed for the triplet reaction: 3-vinylpropargyl – 23% (hydrogen loss from the methyl group), 1-vinylpropargyl – 35% (H loss from vinyl group), cyclopentadienyl – 22% (hydrogen loss from the methyl group), and *i*-C_4H_3 + CH_3 – 17%. Thus, a statistically behaving reaction on the singlet PES alone would produce the methyl hydrogen loss to the vinyl hydrogen loss ratio of 6.1, while the triplet reaction alone would produce the methyl to vinyl hydrogen loss ratio of 1.3. A comparison of the computed branching ratios with the methyl/vinyl hydrogen loss ratio in experiment allowed us to roughly evaluate the $C_2(X^1\Sigma_g^+)/C_2(a^3\Pi_u)$ ratio in the experimental beam to be 76:24, with the assumption that both singlet and triplet reactions follow a statistical behaviour and that singlet and triplet dicarbon molecules react with propene with similar rate constants in the barrierless entrance channels. Purely experimental determination of this ratio so far proved to be difficult if not impossible. Noteworthy, if the evaluated singlet to triplet ratio of dicarbon molecules in the beam is qualitatively correct, then, in contrast to $C(^3P)$ + 1,3-butadiene which mostly forms 1-vinylpropargyl, the C_2 + propene reactions give a higher yield of 3-vinylpropargyl. Experimentally, we did not find conclusive evidence that the most stable C_5H_5 isomer, cyclopentadienyl is formed in the reaction, as the exothermicity of this product is 362–372 kJ mol^{-1}, much higher than the value derived from the maximal translational energy release. Taking the singlet to triplet dicarbon ratio in the beam as 76:24, the statistical yield of cyclopentadienyl should have been ~10%. Cyclopentadienyl might have been synthesised with some internal energy, however, the calculated PES indicate that the dynamics factors are not favourable for the formation of this product as compared to the production of 1- and 3-vinylpropargyls

because the pathways to the precursors of cyclopentadienyl involve multiple hydrogen shifts. Deviations from the statistical behaviour are expected to favour mostly 3-vinylpropargyl and *i*-C_4H_3 + CH_3. The latter products could not be positively identified from the experimental data because this channel is masked by the dissociative ionisation product from the reaction of ground state carbon atoms with propene (C_4H_5).

Although not directly identified experimentally, 1,3-divinylpropargyl radical was predicted to be an important product of the reaction of singlet dicarbon with 1,3-pentadiene, $C_2(X^1\Sigma_g^+)$ + $CH_3CHCHCHCH_2$ [116]. Ab initio/RRKM calculations gave the branching ratio for the formation of 1,3-divinylpropargyl + H in this reaction as close to 30% in the collision energy range of 0–50 kJ mol^{-1} and the pathway to these products involves barrierless addition of singlet dicarbon to the C_3=C_4 double bond of 1,3-pentadiene followed by insertion of the C_2 unit into this bond leading to the $CH_3CHCCCHCHCH_2$ complex and emission of atomic hydrogen from the methyl group. The formation of 1,3-divinylpropargyl was calculated to have exothermicity of 239 kJ mol^{-1} Alternatively, the complex can split the methyl group and produce a substituted *i*-C_4H_3 radical, 4-vinylbutatrienyl, which was computed to be 196 kJ mol^{-1} exothermic and to contribute 18–19% of the total yield. When the initial C_2 addition occurs to the C_1=C_2 bond of 1,3-pentadiene, the insertion of dicarbon into this double bond leads instead to the $CH_3CHCHCHCCCH_2$ complex, which mostly fragments emitting H from the methyl group to a C_7H_7 isomer, which belongs to a class of allylic radicals, $CH_2CHCHCHCCCH_2$, with exothermicity of 227 kJ mol^{-1} and branching ratios of 44–45%. Thus, the chain C_7H_7 radicals, including the allylic isomer and 1,3-divinylpropargyl, as well as 4-vinylbutatrienyl + CH_3 were calculated to be the major products of the reaction of singlet dicarbon with 1,3-pentadiene; the only other noticeable products (1–2%) were 3-methylpropargyl plus propargyl radicals.

3.4.3. *Vinylmethylpropargyls*

The reactions of atomic carbon with two C_5H_8 isomers, isoprene (2-methyl-1,3-butadiene) and 1,3-pentadiene (1-methyl-1,3-butadiene) can be expected to form various isomers of the vinylmethylpropargyl radical, together with other products, if they proceed by the mechanism similar to that for C(^{3}P) + 1,3-butadiene (Figure 3). For instance, it is likely that atomic carbon would add to a double C=C bond in isoprene or 1,3-pentadiene barrierlessly forming triplet three-member ring isomers i1-i4, which then ring-open to i5 ($H_2CCC(CH_3)CHCH_2$) and i6 ($H_2CC(CH_3)CHCCH_2$) in the isoprene reaction and i7 ($H_3CCHCCHCHCH_2$) and i8 ($H_3CCHCHCHCCH_2$) for 1,3-pentadiene. Next, i5 can emit a hydrogen atom from different positions yielding 1,1-vinylmethylpropargyl ($HCCC(CH_3)CHCH_2$), $H_2CCC(CH_2)CHCH_2$, $H_2CCC(CH_3)CCH_2$ and $H_2CCC(CH_3)CHCH$ or undergo a single C–C bond cleavage producing 3-vinylpropargyl + CH_3 or 3-methylpropargyl + C_2H_3. Possible decomposition channels of i6 include hydrogen losses to 1- and 3-propenylpropargyl radicals, $H_2CC(CH_2)CHCCH_2$, and $HCC(CH_3)CHCCH_2$, as well as $H_2CCCHCCH_2$ + CH_3 and propenyl (H_2CCCH_3) + propargyl. In the C(^{3}P) + 1,3-pentadiene reaction, possible dissociation channels of i7 and i8 include among others 1-methyl-3-vinyl- and 1-vinyl-3-methyl-propargyl radicals, as well as 1-methylpropargyl + C_2H_3, 1-vinylpropargyl + CH_3, and propenyl + propargyl. Relative yields of the reaction products will be governed by their relative energies, the energetics of the exit transition states for the corresponding H/CH_3/C_2H_3/C_3H_5 splitting steps, and possibly by reaction dynamics factors. Based on higher stability of RSFRs, we anticipate that the radicals of this type including vinylmethylpropargyls,

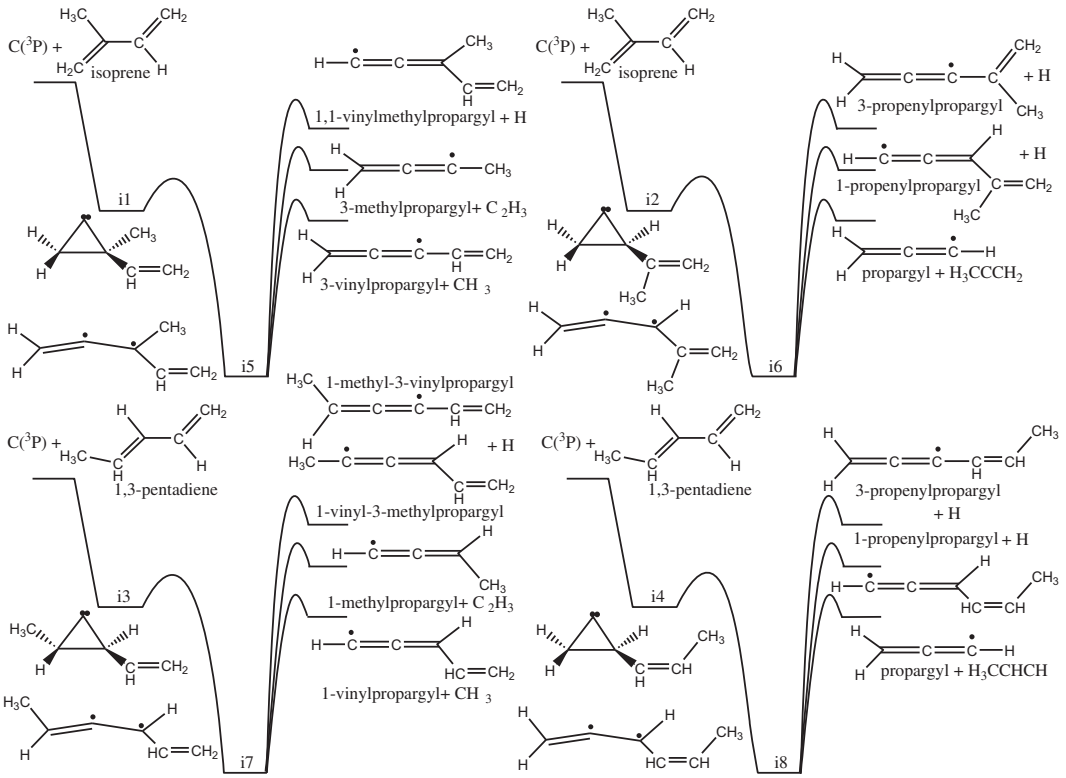

Figure 3. Proposed mechanism and products for the reaction of $C(^3P)$ with C_5H_8 isomers, isoprene and 1,3-pentadiene.

propenylpropargyls, methylpropargyls, and vinylpropargyls will be major reaction products.

3.5. *Methyl-substituted C_5H_3 radicals*

Methyl-substituted *i*- and *n*-C_5H_3 radicals together with other acyclic C_6H_5 isomers were identified in our study of the reaction dynamics of singlet and triplet C_2 with C_4H_6 isomers 2-butyne, 1-butyne and 1,2-butadiene investigated at collision energies of about 26 kJ mol^{-1} [131]. All the reactions were found to be indirect, forming C_6H_6 complexes through barrierless additions by dicarbon on the triplet and singlet PESs, which then isomerized and formed a variety of acyclic C_6H_5 products by hydrogen loss in overall exothermic reactions. No other product channels were detected, although lighter products like C_5H_3 produced by methyl group emission might have been masked by dissociative ionisation of products of the concomitant $C(^3P) + C_4H_6$ reactions, with atomic carbon also present in the molecular beam. The centre-of-mass angular distributions were isotropic and showed intensity over the full angular range, which evidenced for indirect scattering dynamics via long lived collision complex(es) that undergone multiple isomerisations before they decomposed. Overall, according to our experiments combined with calculations, 10 different acyclic C_6H_5 and C_5H_3 RSFRs were found to be produced in the reaction of $C_2(^1\Sigma_g^+/^3\Pi_u)$ with 2-butyne, 1-butyne and 1,2-butadiene.

The $C_2(^1\Sigma_g^+/^3\Pi_u)$ + 2-butyne (CH_3CCCH_3) reactions featured the maximal translational energy release of its C_6H_5 products consistent with the reaction exothermicity of 218 ± 22 kJ mol^{-1}. The reaction energy most closely matches the formation of the 5-methyl-2,4-pentadiynyl-1 product, methyl-substituted *i*-C_5H_3, + H on the singlet surface residing 223 kJ mol^{-1} below the reactants. The *ab initio* calculations of the reaction PES showed this product as the only C_6H_5 isomer, which can be produced in this reaction: addition of singlet dicarbon occurs to the acetyl bond creating a three-member ring C_6H_6 intermediate that eventually ring opens to 2,4-hexadiyne and the latter emits an H atom from one of the terminal CH_3 groups producing 5-methyl-2,4-pentadiynyl-1 without an exit barrier, in line with the near zero peaking of the observed translational energy distribution. In the $C_2(^3\Pi_u)$ + 2-butyne reaction on the triplet surface, RRKM calculations at the experimental collision energy show the formation of 44% of 3-methyl-1,4-pentadiynyl-3 (methyl-substituted *n*-C_5H_3), 14.5% of 5-methyl-2,4-pentadiynyl-1, and 41.5% of CH_3CCCC (methyl-substituted *l*-C_4H) + CH_3. The experimental reaction energy matches the products 3-methyl-1,4-pentadiynyl-3 (exothermic by 228 kJ mol^{-1}) and 5-methyl-2,4-pentadiynyl-1 (exothermic by 234 kJ mol^{-1}), in concurrence with theoretical predictions that these C_6H_5 isomers are the dominant reaction products. The existence of exit barriers for H loss to form 3-methyl-1,4-pentadiynyl-3 and 5-methyl-2,4-pentadiynyl-1 on the triplet PES, 14 and 88 kJ mol^{-1}, respectively, does not contradict to the nearly zero peaking of the experimental translational energy distribution as long as the abundance of triplet dicarbon in the beam is smaller than that of singlet C_2.

For C_2 + 1-butyne, the reaction energy of -228 ± 31 kJ mol^{-1} derived from the translational energy distribution matched the computed exothermicity of 230 kJ mol^{-1} for the formation of 1-methyl-2,4-pentadiynyl-1 + H on the singlet PES. The reaction initiates by singlet dicarbon addition to the triple C≡C bond producing three- or four-member ring intermediates without entrance barriers; the two initial adducts easily rearrange into one another and can undergo a formal insertion of the new C_2 unit into the triple carbon-carbon bond of 1-butyne forming 1,3-hexadiyne. Next, 1,3-hexadiyne emits atomic hydrogen from its CH_2 group to yield 1-methyl-2,4-pentadiynyl-1 or the CH_3 group to form *i*-C_5H_3; both processes occurring without exit barriers, in accord with the near-zero peaking of the experimental product translational energy distribution, at least for the C_6H_5 products. RRKM calculations predicted 86% of the H loss products to be 1-methyl-2,4-pentadiynyl-1 and the rest to be $HC{\equiv}C{-}C{\equiv}C{-}CH_2{-}C^{\bullet}H_2$, a C_6H_5 isomer which is not resonance stabilised and resides 64 kJ mol^{-1} higher in energy than 1-methyl-2,4-pentadiynyl-1. The calculations also predicted that *i*-C_5H_3 + CH_3 are responsible for 92% of the total product yield. In the triplet $C_2(^3\Pi_u)$ + 1-butyne reaction, RRKM calculations pointed at $HCCCHCCHCH_2$ as the major product. This radical is best described by the following resonance structures:

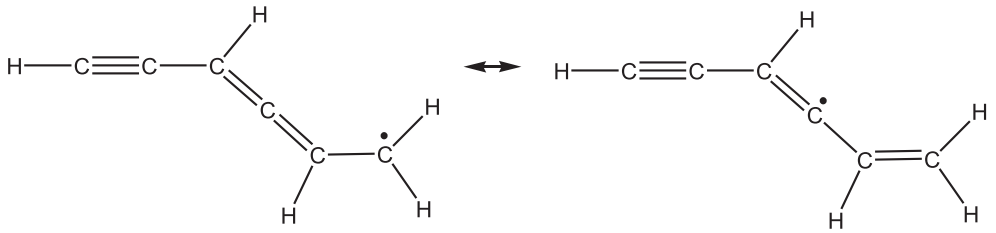

and belongs to the class of substituted allylic radicals, with two H atoms on one carbon replaced by a C_3H_2 group. The $HCCCHCCHCH_2$ + H products on the triplet PES were

predicted to be exothermic by 214 kJ mol^{-1} matching the observed reaction energy. In the meantime, five other C_6H_5 products were computed to lie within the error bars of the experimental reaction exothermicity, including 1-methyl-2,4-pentadiynyl-1, two conformers of $HCCCHCHCCH_2$, $HCCCHCCHCH_2$, and $HCCCCHCHCH_2$. Since these C_6H_5 isomers were close in energy within our experimental/theoretical error limits, we solely referred to the *ab initio*/RRKM calculations to conclude that $HCCCHCCHCH_2$ + H are the major products of the triplet reaction.

The reaction of dicarbon with 1,2-butadiene was determined to be exothermic by 213 ± 28 kJ mol^{-1}, matching the computed reaction energies of 5-methyl-2,4-pentadiynyl-1 (-239 kJ mol^{-1}), 1-methyl-2,4-pentadiynyl-1 (−225 kJ mol^{-1}), and the allylic $HCCCHCCHCH_2$ radical (−226 kJ mol^{-1}) plus atomic hydrogen on the singlet surface. Indeed, RRKM calculations predicted these C_6H_5 products to be formed in nearly equal amounts and to be responsible in total for 23% of the product yield, whereas *i*-C_5H_3 + CH_3 was computed to be the major product (77%) of the singlet reaction. On the triplet surface C_6H_5 products 5-methyl-2,4-pentadiynyl-1, 1-methyl-2,4-pentadiynyl-1, $HCCCHCCHCH_2$, $HCCCH_2CCCH_2$, $HCCC(CH_2)CCH_2$, and $HCCCHCCHCH_2$ were in the exothermicity range of 199–251 kJ mol^{-1}, close to the experimentally observed reaction energy bracket of 213 ± 28 kJ mol^{-1}. According to the *ab initio*/RRKM theoretical results, barrierless addition of triplet dicarbon to the C2 atom of 1,2-butadiene predominantly favours the formation of $HCCC(CH_2)CCH_2$, the addition to C1 produces mostly $HCCCH_2CCCH_2$ (67%) and $HCCCHCCHCH_2$ (27%), whereas the addition to C3 yields mostly *i*-C_5H_3 + CH_3 (81%) together with smaller amounts of 5-methyl-2,4-pentadiynyl-1, 1-methyl-2,4-pentadiynyl-1, and $HCCCHCCHCH_2$ at the levels of 4.4, 7.6, and 7.0%, respectively. The reaction outcome was thus predicted to strongly depend on the site of the initial dicarbon attack; when dicarbon adds to C1 or C2, mostly the $HCCCH_2CCCH_2$, $HCCC(CH_2)CCH_2$, and $HCCCHCCHCH_2$ products exothermic by 199–209 kJ mol^{-1} were predicted to form, but when C3 is attacked, more exothermic C_6H_5 products (236–251 kJ mol^{-1}) were anticipated. Clearly, the first group better correlated with the experimental reaction energy which may be due to the fact that the C3 addition is dynamically least favourable due to steric hindrance.

3.6. C_xH_3 (x = 4, 6)

This class of RSFRs includes C_4H_3 and C_6H_3 that are designated by the general formula $H_2C{=}C{-}(C{\equiv}C)_n{-}H$ with n = 1, 2. The butatrienyl (or 1-butene-3-yne-2-yl) radical, *i*-C_4H_3, and the hexenediynyl radical, *i*-C_6H_3, can be described in terms of two and three resonance structures:

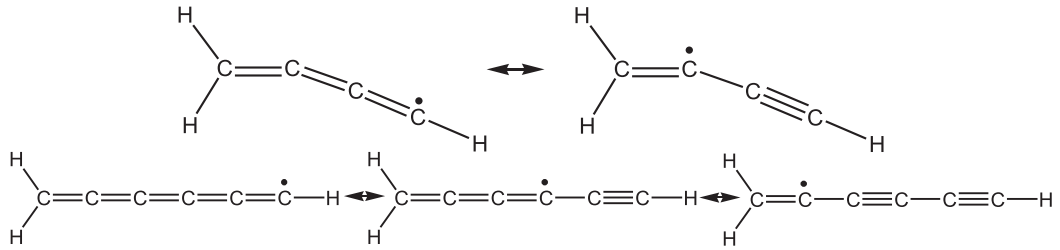

The *i*-C_4H_3 radical has a slightly non-linear C_4 skeleton and a $^2A'$ electronic term according to the most accurate CCSD(T) calculations [132], but H_2C_6H maintains linear C_6 arrangement within C_{2v} symmetry and has a $^2B_2$ ground electronic state [133].

3.6.1. *Butatrienyl radical, i-C_4H_3*

i-C_4H_3 (incorrectly denoted as *n*-C_4H_3 in our earlier articles) was found to be produced in the reaction of atomic carbon with C_3H_4 isomers methylacetylene and allene and also in the reactions of $C_2(X^1\Sigma_g^+/a^3\Pi_u)$ with ethylene. The first report on the formation of *i*-C_4H_3 in CMBs dates back to 1996 [134]. In this work, the $C(^3P_j)$ + CH_3CCH reaction was studied at E_{col} of 20.4 and 33.2 kJ mol^{-1}. The centre-of-mass angular distributions were isotropic at lower, but forward scattered at higher collision energy, supporting indirect reaction dynamics involving a long-lived C_4H_4 complex with a lifetime exceeding or comparable to its rotational period (osculating complex) at the lower and higher E_{col}, respectively. The maximum energy release together with the angular distributions were consistent with the formation of *i*-C_4H_3 in its electronic ground state. Based on the observed distributions, the authors proposed that the carbon atom attacks the π-orbitals of methylacetylene barrierlessly forming a triplet 1-methylpropenediylidene adduct, which rotates in a plane almost perpendicular to the total angular momentum vector around the B\C-axes and undergoes 2,3-H-shift to triplet 1-methylpropargylene and then decomposes to *i*-C_4H_3 within 1–2 ps (here, the rotational period of the complex was used as a molecular clock to estimate its lifetime) by emitting a hydrogen atom from the CH_3 group via a tight exit transition state located at least 30–60 kJ mol^{-1} above the products. The subsequent theoretical study [135] generally corroborated the proposed reaction mechanism and also provided additional details, such as the initial carbon atom addition can occur without barrier not only to both acetylenic carbon atoms in CH_3CCH but also to the triple bond forming a three-member ring triplet C_4H_4 complex (methylcyclopropenylidene), which is the most stable initial adduct. The two complexes formed by C additions to C1 and C2 of methylacetylene (1- and 2-methylpropendiylidenes) easily rearrange to the three-member ring adduct via low barriers and the latter then ring opens to 1-methylpropargylene, providing an alternative path to this key precursor of the *i*-C_4H_3 product. 1-methylpropargylene loses a methyl group hydrogen atom via an exit barrier of 24 kJ mol^{-1} and the resulting *i*-C_4H_3 + H products were computed to be exothermic by 177 kJ mol^{-1}, the value which was somewhat off the energy range of 192–212 kJ mol^{-1} inferred from the crossed beam study. The reaction mechanism and dynamics were further clarified in a later study [136], in which the deuterated CD_3CCH methylacetylene was used as the reactant. The CMB experiment on $C(^3P)$ + CD_3CCH was carried out at the collision energy of 21.1 kJ mol^{-1}. Isotropic angular distribution supported the indirect character of the reaction dynamics proceeding via a long-lived complex. It was also established that initial collisions with large impact parameters dominate the reaction and form triplet trans-1-methylpropenediylidene complex, whereas small impact parameter collisions of relatively minor significance lead to triplet methylcyclopropenylidene. Both adducts rearrange via hydrogen migration and ring opening, respectively, to the same triplet methylpropargylene intermediate but with the attacking C atom located in two distinct positions. The translational energy distribution peaked at a broad plateau between 25–35 kJ mol^{-1}, which is close to the computed height of the exit barrier above the *i*-C_4H_3 product for a deuterium atom loss from triplet methylpropargylene. The translational energy distribution showed that the reaction is exothermic by at least 70–100 kJ mol^{-1} and its long tail could justify an exothermicity up to 180 kJ mol^{-1} corresponding to the formation of *i*-C_4H_3. RRKM calculations of product branching ratios at the experimental collision energy gave 90% of *i*-C_4H_3 and 9% of *n*-C_4H_3 (HCCHCCH). Since the latter was computed to be exothermic by 132 kJ mol^{-1} and to be produced by 1,2-H(D)-shift in triplet methylpropargylene followed by H(D) emission from the

remaining $CH_2(CD_2)$ group, the formation of n-C_4H_3 also does not contradict the experimental observations. The latest crossed beam study of the atomic carbon with methylacetylene was performed at very low collision energies of 0.8 and 3.4 kJ mol^{-1} with additional characterisation of the recoiling hydrogen atoms using Doppler-Fizeau spectra [41]. This report established the $C(^3P) + CH_3CCH \rightarrow i\text{-}C_4H_3 + H$ reaction energy as −185 kJ mol^{-1} (8 kJ mol^{-1} lower than the earlier theoretical value) and confirmed the viability of this reaction under the condition prevailing in interstellar clouds.

The reaction of atomic carbon with another C_3H_4 isomer, allene H_2CCCH_2, also produces i-C_4H_3. This reaction was first investigated in CMB at two collision energies of 19.6 and 38.8 kJ mol^{-1}, these experiments were combined with *ab initio*/RRKM calculations [7,137]. The observed angular distributions of the C_4H_3 products were isotropic at lower, but forward scattered at a higher collision energy. This observation was an evidence of indirect reactive scattering dynamics via a long-lived C_4H_4 complex with a lifetime above or comparable to its rotational period (osculating complex) at the lower and higher E_{col}, respectively. The maximum translational energy release corresponding to the reaction exothermicity of 195–201 kJ mol^{-1} estimated to be accurate within ~25 kJ mol^{-1} and the angular distributions combined with the computed reaction energy of 180 kJ mol^{-1} were consistent with the formation of i-C_4H_3. Reaction dynamics derived from the experimental data indicated that the carbon atom attacks the π-orbitals of the allenic carbon–carbon double bonds without a barrier and the initially formed cyclopropylidene complex rotates in a plane almost perpendicular to the total angular momentum vector around its *C*-axis and undergoes ring opening to triplet butatriene. At higher collision energy, the butatriene complex emits atomic hydrogen within 0.6 ps to form the i-C_4H_3 isomer through an exit transition state located 9.2 kJ mol^{-1} above the products. The channel to the n-C_4H_3 isomer was calculated to contribute less than 1.5%. The much smaller, nearly insignificant yield of the higher-energy n-C_4H_3 isomer slightly distinguishes the reaction of atomic carbon with allene from that with methylacetylene and might be responsible for some differences seen in the dynamics of the two reactions at the lower collision energy, in particular in the fragmentation ratios observed in the mass spectra at $m/z = 51$, 50, and 49 and in the averaged fraction of energy channelling into the translational degrees of freedom, both reflecting somewhat different patterns of secondary decomposition of the primary C_4H_3 products. The authors considered a possible role of a singlet C_4H_4 surface in the reaction and proposed that ISC can occur in the vicinity of the cyclopropylidene adduct, which can ring open to singlet butatriene after crossing over to the singlet state. Butatriene then fragments to i-C_4H_3 by losing an H atom without an exit barrier. Since the reaction on the singlet PES leads to the identical i-C_4H_3 product, its involvement cannot be completely ruled out. However, the observed peaking in the translational energy distribution in the 30–50 kJ mol^{-1} range supported the product formation via a significant exit barrier and hence the dominant role of the triplet PES in the reaction. The most recent study of the $C(^3P)$ + allene reaction [41] at $E_{col} = 0.8$, 3.4, and 5.2 kJ mol^{-1} gave the most accurate evaluation for the reaction energy at −190 kJ mol^{-1}, 10 kJ mol^{-1} lower than the computed value. Also, a uniform angular distribution could not give a satisfying fit for the experimental spectra and, to reconcile the differences, the authors proposed a slightly equatorial distribution with a weak forward/backward dissymmetry. Although the product recoil energy distributions were comparable to those earlier measured by us [136], they departed from the almost isotropic one and this was interpreted in terms of the equatorial contribution due to complexes resulting from C-atom addition on one allenic

bond and dissociating before completing a full rotation. The authors suggested that reactive collisions even at the very low collision energies sampled in their study could keep a relatively direct character.

Chastaing *et al.* [138,139] reported kinetic measurements for the $C(^3P) + C_3H_4$ reactions performed at temperatures between 15 and 295 K and found rate constants to be high, $2.4–4.7\times10^{-10}$ cm^3 mol^{-1} s^{-1}, and to exhibit a slightly negative temperature dependence (methylacetylene) or to be virtually independent of temperature (allene). In the same work, the authors conducted crossed beam experiments in the range of collision energies of 0.5–27 kJ mol^{-1} and measured integral cross sections for the production of hydrogen atoms. The integral cross sections appeared to be in excellent agreement with the temperature dependencies of the rate coefficients. The reactions were thus concluded to proceed without any barrier on at least one reaction path leading to hydrogen atom elimination, which agreed with our observations. If other product channels were present (in addition to $C_4H_3 + H$), the consistency between the rate constants and integral cross sections would indicate that all these channels exhibited similar energy/temperature dependence and thus the reactions are governed by the initial atomic carbon addition step. Another kinetic study by Loison and Bergeat [124] at room temperature reported rate constants for $C(^3P)$ + allene/methylacetylene similar to those obtained by Chastaing *et al.* [137,138] and obtained absolute yields of H atoms as 1.00 and 0.85 ± 0.06 for the allene and methylacetylene reactions, respectively. While the result for allene agrees with the conclusions from CMB experiments and theoretical calculations, the measured hydrogen atom branching for the methylacetylene reaction is in discord with the CMB and *ab initio*/RRKM results. The authors argued that some other channels may be open in the $C(^3P) + CH_3CCH$ reaction, such as $CH_3 + l\text{-}C_3H$ and $H_2 + C_4H_2(^3B_u)$. Although the key decomposing intermediate, triplet methylpropargylene, may indeed decompose to $CH_3 + l\text{-}C_3H$ via a loose variational transition state without an exit barrier, these products were computed to reside only 28 kJ mol^{-1} below the reactants and 125 kJ mol^{-1} higher in energy that the transition state for hydrogen atom emission to form $i\text{-}C_4H_3$ and hence it is unlikely that the yield of $CH_3 + l\text{-}C_3H$ could be as high as 0.15 ± 0.06, if the reaction follows statistical behaviour. Meanwhile, dynamics factors may favour this product channel as it involves the C–C bond cleavage only one bond from the attacking carbon atom. In our theoretical calculations we were not able to locate any transition state for H_2 elimination from methylpropargylene on the triplet PES, attempts to search such a TS usually converge to H abstractions transition states from $i\text{-}C_4H_3$: $H + i\text{-}C_4H_3 \rightarrow H_2 + C_4H_2(^3B_u)$. The situation here is similar to H_2 elimination from triplet CH_3CH, which was ruled out in our theoretical study [140]. We argued then that the molecular orbital picture strongly favours the hydrogen abstraction geometry, with nearly linear C–H–H fragments, for the transition state, as compared to H_2 loss structures. Nevertheless, it may be possible that H_2 is eliminated from triplet methylpropargylene via a roaming mechanism, i.e. via an H-abstraction-type transition state, and hence a minor contribution of the H_2 loss channel may not be completely disregarded. Considering that no H_2 (D_2) loss channels were detected under single-collision conditions [133,135], we may conclude that the hydrogen branching ratio in the $C(^3P) + CH_3CCH$ reaction obtained Loison and Bergeat is likely underestimated due to complications of the analysis caused by secondary reactions and wall effects in their low-pressure fast-flow reactor.

For the $C(^3P)$ + allene reaction, we performed calculations of absolute unimolecular rate constants and branching ratios using microcanonical VTST [141] with full energy and angular momentum resolution, based upon *ab initio* computed interaction potential

between carbon and allene as a function of the angle of attack. The kinetic scheme included an explicit treatment of the entrance channels to predict the overall input flux and allowed for the possibility of redissociation via the entrance channels. The computed rate constants were within a factor of ~2 from the experimental values by Chastaing *et al.*, but showed a positive temperature dependence, whereas the experimental rate constants were found to be nearly temperature-independent. The calculated product branching ratios at different temperatures agreed with the values computed earlier for single-collision conditions [136] – 98–99% of *i*-C_4H_3 were predicted to be formed at $T = 100$–700 K, with the yield of *n*-C_4H_3 not exceeding 1–2%.

The alternative source of C_4H_3 is the reaction of $C_2(X^1\Sigma_g^+/a^3\Pi_u)$ with ethylene. The dynamics of this reaction were first revealed by our CMB experiments at collision energies of 14.6 and 28.9 kJ mol^{-1} combined with theoretical calculations [142]. The results showed the existence of a C_4H_3 + H channel via bound C_4H_4 intermediates. The calculations of the singlet and triplet PESs demonstrated that dicarbon in both electronic states adds to the π-system of C_2H_4 without a barrier and then formally inserts into the C=C double bond proceeding via three- or four-member ring intermediates to singlet or triplet butatriene complexes. In the triplet state, 90% of the total reaction flux goes via a cyclobutyne intermediate. The butatriene complexes emit atomic hydrogen to form *i*-C_4H_3 without an exit barrier (singlet) or via a tight transition state residing 9.2 kJ mol^{-1} above the products (triplet). The reaction exorgicity determined from the maximal translational energy release in experiment was in the range of 121–180 kJ mol^{-1} and consistent with the formation of *i*-C_4H_3 exothermic by 156 and 165 kJ mol^{-1} in the singlet and triplet reaction, respectively. The distribution maximum of the translational energy at the higher E_{col} stretched to 46 kJ mol^{-1}, but peaked near zero at the low collision energy – this change was attributed to an opening of a second channel at higher collision energy, i.e. the reaction of $C_2(^3\Pi_u)$, the abundance of which in the beam increases with E_{col}. The butatriene complexes reside in deep potential energy wells and were therefore long-lived, which was reflected in a backward-forward symmetric angular distribution. We performed detailed calculations of the singlet and triplet C_4H_4 PESs and RRKM computations of product branching ratios for the $C_2(^1\Sigma_g^+/^3\Pi_u) + C_2H_4$ reactions at collision energies between 0 and 42 kJ mol^{-1} [134,143]. Theoretical results confirmed *i*-C_4H_3 to be the dominant product of the triplet reaction, which is mostly formed by H emission from triplet butatriene. However, the calculated product distribution in the singlet reaction appeared to be more complex. Here, the yield of *i*-C_4H_3 was predicted only as 41–52% in the considered collision energy range, with 31–42% originating from singlet butatriene and the rest, 5–6% coming from two other precursors, vinylacetylene and methylpropargylene. The yield of another C_4H_3 isomer, *n*-C_4H_3, appeared to be minimal, under 1%. Another major reaction products with the branching ratio of 49–35% were $C_2H_2 + H_2CC$. The H_2 elimination products, mostly H_2CCCC and to less extent diacetylene, HCCCCH, contributed only 8–9%.

Later, we revisited the $C_2(X^1\Sigma_g^+/a^3\Pi_u) + C_2H_4$ reactions [102] and probed them in crossed beams in more detail, in a broad range of collision energies from 12.1 to 40.9 kJ mol^{-1} and using not only C_2H_4 but also fully and partially deuterated ethylenes as the reactant [144]. With the improved single-to-noise ratio, we tried to detect the molecular hydrogen elimination channel and to evaluate the relative importance of the singlet vs. triplet PESs. From the maximal translational energy release at different E_{col} we were able to more accurately evaluate the reaction exothermicity to produce *i*-C_4H_3 + H as 167 ± 10 and 176 ± 10 kJ mol^{-1} for the singlet and triplet reactions,

respectively – this put our theoretical values close to the experimental margins. We were not able to identify the H_2 elimination channel. This non-observation may be due to dynamical (non-statistical) effects that could favour the atomic hydrogen loss compared to H_2 elimination. Alternatively, considering that molecular hydrogen was predicted to be produced only on the singlet PES, any contribution from the triplet reaction should reduce the overall yield of H_2. Even if the beam contained a 1:1 ratio of triplet vs. singlet dicarbon, this would reduce the H_2 branching ratio to about 4% – below to the sensitivity limit of our fits. Indeed, an inclusion of up to 5% of the $C_4H_2 + H_2$ pathway did not influence the quality of the TOF and laboratory fits at $m/z = 50$. The observation of C_2H_2 was not possible because of the overlap with dissociative ionisation products from C_2H_4. The collision-energy dependence of the angular distributions, which were isotropic at the lowest collision energy but exhibited increasing backward scattering with E_{col}, suggested that the reaction dynamics on the singlet and triplet surfaces are indirect and involve butatriene reaction intermediates. The symmetric singlet butatriene intermediate would lead solely to a symmetric angular distribution; however, in combination with isotopically labelled reactants, we concluded that triplet butatriene excited to B/C like rotations likely account for the observed asymmetries in the angular distributions at higher collision energies. The translational energy distributions pointed at the involvement of both the triplet and singlet reactions, both leading to *i*-C_4H_3 through loose (singlet) and tight (triplet) exit transitions states. According to RRKM computed rate constants the lifetime of the decomposing C_4H_4 complexes was predicted to increase with an increase of the number of D atoms replacing H atoms; this behaviour was reflected in more symmetric forward–backward angular distributions for partially deuterated ethylene and especially for C_2D_4. Finally, the *i*-C_4H_3 radical was predicted to be produced in the reactions of dicarbon $C_2(X^1\Sigma_g^+/a^3\Pi_u)$ with propene, where it is formed by CH_3 elimination from C_5H_6 complexes. The RRKM computed branching ratios for *i*-C_4H_3 constituted 29 and 17% on the singlet and triplet PESs, respectively, but its experimental identification was not possible (see Section 3.4.2).

3.6.2. *C_6H_3 radicals*

The formation of C_6H_3 radicals was observed in the joint CMB/theoretical study [145] of $C_2(^1\Sigma_g^+/^3\Pi_u)$ with vinylacetylene, $H_2C{=}CH{-}C{\equiv}CH$, carried out at a collision energy of 31.0 kJ mol^{-1}. Both singlet and triplet reactions were established to be initiated by a barrierless addition of dicarbon to vinylacetylene and to exhibit indirect scattering dynamics via long-lived C_6H_4 complexes, as indicated by almost forward-backward symmetric angular distribution. The reaction energy of -169 ± 25 kJ mol^{-1} experimentally determined from the maximal translational energy release was close to the predicted energies of *i*-C_6H_3 (hexenediynyl/1-hexene-3,4-diynyl-2, −187 and −197 kJ mol^{-1} on the singlet and triplet PESs, respectively) and of 1,2,3-tridehydrobenzene (−194 and −204 kJ mol^{-1}) as well as 1,2,4-tridehydrobenzene (−185 and −195 kJ mol^{-1}). Since these aromatic and resonantly stabilised C_6H_3 radicals are too close in energy, well within the experimental error limits, we utilised the results of *ab initio*/RRKM calculations to identify the reaction products. These results showed that in the singlet reaction, ethynylbutatriene and vinyldiacetylene produced by insertion of the C_2 unit to the double and triple C–C bonds of vinylacetylene, respectively, emit atomic hydrogen via loose exit transition states (no exit barrier) to form nearly exclusively the *i*-C_6H_3 radical. In the triplet reaction, ethynylbutatriene splits a

hydrogen atom through a tight exit transition state located about 20 kJ mol^{-1} above the *i*-C_6H_3 + H products (> 95%); to a minor amount (~ 4% at low collision energies but less than 1% at the collision energy of our experiment) theory predicted the formation of cyclic 1,2,4-tridehydrobenzene. The translational energy distribution showed a small plateau-like structure from 10 to 27 kJ mol^{-1} supporting the presence of at least two exit channels (one from the singlet and triplet surface each) and that at least one channel involves a tight exit barrier – the involvement of the triplet surface is responsible for this feature; the presence of both singlet and triplet dicarbon in the reactant beam was confirmed by its LIF spectra. RRKM calculations have also predicted C_4H_2 + C_2H_2 as minor reaction products on the singlet surface (8–9%), however, these products could not be identified in experiment because of the interference with dissociative ionisation of the reactants.

The *i*-C_6H_3 product was also seen the CMB study of the reaction dynamics between tricarbon molecules and allene (H_2CCCH_2) and methylacetylene (CH_3CCH and CD_3CCH) at E_{col} ranging from 74 to 123 kJ mol^{-1} [146]. Experimental results indicated that both reactions featured characteristic threshold energies of 40–50 kJ mol^{-1}, consistent with typical reaction barriers for C_3 additions to double and triple C–C bonds [90, 91]. The reaction dynamics were found to be indirect and suggested the reactions proceeded via an initial C_3 addition to the unsaturated hydrocarbon molecules forming cyclic C_6H_4 adducts, most likely five-member rings with out-of-ring CH_2 or CH_3 groups. The cyclic intermediates isomerize to yield eventually the acyclic isomers $CH_3CCCCCH$ (methylacetylene reaction) and $H_2CCCCCCH_2$ (allene reaction) via formal insertion of the tricarbon unit into the triple and double C–C bonds, respectively. Both structures decompose via atomic hydrogen elimination to form *i*-C_6H_3. The support for this mechanism for the methylacetylene reaction came from the fact that no H atom emission was observed in the C_3 + CD_3CCH experiments; only the deuterium atom was emitted from the D3-methyl group and thus the atomic hydrogen loss originated from the methyl group. The lifetime of the intermediate complexes was proposed to be rather short due to very high collision energies. In fact, the observed average fraction of energy channelling into the translational degrees of freedom of the reactants was about 27–43% and 41–53% at lower and higher collision energies, respectively – this order of magnitude confirms that the reaction goes through a relatively short-lived intermediate. These dynamical effects can result in off-zero peaking of the translational energy distributions, which was observed despite the fact that the singlet C_6H_4 complexes are expected to emit atomic hydrogen without an exit barrier. The experimental reaction exothermicities of 50–70 kJ mol^{-1} derived from the maximal translational energy releases agreed well with the computed values for *i*-C_6H_3, 53 and 59 kJ mol^{-1} for the methylacetylene and allene reactions, respectively. The six-member ring C_6H_3 isomers, such as 1,2,3- and 1,2,4-tridehydrobenzenes close in energy to *i*-C_6H_3, were ruled out on the basis of the short lifetime of intermediates; rearrangements of $CH_3CCCCCH$ and $H_2CCCCCCH_2$ to cyclic C_6H_4 benzyne isomers required multiple H atom migrations and were deemed to be too slow to play a role in the reaction under the experimental conditions. The same argument applies to another chain C_6H_3 isomer, HCCCHCCCH, which was computed to be 35 (41) kJ mol^{-1} exothermic in the methylacetylene (allene) reaction.

3.7. *Substituted i-C_4H_3 radicals*

Methyl-substituted *i*-C_4H_3 radicals were found to be formed as major products of the reaction of $C(^3P_j)$, with 1,2-butadiene, $H_2CCCHCH_3$ [128], and 2-butyne, H_3CCCCH_3 [147]. Other substituted *i*-C_4H_3 radicals, 1- and 4-vinylbutatrienyls, were identified or computed to be significant products of the $C_2(X^1\Sigma_g^+)$ + 1,3-butadiene [43] and $C_2(X^1\Sigma_g^+)$ + C_5H_8 [115,116] reactions, as described in Section 3.8, and here we focus on the formation of methylbutatrienyls. The reaction of atomic carbon with 1,2-butadiene probed in crossed beams at three collision energies of 20.4, 37.9, and 48.6 kJ mol^{-1} has shown peculiar dynamics. The experiments together with *ab initio*/RRKM calculations revealed that the reaction is initiated by a barrierless addition of the carbon atom to the π system of the 1,2-butadiene molecule. When $C(^3P)$ attacks $H_2CCCHCH_3$ with large impact parameters, the carbon atom adds preferentially the C2=C3 double bond to form a three-member ring C_5H_6 intermediate i1 with CH_3 on the side chain (mechanism 1); whereas the attack with small impact parameters results in an addition of atomic carbon to the C1=C2 bond yielding another three-member ring intermediate i2 with the methyl group directly linked to the ring (mechanism 2). Both ring structures i1 and i2 open to the same triplet methylbutatriene complex i3, but with differing arrangement of carbon atoms, $H_2C\mathbf{C^*}CCHCH_3$ and $H_2CC\mathbf{C^*}CHCH_3$, respectively, where **C*** designates the attacking carbon atom. Triplet methylbutatriene is suggested to undergo a nonstatistical decay faster than a complete energy randomisation via an H atom loss producing 1- and 4-methylbutatrienyl $H_2CCCCCH_3$ and $HCCCCHCH_3$, respectively. Alternatively, the energy randomisation in $H_2CC\mathbf{C^*}CHCH_3$ is likely to be complete and this isomer emits H atom to form 3-vinylpropargyl, $H_2CCCCHCH_2$ together with the 1- and 4-methylbutatrienyl radicals. The measured translational energy distributions showed that the reaction forming the C_5H_5 product(s) is 190 ± 20 kJ mol^{-1} exothermic, but the additional tail in the distributions could account to exothermicity up to 270 kJ mol^{-1}. Thus, 3-vinylpropargyl isomer lying 260 kJ mol^{-1} below the reactants can be concluded to be only a minor reaction product. The observed reaction energetics rather suggests the dominant formation of 1-methylbutatrienyl and/or 4-methylbutatrienyl, that are calculated to be exothermic by 189 and 177 kJ mol^{-1}, respectively. This conclusion is in contradiction with the RRKM branching ratios of 71.8:2.3:1.4:24.4 for the fragmentation of triplet methylbutatriene i3 into 1-vinylpropargyl:4-methylbutatrienyl:1-methylbutatrienyl:*i*-C_4H_3 + CH_3, indicating that i3 dissociates nonstatistically, apparently due to the fact that its intramolecular energy re-distribution is not fast enough on the reaction time scale, i.e. the lifetime of the complex is too short for a complete energy randomisation to take place. We proposed the following explanation of the observed results. In mechanism 1 (at large impact parameters) the decomposing complex is $H_2C\mathbf{C^*}CCHCH_3$ and in order to form the statistically favoured 3-vinylpropargyl product, $H_2CCCCHCH_2$, the energy has to transfer over four bonds, while in mechanism 2 (at small impact parameters) the decomposing complex is $H_2CC\mathbf{C^*}CHCH_3$ and the energy has to be transferred over three bonds to break the C–H bond and produce 3-vinylpropargyl. The experimental results suggest $H_2C\mathbf{C^*}CCHCH_3$ does not survive long enough for the energy transfer to occur over four bonds; instead, closer C–H bonds are cleaved over two and three bonds producing $HCCCCHCH_3$ (4-methylbutatrienyl) and $H_2CCCCCH_3$ (1-methylbutatrienyl), respectively. Mechanism 1 dominates over mechanism 2 according to the experimental data since 3-vinylpropargyl is clearly only a minor product; the large impact parameter pathway is favoured because the bulky CH_3 group reduces the cone

of acceptance of the C1 atom thus directing the initial carbon atom addition to preferentially form i1. Finally, at lower collision energy, the lifetimes of the decomposing C_6H_5 complexes are apparently longer than their rotational periods giving symmetric forward–backward angular distributions, but too short before a complete energy randomisation occurs. The preference for backward scattering observed in the high energy experiments was attributed to the quenching of the large impact parameters and a decrease of the complex' lifetimes with the collision energy.

The reaction of ground state atomic carbon with 2-butyne was studied in crossed beams at three collision energies between 21.2 and 36.9 kJ mol^{-1} [146]. Experimental results combined with *ab initio*/RRKM calculations allowed us to conclude that the reaction is barrierless and follows indirect scattering dynamics through a long-lived C_5H_6 complex. The angular distributions were almost invariant of the collision energy and their best fits were isotropic and symmetric around 90°, implying that the lifetime of the decomposing C_5H_6 complex was longer than its rotational period. $C(^3P)$ can attack the π system of 2-butyne to form a dimethylcyclopropenylidene intermediate either in one step via an addition to the acetylenic bond or through an addition to only one carbon atom to give short-lived cis/trans dimethylpropenediylidene intermediates, which rapidly ring close. The cyclic intermediate then ring opens to a triplet dimethylpropargylene complex, completing the insertion of the attacking carbon atom into the triple bond. Dimethylpropargylene rotates almost parallel to the total angular momentum vector *J* and decomposes to 1-methylbutatrienyl + H via a tight exit transition state located about 18 kJ mol^{-1} above the separated products; this theoretical values correlates well with off-zero peaking of all translational distributions exhibiting maxima around 20–30 kJmol^{-1}. The experimentally determined exothermicity of 190 ± 25 kJ mol^{-1} was in agreement with the calculated energy to form $H_2CCCCCH_3$, 180 kJ mol^{-1}; 1-methylbutatrienyl + H were also predicted to be the nearly exclusive reaction products by RRKM calculations.

We can predict that the other isomer of the methyl substituted *i*-C_4H_3 radical, 4-methylbutatrienyl, should be one of the major products of the reaction of $C(^3P)$ with 1-butyne (ethylacetylene), $HCCCH_2CH_3$. Although we have not studied this reaction explicitly, we anticipate that it should proceed by barrierless addition of atomic carbon to the terminal acetylenic C atom or to the triple C≡C bond of 1-butyne producing triplet 1-ethylpropendiylidene or ethylcyclopropenylidene adducts, which rapidly rearrange to 1-ethylpropargylene by hydrogen shift or three-member ring opening, respectively (Figure 4). 1-ethylpropargylene, $HCCCCH_2CH_3$, can then decompose to 4-methylbutatrienyl by emitting an H atom from the CH_2 group or to *i*-C_4H_3 by splitting CH_3, both likely via tight exit transition states. The computed exothermicities of these channels, 196 and 238 kJ mol^{-1}, are high and will likely allow them to dominate all other product channels and to compete with one another, with *i*-C_4H_3 + CH_3 being more favourable. On the other hand, the *c*-/*l*-C_3H + C_2H_5 products are not likely to contribute since, by analogy with the $C(^3P)$ + C_2H_2 reaction, they are expected to be thermoneutral or only slightly exothermic – no C_3H products were observed in the reaction of atomic carbon with methylacetylene.

3.8. *Formation of five-, six-, and seven-member cyclic and aromatic radicals*

In some reactions of $C(^3P)$ or $C_2(X^1\Sigma_g^+/a^3\Pi_u)$ with unsaturated hydrocarbons the initial addition steps can be followed by cyclisation leading to five-, six-, or even seven-member rings, which, after rearrangement of hydrogen atoms and emission of either atomic

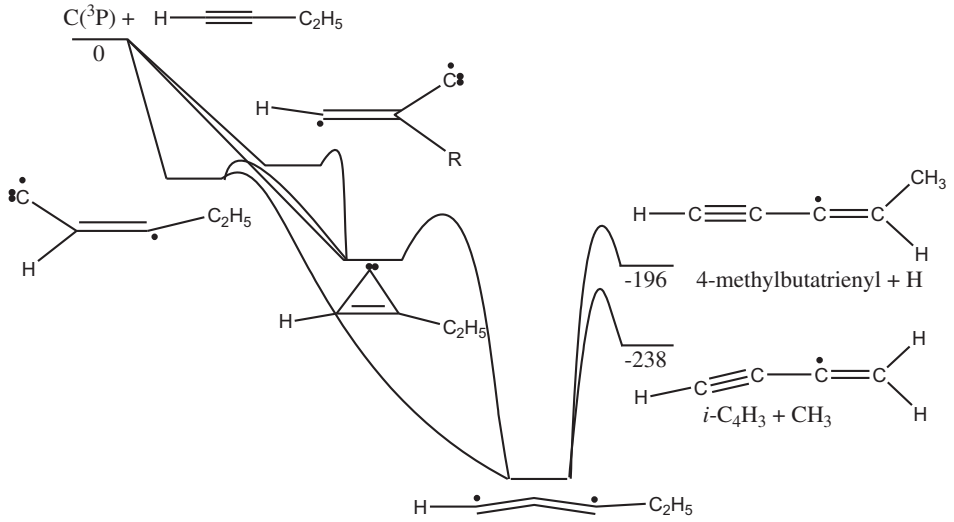

Figure 4. Proposed mechanism and products for the reaction of $C(^3P)$ with 1-butyne, $HCCCH_2CH_3$.

hydrogen or a methyl group, can produce most stable and aromatic isomers of the C_5H_5, C_6H_5, and C_7H_7 radicals.

3.8.1. *Cyclopentadienyl, C_5H_5*

We were not able to detect the cyclopentadienyl radical as a reaction product experimentally, but proposed several pathways for its formation based on theoretical calculations. One of such pathways is the reaction of $C(^3P)$ with an excited cis-conformer of 1,3-butadiene [127], which resides 12.6 kJ mol^{-1} above the most stable trans form; the two conformations are separated from one another by a 23.5 kJ mol^{-1} high barrier. 1,3-butadiene mostly exists in its trans conformation, but a fraction of the cis form may be present at higher temperatures. Our *ab initio*/RRKM calculations show that atomic carbon can add without a barrier to the cis-1,3-butadiene molecule between its two ends to form a cyclic triplet $–CCH_2CHCHCH_2–$ adduct. This complex can undergo a direct H atom loss from one of the CH_2 groups forming an excited cyclic C_5H_5 isomer $–CCHCHCHCH_2–$ via a barrier of 160 kJ mol^{-1} (exit barrier 9 kJ mol^{-1}) and with the overall exothermicity of 189 kJ mol^{-1}. Alternatively, the initial adduct can feature a hydrogen shift from a CH_2 group to the adjacent bare C atom leading to triplet cyclopentadiene via a 172 kJ mol^{-1} barrier and the latter can emit a CH_2 hydrogen forming much more stable cyclopentadienyl exothermic by 332 kJ mol^{-1} via an exit barrier 11 kJ mol^{-1}. However, since the reaction is controlled kinetically, RRKM calculations showed that the $–CCH_2CHCHCH_2–$ adduct produces ~96% of the excited cyclic C_5H_5 isomer and only ~4% of cyclopentadienyl. Overall, cyclopentadienyl can be anticipated as only a trace product of the $C(^3P)$ + 1,3-butadiene reactions and is more likely to be formed through secondary isomerisation of acyclic C_5H_5 isomers, such as vinylpropargyls or methylbutatrienyls.

The calculations have also shown that cyclopentadienyl can be produced as a minor product of singlet and triplet dicarbon with C_3H_6 with relative yields of 7–5 and 31–16%, respectively, at the collision energies of 0–42 kJ mol^{-1} [129]. The pathway to

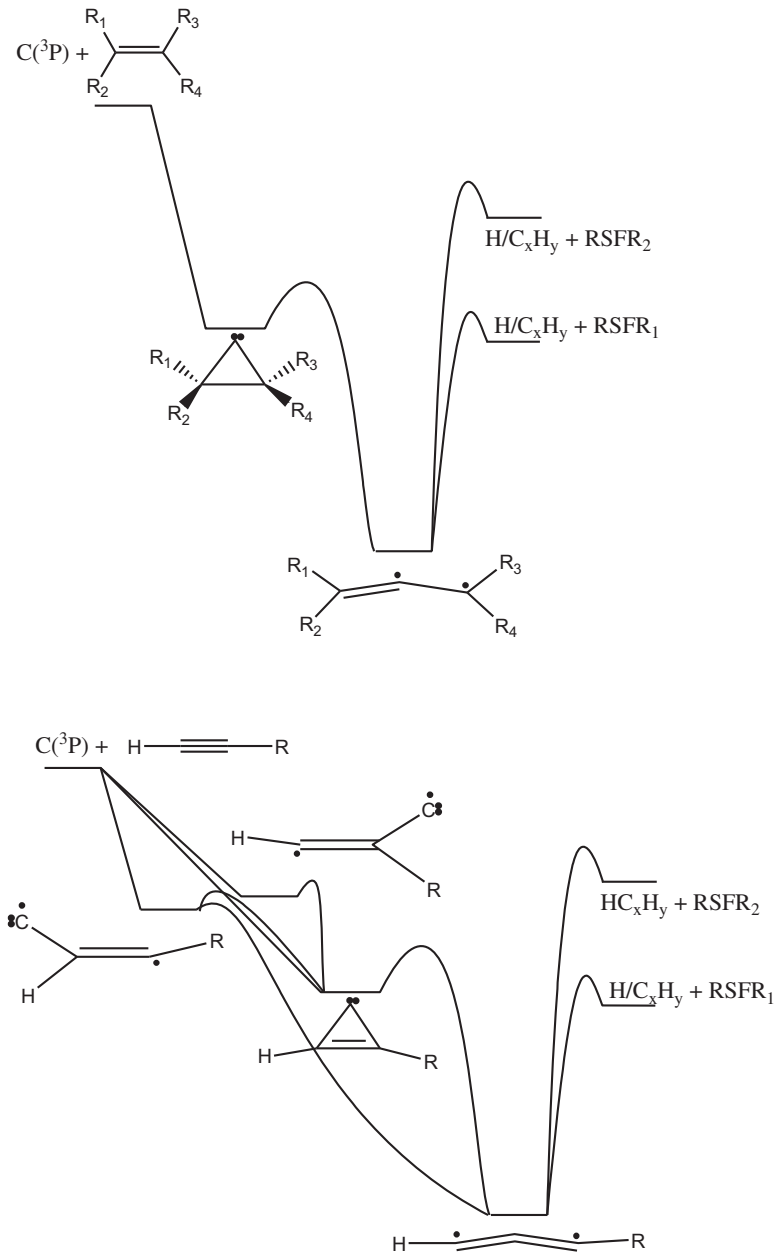

Figure 5. Schematic mechanism of the reactions of $C(^3P)$ with unsaturated hydrocarbons.

c-C_5H_5 on the singlet surface starts at the methyl butatrienyl complex and involves several hydrogen shifts followed by ring closure to cyclopentadiene and H atom emission. The channel leading to cyclopentadienyl on the triplet PES is more feasible and starts from C_2 addition to the terminal CH_2 carbon of propene, proceeds by 1,5-H shift from the methyl group to the opposite end of the molecule followed by another 1,2-H shift, five-member ring closure, and H atom elimination. Since the calculated branching ratio of cyclopentadienyl is significant especially at low collision energies, the $C_2(^3\Pi_u)$ + propene reaction can be considered as a viable source of *c*-C_5H_5 under astrochemical conditions. We have not found conclusive evidence that this isomer is formed in our CMB experiments, as the maximal translational energy release observed

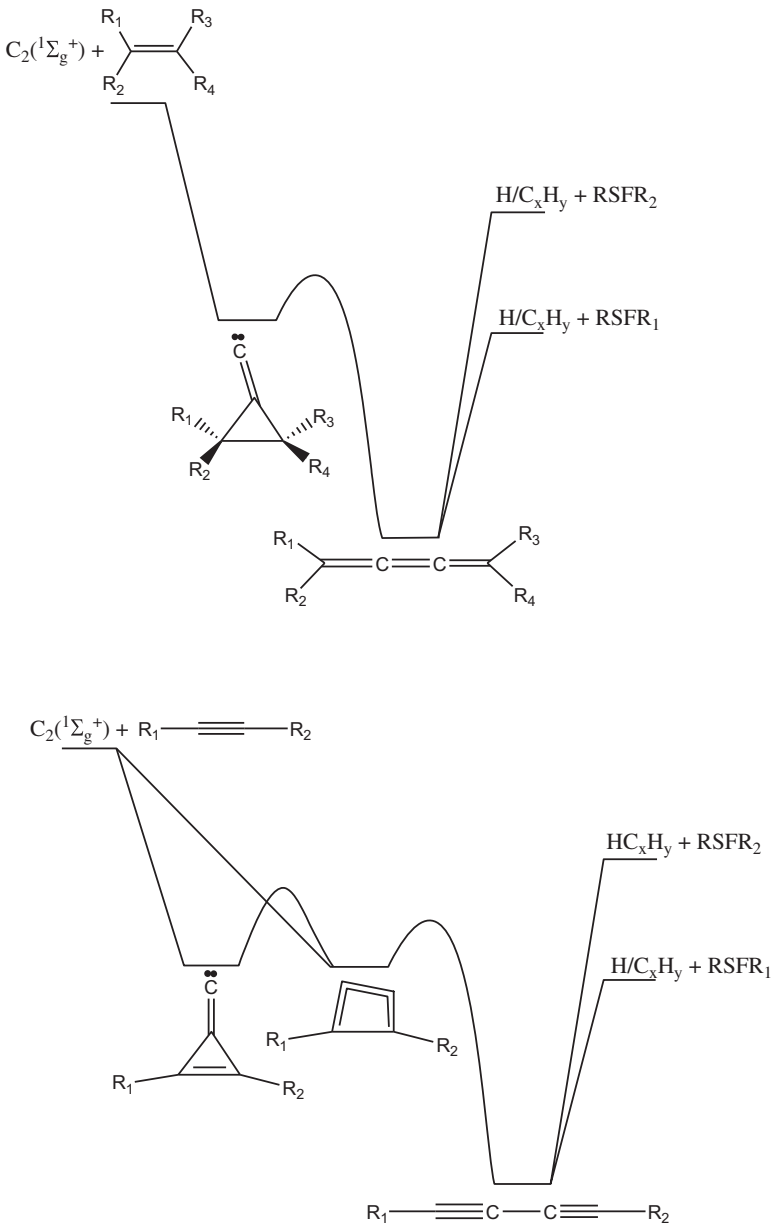

Figure 6. Schematic mechanism of the reactions of $C_2(^1\Sigma_g^+)$ with unsaturated hydrocarbons.

corresponded to the reaction exothermicity of only 200 ± 40 kJ mol^{-1}, whereas the *c*-C_5H_5 + H channel was computed to be 372 kJ mol^{-1} exothermic. However, cyclopentadienyl might have been synthesised with some internal energy; experimental verification for its formation in the $C_2(^3\Pi_u) + C_3H_6$ reaction may come from the measurements of photoionisation cross sections of C_5H_5 reaction products.

3.8.2. *Phenyl, C_6H_5*

CMB experiments of $C_2(X^1\Sigma_g^+/a^3\Pi_u)$ with 1,3-butadiene and its partially deuterated counterparts (1,1,4,4-D4–1,3-butadiene and 2,3-D2–1,3-butadiene) at two collision energies of 12.7 and 33.7 kJ mol^{-1} combined with *ab initio*/RRKM calculations of the

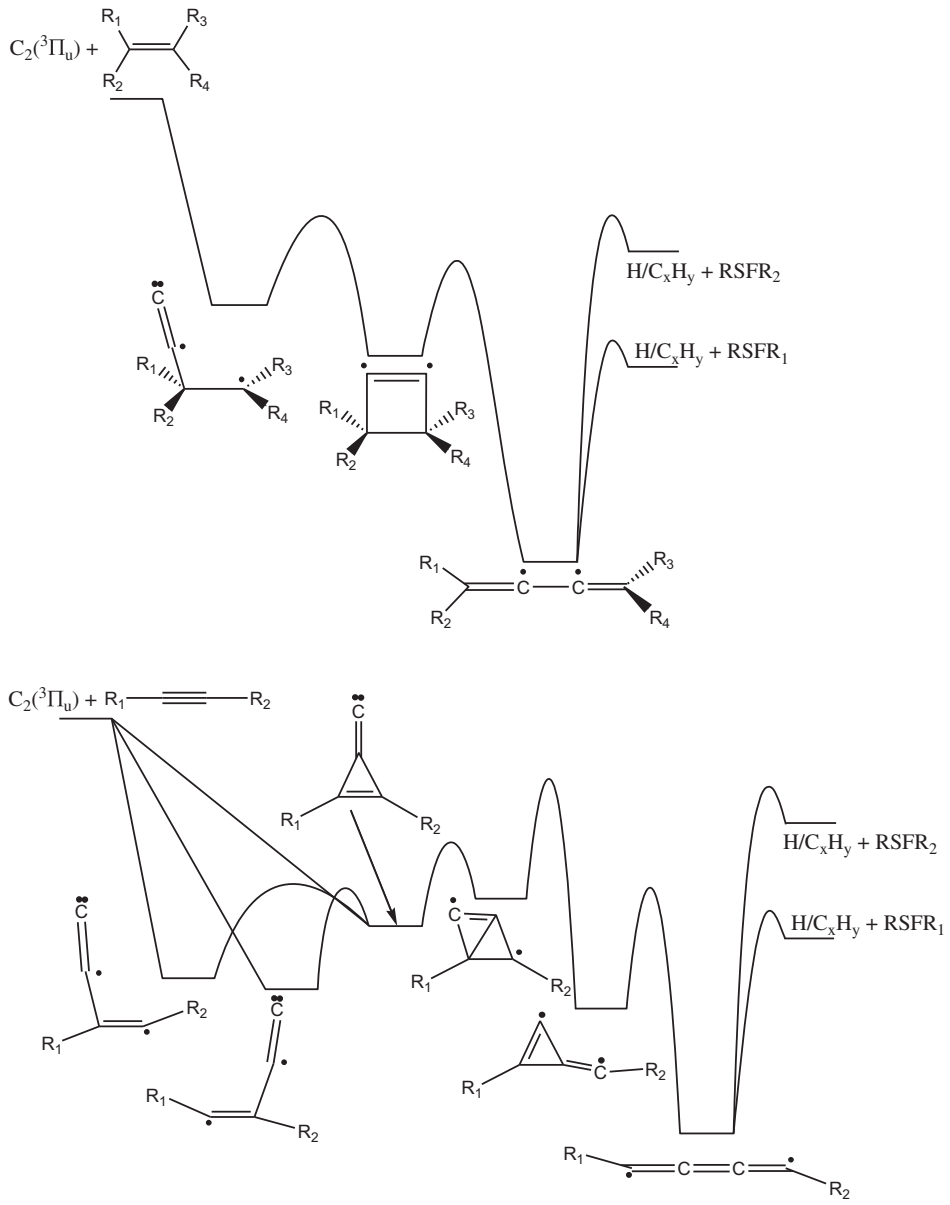

Figure 7. Schematic mechanism of the reactions of $C_2(^3\Pi_u)$ with unsaturated hydrocarbons.

singlet and triplet C_6H_6 surfaces and product branching ratios revealed the formation of the aromatic phenyl radical, *c*-C_6H_5 [43]. The experimental reaction exothermicity to a C_6H_5 product was found to be 337 ± 30 kJ mol^{-1}, which matched the computed exothermicity to produce the phenyl radical, 368 and 379 kJ mol^{-1} on the singlet and triplet PES, respectively. The translational energy distributions had a broad peak from near zero to 35–45 kJ mol^{-1}, indicating that multiple exit channels are likely to exist from the singlet and triplet surfaces, which should involve at least one tight exit transition state for the atomic hydrogen emission. The angular distributions showed flux over the complete angular range and were found to be forward-backward symmetric with respect to 90°. It was concluded therefore that the reaction follows indirect scattering dynamics via the formation of C_6H_6 intermediates and that the lifetime of the

decomposing complex(es) is longer than its (their) rotational period(s). The sideways scattering (maxima at 90°) supported geometrical constraints of the decomposing complex with a preferential hydrogen atom ejection perpendicular to the molecular plane and almost parallel to the total angular momentum vector. Comparing these observations with computed PESs and product yields, we inferred that phenyl is formed predominantly on the triplet surface. The reaction is initiated by a barrierless addition of $C_2(^3\Pi_u)$ to one of the terminal C atoms of 1,3-butadiene, and then the collision complex undergoes trans-cis isomerisation followed by ring closure, H atom migration from CH_2 to the adjacent bare C atom, and H elimination from the remaining CH_2 group forming the phenyl radical via an exit barrier of 27 kJ mol^{-1}. The product precursor emits the hydrogen atom almost perpendicularly to its rotational plane, in accord with the observed sideways scattering. The results of RRKM calculations showed that on the triplet surface, *c*-C_6H_5 is nearly an exclusive reaction product with branching ratios of 98–99%. The proposed mechanism was corroborated by the isotopically labelled experiments, which showed a much stronger signal for the H loss channel in the 2,3-D2–1,3-butadiene reaction as compared to 1,1,4,4-D4–1,3-butadiene and thus indicated that the emitted hydrogen atom mainly originates from the terminal CH_2 group of 1,3-butadiene in the C1/C4 position. On the singlet surface, the reaction proceeds by addition of dicarbon to one of the double C=C bonds followed by insertion of the C_2 unit into this bond resulting in the formation of a vinylbutatriene complex. The complex then decomposes by emitting an H atom from various positions and producing acyclic C_6H_5 isomers, 1- and 4-vinylbutatrienyls and allylic $H_2CCCHCCCH_2$ with branching ratios of 13–20, 5–9, and 8–15% at E_{col} = 0–34 kJ mol^{-1} and exothermic by 172, 152, and 164 kJ mol^{-1}, respectively, or features a 1,3-H shift to trans-bisallene, which dissociates to $C_3H_3 + C_3H_3$ (31–35%, 203 kJ mol^{-1}). The pathway from bis-allene to the phenyl radical involves multiple H migrations before the ring closure and the upper limit of the relative yield of this product if the reaction behaves statistically was evaluated as 41–21%, decreasing with the collision energy. However, a significant yield of the phenyl radical from the singlet reaction was ruled out due to two experimental observations contradicting to the mechanism on the singlet surface: sideways peaking of the angular distributions and the fact that the H atom was preferentially emitted from an original CH_2 group of 1,3-butadiene based on the measurements with partially deuterated 1,3-butadienes. In the meantime, these experiments supported at least the formation of the acyclic 1-vinylbutatrienyl isomer. The formation of this particular isomer is favoured dynamically, because the C–H bond in the decomposing vinylbutatriene intermediate is cleaved only one bond away from the site of the dicarbon attack and insertion, so that energy transfer over many bonds or its complete intramolecular redistribution is not required. Additionally, 1-vinylbutatrienyl is preferable energetically over the other dynamically favoured product 4-vinylbutatrienyl.

3.8.3. *C_7H_7 radicals: benzyl, tolyls, and cycloheptatrienyl*

The benzyl radical, $C_6H_5CH_2$, which is both aromatic and resonance stabilised, was found to be produced in CMB at collision energy of 42.7 kJ mol^{-1} in the reaction of $C_2(X^1\Sigma_g^+/a^3\Pi_u)$ with isoprene via the triplet and singlet C_7H_8 PESs [115]. The reactions on the singlet and triplet surfaces were initiated by the barrierless addition of dicarbon to the carbon–carbon double bond of the isoprene molecule. The initial adducts rearranged via several isomerisation steps eventually leading to the formation of C_7H_7 radicals by emitting atomic hydrogen and the thermodynamically most stable

benzyl isomer was determined to be a major product. Based on the maximal translational energy release, the reaction to the C_7H_7 product(s) was found to be 482 ± 32 kJmol^{-1} exothermic, in line with the computed exothermicity to produce $C_6H_5CH_2$, 468 and 477 kJ mol^{-1} for the singlet and triplet reactions, respectively; the other C_7H_7 isomers (tolyl radicals) are at least ~90 kJ mol^{-1} less stable than benzyl and thus cannot account for the observed maximal reaction energy. The translational energy distribution peaked slightly away from zero, at 20–30 kJmol^{-1}, pointing at the existence at least one C_7H_8 decomposition channel with a tight exit transition state and hence at the involvement of the triplet reaction, as all fragmentation pathways on the singlet surface do not have exit barriers. The angular distribution was forward–backward symmetric with respect to 90° and was spread over the complete angular range of 0°–180° supporting indirect scattering dynamics via the C_7H_8 reaction intermediate(s). The maximum of the angular distribution at 90° indicated sideways scattering, in which the departing atomic hydrogen atom was emitted preferentially perpendicular with respect to the rotational plane of the decomposing complex. Based on the analysis of the calculated PESs and RRKM product branching ratios, it was proposed that benzyl was mostly formed in the triplet reaction via the following mechanisms: triplet dicarbon adds to the C4 or C1 carbon atom of isoprene, yielding intermediates $CCCH_2CHC(CH_3)CH_2$ and $CCCH_2C(CH_3)CHCH_2$, respectively. The former undergoes hydrogen migration from the methyl group to form $CCHCH_2CHC(CH_2)CH_2$, which then ring-closes to –$CCHCH_2CHC(CH_2)CH_2$– and then features another H shift from the CH_2 group in the ring (the former methyl group in isoprene) to the neighbouring bare carbon to yield a cyclic precursor of benzyl, –$CHCHCH_2CHC(CH_2)CH$–. Alternatively, $CCCH_2C(CH_3)CHCH_2$ is subjected to a hydrogen shift from the methyl group yielding $CHCCH_2C(CH_2)CHCH_2$ followed by rotation around a CC bond and a ring closure to –$CCHCH_2CHC(CH_2)CH_2$–, and the two pathways merge. The H loss from the ring CH_2 group in the cyclic precursor of benzyl occurs via an exit barrier of 16 kJ mol^{-1} and in the direction nearly perpendicular to the molecular plane (81.3°) accounting for the observed sideways scattering. The statistical RRKM calculations predicted that the dicarbon addition to C1 under our experimental conditions should produce ~61% of the benzyl radical and ~37% of tolyl radicals with nearly equal contributions of m- and p-tolyls, whereas adding triplet dicarbon to C4 should produce ~25% of benzyl and 75% m- and p-tolyls. On the other hand, the benzyl radical is unlikely to be formed in the singlet reaction both due to the statistical factor – the RRKM branching ratio was estimated to be under 21%, and dynamical unfavorability – the pathway requires multiple isomerisation steps including hydrogen shifts. Instead, we predicted that the reaction on the singlet surface should mostly form acyclic C_6H_5 RSFRs, including allylic $H_2CCCHCCCH_2$ and 1-vinylbutatrienyl, by emitting CH_3, or C_7H_7 radicals, such as $H_2CCCCHC(CH_2)CH_2$, $H_2CCCCC(CH_2)CH_3$, $HCCCCHC(CH_2)CH_3$, and $H_2CCCC(CH_2)CHCH_2$, by H elimination, with exothermicities of 163–215 kJ mol^{-1}.

The CMB study of the reactions of singlet and triplet dicarbon with 1,3-pentadiene at E_{col} = 43 kJ mol^{-1} revealed the formation of less stable cyclic and aromatic C_7H_7 isomers [116]. The experimentally reaction exothermicity of 412 ± 52 kJ mol^{-1} derived from the translational energy distribution was consistent with the formation of o-, m-, and p-tolyl radicals (exothermic by 373–386 kJ mol^{-1}), cycloheptatrienyl (exothermic by 411 kJ mol^{-1} on the triplet PES) and benzyl, but the *ab initio*/RRKM calculations predicted cycloheptatrienyl, m-tolyl, and benzyl to be the major products on the triplet surface with the branching ratios of 45:14:9; the remaining products were formed by CH_3 loss and included the phenyl and acyclic $CCCHCHCHCH_2$ radicals. On both the singlet

and triplet surfaces, the reactions involve indirect scattering dynamics, as followed from the forward–backward symmetric angular distribution spread over the complete angular range of 0°–180°, and were initiated by the barrier-less addition of C_2 to the C=C double bond of 1,3-pentadiene. These initial addition complexes rearrange via multiple isomerisation steps leading eventually through atomic hydrogen elimination to the formation of distinct C_7H_7 radical species. For instance on the triplet surface, the initial complexes $CCC(CH_3)HCHCHCH_2$ and $CCCH_2CHCHCHCH_3$ are formed by dicarbon addition to the C1 and C4 atoms of 1-methyl-1,3-butadiene. From $CCC(CH_3)HCHCHCH_2$, a large amount of the acyclic $CCCHCHCHCH_2$ product is predicted to be produced by a direct CH_3 loss. The other significant products include m-tolyl, cycloheptatrienyl, phenyl plus methyl, and benzyl. The m-tolyl radical is formed via the route initiated by trans-cis isomerisation of the initial adduct and followed by ring closure to a cyclic –$CCC(CH_3)HCHCHCH_2$– complex, H migration from CH_2 to the bare C atom next to it to produce cyclic –$CHCC(CH_3)HCHCHCH$–, and H loss from the carbon linked to the methyl group. The pathway to cycloheptatrienyl branches off at the cyclic –$CCC(CH_3)HCHCHCH_2$– intermediate when it undergoes a hydrogen shift from the methyl group to the ring leading to –$CCHC(CH_2)HCHCHCH_2$–, which then reopens to a chain structure, closes to a seven-member ring, features a hydrogen shift from CH_2 and finally loses atomic hydrogen from CH_2. Alternatively, the reaction can proceed from cyclic –$CCHC(CH_2)HCHCHCH_2$– to benzyl by H shift to –$CHCHC(CH_2)HCHCHCH$– followed by H emission from the C atom linked to external CH_2. Phenyl is formed by H migration in –$CCC(CH_3)HCHCHCH_2$– followed by CH_3 loss. If the reaction begins with $CCCH_2CHCHCHCH_3$, the formation of cycloheptatrienyl is favourable due to the kinetic preference of the route going through conformational changes of the initial adduct, H migration from CH_3 to the opposite end of the molecules, seven-member ring closure to cyclic –$CHCCH_2CHCHCHCH_2$–, H migration from CH_2 to and H elimination from CH_2. All H elimination steps on these pathways go via the structures in which the H atom leaves almost perpendicularly to the molecular plane, which explains the observed sideways scattering. The off-zero peaking of the translational distribution at 20–30 kJ mol^{-1} can be attributed to the exit barrier on the path leading to the m-tolyl product. Meanwhile, on the singlet surface, only acyclic C_6H_5 (+CH_3) and C_7H_7 (+H) isomers can be formed as discussed in Section 3.4.2.

3.9. $C_6H_5C_x$ (x = 1, 2, 3)

The $C_{6+x}H_5$ radicals containing six- and seven-member rings can be produced in the reactions of atomic carbon, dicarbon, and tricarbon with benzene. For instance, the reactions of carbon atoms with benzene and its derivatives were studied in bulk experiments, which suggested a mechanism of C−H insertion to form phenylcarbene [148–152]. Isotope labelling studies by Shevlin and co-workers for the reaction of ^{13}C with C_6D_6 allowed to propose a reaction pathway in which the initial C−H insertion is followed by the phenylcarbene ring-expansion to cycloheptatetrene [153–155]. The C (^3P) + C_6H_6/C_6D_6 reactions were first studied in crossed beams in 1999 [156] and then in more detail in 2002 [157,158] at multiple collision energies in the 8.8–52.5 kJ mol^{-1} range. These experiments performed under single-collision conditions provided a more intimate view on the reaction mechanism. The observed translational energy and angular distributions combined with *ab initio* calculations of the singlet and triplet C_7H_6 PESs [159] and RRKM-Master Equation (ME) kinetics studies allowed the authors to conclude that the reaction proceeds on the triplet surface via a barrierless addition

atomic carbon to form a bicyclic intermediate followed by its insertion into the attacked aromatic C–C bond and thus expansion of the original six-member ring to a seven-member ring intermediate, triplet cycloheptatrienylidene. The latter decomposes without exit barrier to the 1,2-didehydro-cycloheptatrienyl radical, $C_7H_5(X^2B_1)$ or its deuterated C_7D_5 counterpart by emitting an H/D atom; the barrierless character of H elimination was supported by zero peaking of the translational energy distributions. The role of ISC to the singlet C_7H_6 surface was ruled out. From the analysis of the observed translational energy distributions the reactions were found to be exothermic by 15.6 ± 4.8 kJ mol^{-1} (C_6H_6) and 12.2 ± 3.7 kJ mol^{-1} (C_6D_6), close to the computed energy for 1,2-didehydrocycloheptatrienyl, 7.9 kJ mol^{-1} below the reactants. The other potential product, the benzocyclopropenyl radical, was computed to be 45.3 kJ mol^{-1} exothermic and the potential reaction pathway to its formation from the initial adduct involves insertion of the attacking C atom into a neighbouring C–H bond to form triplet phenylcarbene, closure of a three-member ring, and H emission. However, the production of the more thermodynamically stable benzocyclopropenyl is hindered by significantly higher barriers for C–H insertion and H loss as compared with the ring expansion processes leading to the seven-member ring cycloheptatrienylidene complex, the precursor of 1,2-didehydrocycloheptatrienyl. RRKM-ME calculations estimated the relative yield of benzocyclopropenyl to be less than 20%, with a rather small dependence on the collision energy. The maximal contribution of benzocyclopropenyl was evaluated as 10–15%, from the analysis of the fits of translational energy distributions; a one-channel fit without any contribution of this product could also reproduce the experimental data satisfactorily. In addition to the C-for-H/D replacement channels, a C_7D_6 adduct was observed at E_{col} = 21.4 kJ mol^{-1}, because the time needed for this species to reach the ioniser from the interaction region, about 430 ms, was shorter than its RRKM predicted lifetime. The observed trend in the angular distributions, which were increasingly backward-scattered with rising collision energy (and, hence, with a decreasing maximum impact parameter), was traced to the initial direction of the atomic carbon approach toward benzene. The closer the C(^{3}P) attack is to the centre-of-mass of benzene, the more backward-scattered the centre-of-mass angular distribution should be. It was concluded therefore that the dynamics is controlled by large impact parameters at low collision energies when the reaction can proceed either via edge-on or face-on attacks of the benzene ring, resulting in forward–backward symmetric angular distribution. As E_{col} increases, the maximum impact parameter diminishes, and reactive collisions are more likely to occur with smaller impact parameters closer to the centre-of-mass of the ring, giving rise to an enhanced backward scattering due to a direct component of the reaction mechanism via short-lived C_7D_6 /C_7H_6 intermediates.

The formation of stabilised C_7H_6 isomers in the C + C_6H_6 reactions was recently revisited in a combined matrix isolation and *ab initio* molecular dynamics (AIMD) study [160]. The calculations showed that in the C(^{1}D) reaction nearly every collision does not follow the minimum energy path but is controlled by dynamics and yields a product determined by the initial encounter geometry, which is divided into a surface fraction giving the C−H insertion product, phenylcarbene, and a surface area giving the C−C addition product, cycloheptatetraene. Alternatively, in a 10 K solid argon matrix, ground state C(^{3}P) atoms mostly followed the RRKM behaviour, where only cycloheptatetraene is expected, and indeed only this product was detected; the triplet cycloheptatrienylidene intermediate was quenched to the stable singlet molecule. The AIMD calculations indicated that a significant fraction of C−H insertion occurs to form phenylcarbene (55% and 47% for the C(^{1}D) and C(^{3}P) trajectories, respectively), in

contrast to the Ar matrix isolation measurements where the phenylcarbene intermediate was not observed. The AIMD results were significantly different from the PES/RRKM consideration and more consistent with vaporised carbon atom experiments where labelling studies indicated the initial formation of phenylcarbene.

Kinetic studies of the $C(^3P) + C_6H_6$ reaction at room temperatures in a low-pressure fast-flow reactor [78], in which Bergeat and Loison measured and compared the rates of consumption of $C(^3P)$ and appearance of atomic hydrogen, gave the rate constant of $2.8 \pm 0.8 \times 10^{-10}$ cm^3 mol^{-1} s^{-1} consistent with barrierless carbon atom addition to benzene, but the overall yield of the H production was evaluated as only $17 \pm 5\%$. To explain the relatively low branching ratio of the H production channel, the authors proposed acetylene + triplet cyclopentadienylidene or singlet $C_7H_4 + H_2$ (via ISC to the singlet surface) as alternative products. Further theoretical studies [161–164] of the singlet and triplet C_7H_6 PESs performed in relation to the pyrolysis of fulvenallene and other possible reactions accessing these surfaces did not confirm this hypothesis. For instance, da Silva [165] has found a relatively low energy multi-step pathway from the cycloheptatrienylidene complex to the triplet *c*-$C_5H_4 + C_2H_2$ products, but dissociation to these products was predicted to be clearly unfavourable as compared to the fragmentation of the same precursor to fulvenallenyl radical + H. If ISC to the singlet surface occurs, the lowest in energy pathway leads to fulvenallene, which further fragments without an exit barrier to fulvenallenyl + H residing 111 kJ mol^{-1} below the initial reactants. It is apparent that more detailed RRKM calculations would be required to determine the contribution of the fulvenallenyl + H and *c*-$C_5H_4 + C_2H_2$ products on the triplet PES, although the yield of the latter is anticipated to be minor. Also, the dynamical factor clearly favours the formation of 1,2-didehydrocycloheptatrienyl + H from the cycloheptatrienylidene complex because the pathway to fulvenallenyl + H involves multiple isomerisation steps. The exothermicity of the fulvenallenyl radical does not match the experimental energy observed in CMBs. Even if fulvenallenyl is produced predominantly with high internal energy, its formation would have to proceed over an exit barrier of 26 kJ mol^{-1} (compare with the exit barrier of only 1 kJ mol^{-1} found by da Silva for the 1,2-didehydrocycloheptatrienyl + H formation channel), which contradicts to zero peaking of the experimental translational energy distributions. An alternative path to fulvenallenyl + H would involve ISC to the singlet PES, followed by isomerisation to fulvenallene and barrierless emission of atomic hydrogen from the latter. Even if the ISC can be fast for phenylcarbene [166], it is not obvious it could compete with fragmentation of chemically activated triplet complexes under collisionless condition in crossed beams. However, da Silva proposed that in environments where collisional deactivation can compete with fragmentation of the adducts, fulvenallene and fulvenallenyl should the dominant products. The collisional deactivation of C_7H_6 complexes, cycloheptatrienylidene or phenylcarbene on the triplet PES and singlet cycloheptatetraene, phenylcarbene, or fulvenallene if ISC does occur, may explain the observation of only 17% C_7H_5 + H formation in the low-temperature flow reactor [78] studies. Noteworthy, the reaction of carbon atoms with deuterated benzene, C_6D_6, was recently investigated in liquid helium droplets at the temperature as low as 0.37 K [167]. The authors found that a barrierless addition of the carbon atom forming an initial complex is followed by a ring opening and the formation of a seven-member ring. The formation of the seven-member ring C_7D_6 product was supported by calorimetric measurements, which revealed that more than 267 kJ mol^{-1} were released in this reaction, in line with the theoretical energy for the formation of triplet cycloheptatrienylidene [155]. The reaction is frozen after these steps and the hydrogen loss does not

occur because the energy of chemical activation is dissipated into the liquid helium droplet. We can conclude here that the relative yield of various $C_7H_5 + H$ and C_7H_6 products of the $C(^3P) + C_6H_6$ reaction strongly depends on the reaction conditions and RRKM-ME calculations taking into account the ISC rates and energy dissipation into the environment and involving both triplet and singlet PESs would be required to make more accurate predictions of the reaction outcome.

The combined crossed beams and theoretical study [168] of the reactions of dicarbon molecules, $C_2(^1\Sigma_g^+/^3\Pi_u)$, with benzene revealed the formation of the phenylethynyl radical (C_6H_5CC; X^2A_1) + H. The translational energy distributions measured at the collision energies of 56.8 and 72.4 kJ mol^{-1} allowed us to evaluate the reaction exothermicity to form the $C_8H_5 + H$ products as 62 ± 20 kJ mol^{-1}. The experimental reaction energy appeared to be in good agreement with the calculated energy to form the phenylethynyl radical, 33 ± 10 and 41 ± 10 kJ mol^{-1} on the singlet and triplet surfaces, respectively. The reactions to produce ortho, meta, and para-ethynylphenyl radicals were too exothermic by ~70 kJ mol^{-1} and hence could not account for the observed translational energy distributions. The distributions depicted a flat broad plateau between 3 and ~40 kJ mol^{-1} suggesting the existence of at least one reaction channel with a significant exit barrier; this was attributed to the fragmentation of a triplet C_8H_6 complex. The angular distribution showed intensity over the complete angular scan supporting indirect scattering dynamics via C_8H_6 intermediate(s). The shapes of the angular distributions changed dramatically from forward-scattered at lower E_{col} to backward-scattered at higher E_{col}, which indicated that the lifetime of the decomposing complex was shorter than its rotational period, i.e. a few ps. The maximum reactive impact parameter decreases as the collision energy increases, and larger impact parameters could lead to a forward-scattered angular distribution where the attacking C_2 picks up the phenyl unit and leaves H behind; on the contrary, smaller impact parameters could result in a backward scattering of the heavy phenylethynyl product. On the other hand, the backward scattering could also originate from a change of the $C_2(^1\Sigma_g^+)$:$C_2(^3\Pi_u)$ ratio in the beam with increasing collision energy, but this ratio was unknown. Based on the experimental observations and the computed PESs, we proposed the following reaction mechanisms. On the singlet surface, C_2 adds to the aromatic C–C bond and benzene and then one of the two nearest hydrogen atoms is emitted without an exit barrier forming phenylethynyl. Otherwise, a hydrogen atom migration to the terminal C atom of the C_2 unit may lead to the formation of a very stable phenylacetylene molecule via a transition state residing 64 kJ mol^{-1} below the reactants, i.e. about 30 kJ mol^{-1} lower in energy than the phenylethynyl product. Phenylacetylene would preferentially decompose without exit barrier to the ortho, meta, and para-ethynylphenyl radicals rather than to the less stable phenylethynyl radical. This did not happen in experiment due to a short lifetime of the C_8H_6 intermediates. The RRKM computed lifetimes with the assumption of complete energy randomisation were between 114 and 237 ps; the timescales of hundreds of ps would result in long-lived complexes and symmetric centre of mass angular distributions, in contradiction to the experimental results. Hence, the $C_2 + C_6H_6$ reaction did not follow RRKM behaviour under our experimental conditions and, because of this, the thermodynamically most stable isomer(s) were not formed. On the triplet surface, the dicarbon adds to one carbon atom of the benzene molecule and this is followed by elimination of the H atom linked to the attacked C atom via a tight exit transition state located 57 kJ mol^{-1} above the phenylethynyl radical + H products.

The reaction of tricarbon with benzene was investigated first in cryogenic matrices using FTIR spectroscopy [169] and was found to produce only weakly bound $C_3 \cdot C_6H_6$ π-complexes stabilised by ~8 kJ mol^{-1} in which the tricabon unit is parallel to the molecular plane of C_6H_6; the complexes were identified via a comparison of the observed infrared absorption peaks and calculated vibrational frequencies. To better understand possible reaction pathways, the authors carried out DFT calculations of the pertinent PES. Based on the calculations, they concluded that the reaction likely ends at the π-complexes under their cryogenic experimental conditions. Most of the computed potential barriers from the weak complexes to covalently bound intermediates were in the range of 53–54 kJ mol^{-1} but the authors suggested that the addition of C_3 to the C–C bond may be barrierless and hence, in gas phase molecular beam experiments, the reaction may form much more stable structures, including a seven-member ring C_9H_8 isomer with an out-of-ring ethynyl group and C_6H_5–C(H)C_2, exothermic by ~280 kJ mol^{-1} with respect to the reactants, didehydroindene (239 kJ mol^{-1} below the reactants), and a nine-member ring isomer (101 kJ mol^{-1} below the reactants). However, our crossed beam experiments did not confirm this proposition [90]. The experiments were performed at the collision energy as high as 174 ± 14 kJ mol^{-1} and only a C_9H_5 (+H) product(s) was detected. The reaction energy threshold was found to in the 90–110 kJ mol^{-1}. A large fraction of energy was released into the translational degrees of freedom of the reaction products, indicating most likely that the reaction proceeds through short-lived singlet C_9H_6 reaction intermediates, which was also corroborated by the necessity to fit the data with intensity over the complete angular range from 0° to 180°. By comparing with the experimentally derived energetics and the reaction threshold, we identified phenyltricarbon, C_6H_5CCC, endothermic by 104 kJ mol^{-1} according to our high-level calculations, as the reaction product. Thus, an H atom of benzene is replaced by the C_3 unit, which is similar to the $C_2 + C_6H_6$ reaction producing phenylethynyl. The relevant part of the C_9H_6 singlet PES shows that tricarbon attacks a C–C bond in the aromatic ring via an entrance barrier of 43 kJ mol^{-1} leading to a bicyclic C_6H_6CCC intermediate stabilised by about 60 kJ mol^{-1} and the latter may lose atomic hydrogen to form C_6H_5CCC without an exit barrier. The existence of the exit barrier seems to contradict the observed off-zero peaking of the translational distribution, however, this off-zero peaking was attributed to dynamical effects caused by a short lifetime of the fragmenting intermediate and the large collision energy in the experiment.

4. Summary of reaction pathways for the C(^{3}P) and $C_2(X^1\Sigma_g^+/a^3\Pi_u)$ reactions

Let us now summarise mechanisms for the reactions of carbon atoms and dicarbon with unsaturated hydrocarbons leading to the formation of RSFRs. Note only briefly that tricarbon, $C_3(X^1\Sigma_g^+)$, is unreactive at low temperatures and can react with C=C and C≡C, and aromatic C–C bonds only under conditions where high energy thresholds of 40–50, 80–90, 90–110 kJ mol^{-1}, respectively can be overcome. Then, the C_3 unit can step-wisely de facto insert via addition – ring opening into the double and triple bonds and RSFRs can be produced by atomic hydrogen emission, whereas the reaction of C_3 with an aromatic ring proceeds by a simple C_3-for-H replacement mechanism [90, 145].

Atomic carbon adds to a double C=C bond without a barrier and forms a triplet three-member ring cyclopropylidene-like intermediate, which then ring-opens to a triplet cummulene complex completing the insertion of the attacking carbon atom into the C=C bond (Figure 5). Fragmentation of the cummulene intermediate occurs by a

cleavage of the weakest C–H or single C–C bonds if the system behaves statistically, when the lifetime of the complex is longer than the time required for its IVR. However, if the lifetime is not long enough, the reaction can be dynamically controlled and then a single bond closest to the inserted C atom can be cleaved, as this happens for example in the $C(^3P)$ + 1,2-butadiene reaction. The fragmentation of a triplet complex usually occurs via a tight transition state and an exit barrier. Hydrogen migrations in the cummulene intermediate followed by dissociation may lead to alternative products but their contributions are usually minor. Reactions of $C(^3P)$ with an alkyne proceed by C addition either to individual acetylenic carbons or to the triple C≡C bond forming triplet propendiylidene- and cyclopropenylidene-like complexes, respectively, which can easily rearrange to one another and also rapidly isomerize to a (substituted) propargylene intermediate. The latter decomposes by cleaving the weakest C–H or C–C bonds via tight transition states. For the smallest C + alkyne system, in which atomic carbon reacts with acetylene, ISC was found to play an important role; the system crosses over to the singlet C_3H_2 surface and can form $C_3(X^1\Sigma_g^+) + H_2$ as significant products. This unique behaviour has not been observed in the reactions of $C(^3P)$ with larger alkenes and the phenomenon can be attributed to a relative long lifetime of the decomposing C_3H_2 complexes caused by the fact that the products on the triplet surface, *c*- and *l*-C_3H are nearly thermoneutral or only slightly exothermic. A long lifetime allows the triplet-singlet ISC to occur. Alternatively, in the reactions involving larger alkynes, much more exothermic products can be formed and the lifetime of the triplet intermediates is shorter and hence no evidence of ISC was observed so far. The only other reaction of $C(^3P)$ in which ISC apparently does play a role is with benzene, but only in bulk conditions not in gas phase molecular beam experiments.

Singlet dicarbon reacts with alkenes by barrierless addition to the double on in head-on fashion to form a three-member ring intermediate (Figure 6). Next, the C_2 unit inserts into the attacked C=C bond producing a butatriene-like singlet molecule. A rupture of a C–H or a C–C bond follows, which occurs without an exit barrier and could be either kinetically or dynamically controlled. Hydrogen migrations in the (substituted) butatriene intermediate may lead to other singlet isomers which would dissociate to alternative products, but the contributions of such pathways are usually not very significant. In the reactions of $C_2(X^1\Sigma_g^+)$ with alkynes, the addition of the dicarbon unit to C≡C may take place in head-on or side-on manner forming three- or four-member intermediates, respectively. The three-member ring structure isomerizes to the four-member ring complex, which ring-opens to a (substituted) singlet diacetylene; the latter fragments to products via a C–H or C–C bond cleavage without exit barriers.

The reactions of $C_2(a^3\Pi_u)$ are the most complex and may form the largest variety of products. The simplified mechanisms illustrated in Figure 7 do not show all the possibilities but help to understand why multiple pathways could occur. The addition of triplet dicarbon to the double C=C bond proceeds without a barrier to a single sp^2 carbon producing a triplet chain adduct. The adduct undergoes a four-member ring closure to a cyclobutyne-like structure, which then opens to a (substituted) triplet butatriene complex. Triplet butatriene fragments to RSFR products via tight transition states. However, when ligands R_1–R_4 are not simply an H atom, a possibility opens for facile hydrogen migrations to the terminal C atom in the initial reaction adduct. The migration can be followed (or preceded) by a five-, six-, or seven-member ring closure and the reaction can move to the formation of very stable cyclic and aromatic radicals, such as cyclopentadienyl ($C_2(a^3\Pi_u)$ + propene), phenyl ($C_2(a^3\Pi_u)$ + 1,3-butadiene), tridehydrobenzene ($C_2(a^3\Pi_u)$ + vinylacetylene), and benzyl, tolyls and cycloheptatrienyl

($C_2(^3\Pi_u) + C_5H_8$). Even if the cyclisation does not occur, H migrations to the terminal carbon opens favourable pathways to alternative RSFR products ($C_2(a^3\Pi_u)$ + vinylacetylene and $C_2(a^3\Pi_u)$ + 1,2-butadiene). The reaction of triplet dicarbon with a triple C≡C bond occurs by addition to either acetylenic C atom or to the bond itself to form a three-member ring intermediate. The C1 and C2 adducts can isomerize to the cyclic intermediate and the latter can undergo a three-step insertion of the dicarbon unit into the attacked C–C bond. The insertion completes at a (substituted) triplet diacetylene structure serving as a product precursor. The pathways, which result in alternative RSFR products, involved H migrations to the terminal carbon atom in the C1 and C2 adducts and appeared to be important in the reactions of $C_2(a^3\Pi_u)$ with methylacetylene, vinylacetylene, and 1- and 2-butynes.

5. Concluding remarks

Extensive experimental and theoretical studies of the reactions of atomic carbon, $C(^3P)$, dicarbon, $C_2(X^1\Sigma_g^+/a^3\Pi_u)$, and tricarbon, $C_3(X^1\Sigma_g^+)$, with unsaturated hydrocarbons, from acetylene to benzene, reviewed in this article show that the reactions can form various types of resonance stabilised hydrocarbon radicals via $C_n(n = 1–3)$ vs. atomic hydrogen, C_n vs. methyl, and C_n vs. hydrocarbon fragment exchange mechanisms. The RSFRs produced in the reactions include C_xH ($x = 1-8$), propargyl (C_3H_3) and its substituted analogues, 2,4-pentadiynyl-1 (i-C_5H_3) and 1,4-pentadiynyl-3 (n-C_5H_3) together with their methyl substituted counterparts, butatrienyl (i-C_4H_3) and its substituted analogues, and hexenediynyl (i-C_6H_3). Allylic-type radicals with one or more hydrogen atoms of C_3H_5 replaced with hydrogen deficient C_xH_y substituents can be also produced as minor products. Cyclic five-, six-, and seven-member ring radicals including aromatic phenyl, benzyl, and tolyl radicals can be formed mainly via the reactions of triplet dicarbon when hydrogen-migration and cyclisation steps become competitive with single C–H or C–C bond cleavages in intermediate complexes. The reactions of C and C_2 proceed by barrierless additions of atomic carbon or dicarbon to double, triple, or aromatic bonds in unsaturated hydrocarbons, form highly exoergic products, and therefore are fast with rate constants of a few 10^{-10} cm^3 s^{-1} even at temperatures as low as 10 K [170]. Alternatively, the reactions of singlet tricarbon require high barriers to be overcome, often lead to endothermic products, and thus can occur only at high temperatures as reflected in very low rate constants ranging from 10^{-13} to 10^{-17} of cm^3s^{-1} at 293 K. These reactions have strong implications both for combustion and astrochemistry. The hydrogen replacement by C_n ($n = 1–3$) in the reactions implies that these reactions can lead to highly hydrogen-deficient hydrocarbon molecules, including RSFRs and aromatic radicals, within a single collision event, which may significantly contribute to the PAH formation and growth processes. The inclusion of the reaction products of these neutral–neutral reactions into astrochemical models of carbon rich circumstellar envelopes and molecular clouds should lead to a refined understanding on the formation of PAH, their hydrogen deficient precursors, and carbon-rich nanostructures. Most importantly, the formation of RSFRs presents well-defined alternative routes to hitherto postulated ion-molecule reactions as a ‘one-fits-all’ route. The idea of an ion-molecule dominated interstellar chemistry originated from the 70s, when the molecular complexity of the ISM was highly underestimated and astrochemists had the misconception that ion-molecule reactions are always barrierless and all neutral-neutral reactions possess entrance barriers. Note that although under experimental single collision conditions of CMB experiments the intermediates involved in the reactions cannot

be stabilised via third body collisions, in combustion processes number densities are typically in the order of 10^{17} cm^{-3} at temperatures between 1000 and 2000 K, and ternary reactions might stabilise the reaction intermediates. The elevated temperatures open further reaction pathways like the elementary reactions of singlet tricarbon. The demonstrated capability of reactions of carbon atoms and small carbon molecules with unsaturated hydrocarbons to synthesise hydrogen-deficient molecules as well as RSFRs and aromatic radicals appeals for this important reaction class to be included in new developing models of combustion flames as well as PAH and soot formation.

Funding

This work was supported by the US Department of Energy, Basic Energy Sciences, via [grant number DE-FG02-04ER15570], to FIU and [grant number DE-FG02-03ER15411] to Hawaii.

References

[1] H. Richter and J.B. Howard, Prog. Energy Combust. Sci. **26**, 565 (2000).
[2] M.J. Castaldi, N.M. Marinov, C.F. Melius, J. Huang, S.M. Senkan, W.J. Pit, and C.K. Westbrook, Symp. (Int.) Combust. [Proc.]. **26**, 693 (1996).
[3] M. Frenklach, Phys. Chem. Chem. Phys. **4**, 2028 (2002).
[4] Y.C. Minh and E.F. Dishoeck, *Astrochemistry – From Molecular Clouds to Planetary Systems* (ASP Publisher, San Francisco, 2000).
[5] D.A. Williams, Faraday Discuss. **109**, 1 (1998).
[6] H.J. Fraser, M.R.S. McCoustra, and D.A. Williams, Astron. Geophys. **43**, 2.10 (2002).
[7] R.I. Kaiser, C. Ochsenfeld, D. Stranges, M. Head-Gordon, and Y.T. Lee, Faraday Discuss. **109**, 183 (1998).
[8] C.C. Chiong, O. Asvany, N. Balucani, Y.T. Lee, and R.I. Kaiser, in *Proceedings of the 8th Asia-Pacific Physics Conference, APPC 2000*, (World Scientific Press, Singapore, 2001), p. 167.
[9] R.I. Kaiser and A.M. Mebel, Int. Rev. Phys. Chem. **21**, 307 (2002).
[10] R.I. Kaiser, Chem. Rev. **102**, 1309 (2002).
[11] X. Gu, R.I. Kaiser, and A.M. Mebel, Chem. Phys. Chem. **9**, 350 (2008).
[12] R.I. Kaiser and N. Balucani, Int. J. Astrobiol. **1**, 15 (2002).
[13] R.I. Kaiser, P. Maksyutenko, C. Ennis, F. Zhang, X. Gu, S.P. Krishtal, A.M. Mebel, O. Kostko, and M. Ahmed, Faraday Discuss. **147**, 429 (2010).
[14] M. Frenklach, D.W. Clary, W.C. Gardiner, and S.E. Stein, Symp. (Int.) Combust. [Proc.] **20**, 887 (1984).
[15] J.A. Miller, Symp. (Int.) Combust. [Proc.] **26**, 461 (1996).
[16] N.M. Marinov, W.J. Pitz, C.K. Westbrook, M.J. Castaldi, and S.M. Senkan, Combust. Sci. Technol. **116, 117**, 211 (1996).
[17] J.A. Miller and C.F. Melius, Combust. Flame **91**, 21 (1992).
[18] A. D'Anna, A. violi, and A. D'Alessio, Combust. Flame **121**, 418 (2000).
[19] A. D'Anna and A. Violi, Symp. (Int.) Combust. [Proc.] **27**, 425 (1998).
[20] P. Lindstedt, Symp. (Int.) Combust. [Proc.] **27**, 269 (1998).
[21] J.A. Miller, Faraday Discuss. **119**, 461 (2002).
[22] J.A. Miller and S.J. Klippenstein, J. Phys. Chem. A. **105**, 7254 (2001).
[23] J.A. Miller and S.J. Klippenstein, J. Phys. Chem. A. **107**, 7783 (2003).
[24] P.-T. Howe and A. Fahr, J. Phys. Chem. A. **107**, 9603 (2003).
[25] C.H. Miller, W.Y. Tang, R.S. Tranter, and K. Brezinsky, J. Phys. Chem. A. **110**, 3605 (2006).
[26] A.M. Mebel, S.H. Lin, X.M. Yang, and Y.T. Lee, J. Phys. Chem. A. **101**, 6781 (1997).

[27] P. Linstedt, L. Maurice, and M. Meyer, Faraday Discuss. **119**, 409 (2002).
[28] V.V. Kislov and A.M. Mebel, J. Phys. Chem. A. **111**, 3922 (2007).
[29] A.G. Gordon, *The Spectroscopy of Flames* (Chapman and Hall Ltd., Wiley, New York, 1974).
[30] T. Shiomi, H. Nagai, K. Kato, M. Hiramatsu, and M. Nawata, Diam. Rel. Mater. **10**, 388 (2001).
[31] G. Pascoli and A. Polleux, Astron. Astrophys. **359**, 799 (2000).
[32] N. Herlin, I. Bohn, C. Reynaud, M. Cauchetier, A. Galvez, and J.-N. Rouzaud, Astron. Astrophys. **330**, 1127 (1998).
[33] H.G.M. Hill, A.P. Jones, and L.B. d'Hendecourt, Astron. Astrophys. **336**, L41 (1998).
[34] A.C. Andersen, U.G. Jorgensen, F.M. Nicolaisen, P.G. Sorensen, and K. Glejbol, Astron. Astrophys. **330**, 1080 (1998).
[35] X. Gu, Y. Guo, H. Chan, E. Kawamura, and R.I. Kaiser, Rev. Sci. Instr. **76**, 116103 (2005).
[36] R.I. Kaiser, A.G. Suits, and Y.T. Lee, Rev. Sci. Instr. **66**, 5405 (1995).
[37] R.I. Kaiser, J.W. Ting, L.C.L. Huang, N. Balucani, O. Asvany, Y.T. Lee, H. Chan, D. Stranges, and D. Gee, Rev. Sci. Instrum. **70**, 4185 (1999).
[38] D.S.N. Parker, A.M. Mebel, and R.I. Kaiser, Chem. Soc. Rev. **43**, 2701 (2014).
[39] W.-J. Huang, Y.-L. Sun, C.-H. Chin, and S.-H. Lee, J. Chem. Phys. **141**, 124314 (2014).
[40] Y.-L. Sun, W.-J. Huang, C.-H. Chin, and S.-H. Lee, J. Chem. Phys. **141**, 194305 (2014).
[41] C.-H. Chin, W.-K. Chen, W.-J. Huang, Y.-C. Lin, and S.-H. Lee, J. Phys. Chem. A. **116**, 7615 (2012).
[42] S.-H. Lee, W.-K. Chen, C.-H. Chin, and W.-J. Huang, J. Chem. Phys. **139**, 174317 (2013).
[43] C.-H. Chin, W.-K. Chen, W.-J. Huang, Y.-C. Lin, and S.-H. Lee, Icarus. **222**, 254 (2013).
[44] L. Cartechini, A. Bergeat, G. Capozza, P. Casavecchia, G.G. Volpi, W.D. Geppert, C. Naulin, and M. Costes, J. Chem. Phys. **116**, 5603 (2002).
[45] N. Balucani, Giovanni Capozza, F. Leonori, E. Segoloni, and P. Casavecchia, Int. Rev. Phys. Chem. **25**, 109 (2006).
[46] M. Costes, N. Daugey, C. Naulin, A. Bergeat, F. Leonori, E. Segoloni, R. Petrucci, N. Balucani, and P. Casavecchia, Faraday Discuss. **133**, 157 (2006).
[47] N. Balucani, F. Leonori, R. Petrucci, K.M. Hickson, and P. Casavecchia, Phys. Scr. **78**, 058117 (2008).
[48] F. Leonori, R. Petrucci, E. Segoloni, A. Bergeat, K.M. Hickson, N. Balucani, and P. Casavecchia, J. Phys. Chem. A. **112**, 1363 (2008).
[49] W.D. Geppert, C. Naulin, M. Costes, G. Capozza, L. Cartechini, P. Casavecchia, and G.G. Volpi, J. Chem. Phys. **119**, 10607 (2003).
[50] A.D. Becke, J. Chem. Phys. **98**, 5648 (1993).
[51] C. Lee, W. Yang, and R.G. Parr, Phys. Rev. B: Condens. Matter Mater. Phys. **37**, 785 (1988).
[52] P.J. Stephens, F.J. Devlin, C.F. Chabalowski, and M.J. Frisch, J. Phys. Chem. **98**, 11623 (1994).
[53] A.M. Mebel, K. Morokuma, and M.C. Lin, J. Chem. Phys. **103**, 7414 (1995).
[54] A.G. Baboul, L.A. Curtiss, P.C. Redfern, and K. Raghavachari, J. Chem. Phys. **110**, 7650 (1999).
[55] L.A. Curtiss, K. Raghavachari, P.C. Redfern, A.G. Baboul, and J.A. Pople, Chem. Phys. Lett. **314**, 101 (1999).
[56] L.A. Curtiss, K. Raghavachari, P.C. Redfern, V. Rassolov, and J.A. Pople, J. Chem. Phys. **109**, 7764 (1998).
[57] G.D. Purvis III and R.J. Bartlett, J. Chem. Phys. **76**, 1910 (1982).
[58] T.H. Dunning Jr., J. Chem. Phys. **90**, 1007 (1989).
[59] K.A. Peterson and T.H. Dunning, J. Phys. Chem. **99**, 3898 (1995).
[60] H. Eyring, S.H. Lin, and S.M. Lin, *Basic Chemical Kinetics* (Wiley, New York, NY, 1980).

[61] J.I. Steinfeld, J.S. Francisco, and W.L. Hase, *Chemical Kinetics and Dynamics* (Prentice-Hall, Englewood Cliffs, NJ, 1999).
[62] V.V. Kislov, T.L. Nguyen, A.M. Mebel, S.H. Lin, and S.C. Smith, J. Chem. Phys. **120**, 7008 (2004).
[63] Z. Homayoon, J.M. Bowman, N. Balucani, and P. Casavecchia, J. Phys. Chem. Lett. **5**, 3508 (2014).
[64] R.D. Levine, *Molecular Reaction Dynamics* (Cambridge University Press, Cambridge, 2005).
[65] S. Yamamoto, S. Saito, M. Ohishi, H. Suzuki, S. Ishikawa, N. Kaifu, and A. Murakami, Astrophys. J. **322**, L55 (1987).
[66] A.M. Mebel, W.M. Jackson, A.H.H. Chang, and S.H. Lin, J. Am. Chem. Soc. **120**, 5751 (1998).
[67] J.F. Stanton, Chem. Phys. Lett. **237**, 20 (1995).
[68] J. Takahashi, Publ. Astron. Soc. Japan. **52**, 401 (2000).
[69] Y. Zhang, P. Ning, and J. Zhang, Spectrochim. Acta A: Mol. Biomol. Spectrosc. **101**, 283 (2013).
[70] R.I. Kaiser, C. Ochsenfeld, M. Head-Gordon, Y.T. Lee, and A.G. Suits, J. Chem. Phys. **106**, 1729 (1997).
[71] R.I. Kaiser, D. Stranges, Y.T. Lee, and A.G. Suits, Astrophys. J. **477**, 982 (1997).
[72] R.I. Kaiser, Y.T. Lee, and A.G. Suits, J. Chem. Phys. **103**, 10395 (1995).
[73] R.I. Kaiser, C. Ochsenfeld, M. Head-Gordon, Y.T. Lee, and A.G. Suits, Sci. **274**, 1508 (1996).
[74] X. Gu, Y. Guo, F. Zhang, and R.I. Kaiser, J. Phys. Chem. A. **111**, 2980 (2007).
[75] R.I. Kaiser, A.M. Mebel, and Y.T. Lee, J. Chem. Phys. **114**, 231 (2001).
[76] R.I. Kaiser, L. Belau, S.R. Leone, M. Ahmed, B.J. Braams, and J.B. Bowman, Chem. Phys. Chem. **8**, 1236 (2007).
[77] R.I. Kaiser, C. Ochsenfeld, M. Head-Gordon, and Y.T. Lee, Astrophys. J. **510**, 784 (1999).
[78] M. Costes, P. Halvick, K.M. Hickson, N. Daugey, and C. Naulin, Astrophys. J. **703**, 1179 (2009).
[79] A. Bergeat and J.-C. Loison, Phys. Chem. Chem. Phys. **3**, 2038 (2001).
[80] C. Ochsenfeld, R.I. Kaiser, Y.T. Lee, A.G. Suits, and M. Head-Gordon, J. Chem. Phys. **106**, 4141 (1997).
[81] R. Guadagnini, G.C. Schatz, and S.P. Walch, J. Phys. Chem. A. **102**, 5857 (1998).
[82] E. Buonomo and D.C. Clary, J. Phys. Chem. A. **105**, 2694 (2001).
[83] T. Takayanagi, Chem. Phys. **312**, 61 (2005).
[84] T. Takayanagi, J. Phys. Chem. A. **110**, 361 (2006).
[85] W.K. Park, J. Park, S.C. Park, B.J. Braams, C. Chen, and J.B. Bowman, J. Chem. Phys. **125**, 081101 (2006).
[86] A.M. Mebel, V.V. Kislov, and M. Hayashi, J. Chem. Phys. **126**, 204310 (2007).
[87] B.J. Sun, C.Y. Huang, H.H. Kuo, K.T. Chen, H.L. Sun, C.H. Huang, M.F. Tsai, C.H. Kao, Y.S. Wang, L.G. Gao, R.I. Kaiser, and A.H.H. Chang, J. Chem. Phys. **128**, 244303 (2008).
[88] F. Zhang, Y.S. Kim, L. Zhou, A.H.H. Chang, and R.I. Kaiser, J. Chem. Phys. **129**, 134313 (2008).
[89] Y. Guo, V.V. Kislov, X. Gu, F. Zhang, A.M. Mebel, and R.I. Kaiser, Astrophys. J. **653**, 1577 (2006).
[90] B.J. Sun, C.H. Huang, M.F. Tsai, H.L. Sun, L.G. Gao, Y.S. Wang, Y.Y. Yeh, Y.H. Shih, Z.F. Sia, P.H. Chen, R.I. Kaiser, and A.H.H. Chang, J. Chem. Phys. **131**, 104305 (2009).
[91] X. Gu, Y. Guo, A.M. Mebel, and R.I. Kaiser, Chem. Phys. Lett. **449**, 44 (2007).
[92] A.M. Mebel, G.-S. Kim, V.V. Kislov, and R.I. Kaiser, J. Phys. Chem. A. **111**, 6704 (2007).
[93] R.I. Kaiser, T.N. Le, T.L. Nguyen, A.M. Mebel, N. Balucani, Y.T. Lee, and F. Stahl, P.v.R. Schleyer, and H.F. Schaefer III, Faraday Discuss. **119**, 51 (2001).
[94] A.M. Mebel, M. Hayashi, W.M. Jackson, J. Wrobel, M. Green, D. Xu, and S.H. Lin, J. Chem. Phys. **114**, 9821 (2001).

[95] S. Graf, J. Geiss, and S. Leutwyler, J. Chem. Phys. **114**, 4542 (2001).
[96] Vikas and G. Kaur, J. Chem. Phys. 139, 224311 (2013).
[97] V.M. Donnelly and L.R. Pasternack, Chem. Phys. **39**, 427 (1979).
[98] L.R. Pasternack, J.R. McDonald, and V.M. Donnelly, ACS Symp. Ser. **134**, 381 (1980).
[99] K.H. Becker, B. Donner, C.M.F. Dinis, H. Geiger, F. Schmidt, and P. Wiesen, J. Phys. Chem. (Munich) **214**, 503 (2000).
[100] R.I. Kaiser, N. Balucani, O. Asvany, and Y.T. Lee, Symp. Int. Astron. Union. **197**, 251 (2000).
[101] R.I. Kaiser, N. Balucani, D.O. Charkin, and A.M. Mebel, Chem. Phys. Lett. **382**, 112 (2003).
[102] X. Gu, Y. Guo, A.M. Mebel, and R.I. Kaiser, J. Phys. Chem. A. **110**, 11265 (2006).
[103] X. Gu, Y. Guo, F. Zhang, A.M. Mebel, and R.I. Kaiser, Faraday Disc. **133**, 245 (2006).
[104] A. Canosa, A. Páramo, S.D. Le Picard, and I.R. Sims, Icarus. **187**, 558 (2007).
[105] A. Páramo, A. Canosa, S.D. Le Picard, and I.R. Sims, J. Phys. Chem. A. **112**, 9591 (2008).
[106] F. Leonori, R. Petrucci, K.M. Hickson, E. Segoloni, N. Balucani, S.D. Le Picard, P. Foggi, and P. Casavecchia, Planet. Space Sci. **56**, 1658 (2008).
[107] F. Zhang, Y.S. Kim, R.I. Kaiser, and A.M. Mebel, J. Phys. Chem. A. **113**, 1210 (2009).
[108] T.L. Nguyen, A.M. Mebel, and R.I. Kaiser, J. Phys. Chem. A. **105**, 3284 (2001).
[109] D.S.N. Parker, F. Zhang, Y.S. Kim, and R.I. Kaiser, J. Phys. Chem. A. **115**, 593 (2011).
[110] D. Chastaing, P.L. James, I.R. Sims, and I.W.M. Smith, Phys. Chem. Chem. Phys. **1**, 2247 (1999).
[111] R.I. Kaiser, Y.T. Lee, and A.G. Suits, J. Chem. Phys. **105**, 8705 (1996).
[112] T.N. Le, H.-Y. Lee, A.M. Mebel, and R.I. Kaiser, J. Phys. Chem. A. **105**, 1847 (2001).
[113] C. Naulin, N. Daugey, K.M. Hickson, and M. Costes, J. Phys. Chem. A. **113**, 14447 (2009).
[114] R.I. Kaiser, T.L. Nguyen, A.M. Mebel, and Y.T. Lee, J. Chem. Phys. **116**, 1318 (2002).
[115] F. Zhang, B. Jones, P. Maksyutenko, R.I. Kaiser, C. Chin, V.V. Kislov, and A.M. Mebel, J. Am. Chem. Soc. **132**, 2672 (2010).
[116] B.B. Dangi, D.S.N. Parker, T. Yang, R.I. Kaiser, and A.M. Mebel, Angew. Chem., Int. Ed. **53**, 4608 (2014).
[117] B.B. Dangi, D.S.N. Parker, R.I. Kaiser, D. Belisario-Lara, and A.M. Mebel, Chem. Phys. Lett. **607**, 92 (2014).
[118] A.M. Mebel, V.V. Kislov, and R.I. Kaiser, J. Phys. Chem. A. **110**, 2421 (2006).
[119] Y. Guo, X. Gu, N. Balucani, and R.I. Kaiser, J. Phys. Chem. A. **110**, 6245 (2006).
[120] X. Gu, Y. Guo, F. Zhang, A.M. Mebel, and R.I. Kaiser, Chem. Phys. Lett. **444**, 220 (2007).
[121] Y. Guo, X. Gu, F. Zhang, A.M. Mebel, and R.I. Kaiser, J. Phys. Chem. A. **110**, 10699 (2006).
[122] R.I. Kaiser, D. Stranges, H.M. Bevsek, Y.T. Lee, and A.G. Suits, J. Chem. Phys. **106**, 4945 (1997).
[123] R.I. Kaiser, T.L. Nguyen, T.N. Le, and A.M. Mebel, Astrophys. J. **561**, 858 (2001).
[124] Y. Li, H.-L. Liu, X.-R. Huang, Y.-B. Sun, Z. Li, and C.-C. Sun, J. Phys. Chem. A. **113**, 10577 (2009).
[125] J.-C. Loison, and A. Bergeat, Phys. Chem. Chem. Phys. **6**, 5396 (2004).
[126] Y. Li, H.-L. Liu, X.-R. Huang, D.-Q. Wang, and C.-C. Sun, J. Phys. Chem. A. **113**, 6800 (2009).
[127] I. Hahndorf, H.Y. Lee, A.M. Mebel, S.H. Lin, Y.T. Lee, and R.I. Kaiser, J. Chem. Phys. **113**, 9622 (2000).
[128] R.I. Kaiser, H.Y. Lee, A.M. Mebel, and Y.T. Lee, Astrophys. J. **548**, 852 (2001).
[129] N. Balucani, H.-Y. Lee, A.M. Mebel, Y.T. Lee, and R.I. Kaiser, J. Chem. Phys. **115**, 5107 (2001).
[130] B.B. Dangi, S. Maity, R.I. Kaiser, and A.M. Mebel, J. Phys. Chem. A. **117**, 11783 (2013).

[131] D.S.N. Parker, S. Maity, B.B. Dangi, R.I. Kaiser, A. Landera, and A.M. Mebel, Phys. Chem. Chem. Phys. **16**, 12150 (2014).
[132] T.N. Le, A.M. Mebel, and R.I. Kaiser, J. Comp. Chem. **22**, 1522 (2001).
[133] A. Landera, S.P. Krishtal, V.V. Kislov, A.M. Mebel, and R.I. Kaiser, J. Chem. Phys. **128**, 214301 (2008).
[134] R.I. Kaiser, D. Stranges, Y.T. Lee, and A.G. Suits, J. Chem. Phys. **105**, 8721 (1996).
[135] A.M. Mebel, R.I. Kaiser, and Y.T. Lee, J. Am. Chem. Soc. **122**, 1776 (2000).
[136] R.I. Kaiser, A.M. Mebel, Y.T. Lee, and A.H.H. Chang, J. Chem. Phys. **115**, 5117 (2001).
[137] R.I. Kaiser, A.M. Mebel, A.H.H. Chang, S.H. Lin, and Y.T. Lee, J. Chem. Phys. **110**, 10330 (1999).
[138] D. Chastaing, S.D. Le Picard, I.R. Sims, and I.W.M. Smith, Astron. Astrophys. **365**, 241 (2001).
[139] D. Chastaing, S.D. Le Picard, I.R. Sims, I.W.M. Smith, W.D. Geppert, C. Naulin, and M. Costes, Chem. Phys. Lett. **331**, 170 (2000).
[140] G.-S. Kim, T.L. Nguyen, A.M. Mebel, S.H. Lin, and M.T. Nguyen, J. Phys. Chem. A. **107**, 1788 (2003).
[141] H.W. Schranz, S.C. Smith, A.M. Mebel, and S.H. Lin, J. Chem. Phys. **117**, 7055 (2002).
[142] N. Balucani, A.M. Mebel, Y.T. Lee, and R.I. Kaiser, J. Phys. Chem. A. **105**, 9813 (2001).
[143] A.M. Mebel, V.V. KisIov, and R.I. Kaiser, J. Chem. Phys. **125**, 133113 (2006).
[144] X. Gu, Y. Guo, F. Zhang, A.M. Mebel, and R.I. Kaiser, Chem. Phys. **335**, 95 (2007).
[145] R.I. Kaiser, M. Goswami, P. Maksyutenko, F. Zhang, Y.S. Kim, A. Landera, and A.M. Mebel, J. Phys. Chem. A. **115**, 10251 (2011).
[146] Y. Guo, X. Gu, F. Zhang, A.M. Mebel, and R.I. Kaiser, Phys. Chem. Chem. Phys. **9**, 1972 (2007).
[147] L.C.L. Huang, H.Y. Lee, A.M. Mebel, S.H. Lin, Y.T. Lee, and R.I. Kaiser, J. Chem. Phys. **113**, 9637 (2000).
[148] P.B. Shevlin, Atomic Carbon, in *Reactive Intermediate Chemistry*, edited by R.A. Moss, M.S. Platz, and M. Jones (Wiley, New York, NY, 2004), pp. 463–500.
[149] C.M. Geise, C.M. Hadad, F. Zheng, and P.B. Shevlin, J. Am. Chem. Soc. **124**, 355 (2002).
[150] B.M. Armstrong, F. Zheng, and P.B. Shevlin, P. B. J. Am. Chem. Soc. **120**, 6007 (1998).
[151] F. Sevin, İ. Sökmen, B. Düz, and P.B. Shevlin, Terahedron Lett. **44**, 3405 (2003).
[152] İ. Sökmen, A. Ece, B. Düz, F. Sevin, and F. Lett, Org. Chem. **6**, 650 (2009).
[153] S. Matzinger, T. Bally, E.V. Patterson, and R.J. McMahon, J. Am. Chem. Soc. **118**, 1535 (1996).
[154] M.W. Wong and C. Wentrup, J. Org. Chem. **61**, 7022 (1996).
[155] P.R. Schreiner, W.L. Karney, P.v.R. Schleyer, W.T. Borden, T.P. Hamilton, and H.F. Schaefer. J. Org. Chem. **61**, 7030 (1996).
[156] R.I. Kaiser, I. Hahndorf, L.C.L. Huang, Y.T. Lee, and H.F. Bettinger, P.v.R. Schleyer, H.F. Schaefer III, and P.R. Schreiner, J. Chem. Phys. **110**, 6091 (1999).
[157] I. Hahndorf, Y.T. Lee, R.I. Kaiser, L. Vereecken, J. Peeters, H.F. Bettinger, and P.R. Schreiner, P.v.R. Schleyer, W.D. Allen, and H.F. Schaefer III. J. Chem. Phys. **116**, 3248 (2002).
[158] R.I. Kaiser, L. Vereecken, J. Peeters, H.F. Bettinger, P.v.R. Schleyer, and H.F. Schaefer III, Astronom. Astrophys. **406**, 385 (2003).
[159] H.F. Bettinger, P.v.R. Schleyer, H.F. Schaefer III, P.R. Schreiner, R.I. Kaiser, and Y.T. Lee, J. Chem. Phys. **113**, 4250 (2000).
[160] M.L. McKee, H.P. Reisenauer, and P.R. Schreiner, J. Phys. Chem. A. **118**, 2801 (2014).
[161] G. da Silva, and A. Trevitt, Phys. Chem. Chem. Phys. **13**, 8940 (2011).
[162] G. da Silva, A.J. Trevitt, M. Steinbauer, and P. Hemberger, Chem. Phys. Lett. **517**, 144 (2011).
[163] D. Polino, A. Famulari, and C. Cavallotti, J. Phys. Chem. A **115**, 7928 (2011).
[164] D. Polino, and C. Cavallotti, J. Phys. Chem. A **115**, 10281 (2011).
[165] G. da Silva, J. Phys. Chem. A **118**, 3967 (2014).

[166] M.S. Platz, Acc. Chem. Res. **28**, 487 (1995).
[167] S.A. Krasnokutski, and F. Huisken, J. Chem. Phys. **141**, 214306 (2014).
[168] X. Gu, Y. Guo, F. Zhang, A.M. Mebel, and R.I. Kaiser, Chem. Phys. Lett. **436**, 7 (2007).
[169] J. Szczepanski, H. Wang, and M. Vala, Chem. Phys. **303**, 165 (2004).
[170] http://kinetics.nist.gov/